PLASMA MEMBRANE DYNAMICS REGULATING THE PD-1/PD-L1 PATHWAY

Christopher Charles Bricogne

Thesis submitted to University College London
for the degree of Doctor of Philosophy

2015

DECLARATION

I, Christopher Charles Bricogne, confirm the work presented in this thesis is my own. Where information has been derived from other sources, I confirm that this has been indicated in the thesis.

This work has been funded by The Rosetrees Trust, The Medical Research Council and the UCL Bogue Fellowship.

“ Just be aware that the next worthy pursuit will probably appear in your periphery, which is why you should be careful of long-term dreams – if you focus too far in front of you, you won’t see the shiny thing out the corner of your eye. ”

– Tim Minchin

ABSTRACT

The PD-1/PD-L1 pathway in T lymphocytes is emerging as one of the most promising targets for cancer immunotherapy but few details are yet known about how its inhibitory influence is achieved.

This work set out to investigate the role of plasma membrane dynamics, on both T cells and tumour cells, in modulating the pathway. In eukaryotic cells, calcium influx leads to rapid changes in the plasma membrane. Exocytosis, phospholipid scrambling, membrane shedding and massive endocytosis can all occur. The calcium sensors for these processes, their inter-dependence and their effects on transmembrane protein expression remain largely unknown. Here we show that the ion channel TMEM16F is the calcium sensor for large exocytosis and that phospholipid scrambling and microvesicle shedding are coupled to exocytosis. The absence of TMEM16F not only abrogates exocytosis but also results in massive endocytosis in response to calcium. Intracellular polyamines regulate these phenotypes, switching cell responses from massive exo- to endocytosis by blocking the TMEM16F conductance. This massive endocytosis also occurs during apoptosis via a calcium-independent mechanism. In lymphocytes, PD-1 participates selectively in both shedding and massive endocytosis, targeting that depends on the PD-1 transmembrane region, independent of actin and classical protein adaptors. We also found that PD-L1 on tumour cells can be transferred to lymphocytes, and be maintained in stable complex with PD-1 on in vitro and in vivo. This may modulate the PD-L1/PD-1 pathway in tumours.

Together, these results provide new insights into the plasma membrane reorganization that occurs following calcium transients, establishes a mechanism of PD-1 regulation dependent solely on protein-membrane interaction, and also introduces a new modality by which PD-L1:PD-1 interactions can be sustained beyond cell-cell contact in tumours.

ACKNOWLEDGEMENTS

I am hugely grateful to my supervisor Mary Collins for these fantastic years in her laboratory. She always provided complete freedom, while offering a huge amount of support, wisdom and encouragement. I will really miss working with her. I also thank her family (Aggie, Tim and Mollie) who have been extremely friendly and hospitable to me – I will remember those paper-submission dinners fondly.

I am very grateful to Don Hilgemann whose openness in accepting me into his lab (twice) was integral to the outcomes of this work. It was a privilege to work in his laboratory. As well as being a great mentor scientifically, he was also incredibly generous personally. I will forever remember our trips around Dallas, to the symphony, to dinners, drinks and thanksgiving with his wife Christianne. I will always have Herbert on my wall as a reminder of that great time.

I would like to thank members of the Collins lab past and present. I am really thankful to David Escors for providing me with a fantastic start in science, the feeling that any question can be answered and for getting me hooked on doing experiments. I will really miss working with Mehdi Barachian; his support, help, advice and friendship have been invaluable. I also thank Doug Macdonald for his sage advice early on. Thanks to Maha Tajani and Djamil Damry who both surpassed their master at cloning. I also thank Kam Zaki, Fred Arce, Chris Davis and Gary Britton for their help and humour over the years.

From the Hilgemann lab I thank Michael Fine who taught me to patch clamp, put in many hours in front of the confocal, set me up in Dallas and always put a smile on my face. Thank you to Susan for her generosity in keeping me well fed on salmon and dumplings and for all her technical assistance. Thanks to Youxue for his thoughtful advice and to Linda Patterson who was very kind to me throughout my visits.

This work would not have been possible without our collaborators. I thank Sergio Quezada for his ongoing advice throughout my PhD and his postdoc Dr Dana Briesmeister for her friendship and assistance with the tumour experiment. I am grateful to Ricardo Henriques for being so open to collaborating on the SR-SIM experiments and to Pedro Pereira for staying up to the wee hours over many nights taking the pictures.

I am extremely grateful to my funders who made all this possible – The Rosetrees Trust, the MRC and also the Bogue Fellowship Committee for enabling me to work in Dallas. Many thanks also to Gordon Stewart and the MBPhD programme.

I am so unbelievably lucky to have such wonderful friends - Nick, Lianne, Emma, Lucy, Georgia, Shiv, Sarah, Henry, Faz, Mike etc. you are all so special to me and have kept me going. A particular thank you to lovely Claire who has put up with listening to all my (mostly incorrect) hypotheses and for being so wonderfully supportive at every stage.

Lastly I would like to thank my incredible family for all their love, all they have done and sacrificed on my behalf; especially my wonderful grandparents Granny and Pork, my father, Gérard, for encouraging me to marvel at the world, and my amazing sister and best friend Alice for all her love and support.

Lastly I would like to thank and dedicate this thesis to my mother, Jennifer, without whom none of this would have been possible, and who is a constant source of strength and inspiration.

TABLE OF CONTENTS

LIST OF FIGURES

LIST OF TABLES

ABBREVIATIONS

ABCA1	ATP-binding cassette transporter 1
af	*Aspergillus fumigatus*
Akt	Protein kinase B
ALIX	ALG-2-interacting protein X
AM	Acetoxymethyl ester
AnXV	Annexin V
AP-2	Adaptor protein 2
APC	Antigen presenting cell
ASM	Acid sphingomyelinase
ATP	Adenosine triphosphate
ATP11C	ATPase, Class VI, Type 11C
ATPase	Adenosine triphosphatase
BATF	Basic leucine zipper transcription factor, ATF-like
BEL	Bromoenol lactone
BHK	Baby hamster kidney
BoNT	Botulinum toxin
BTLA	B and T lymphocyte attenuator
Ca^{2+}	Calcium ions
cAMP	Cyclic AMP
Cas 9	CRISPR associated protein 9
Cbl-b	E3 Ligase Casitas B Lineage Lymphoma b
CCP	Clathrin-coated pits
CD	Cluster of differentiation
$CD4^+$	CD4 expressing T lymphocyte
$CD8^+$	CD8 expressing T lymphocyte
CHMP	Chromatin modifying protein
Cl^-	Chloride ions
C_m	Membrane capacitance
CoA	Coenzyme A
CRAC	Calcium release activated channel

CRISPR	Clustered regularly interspaced short palindromic repeats
cSMAC	Central supramolecular adhesion complex
CTL	Cytotoxic T lymphocyte
CTLA-4	Cytotoxic T-lymphocyte-associated protein 4
DAG	Diacyl-glycerol
DC	Dendritic cell
DHHC5	Zinc Finger DHHC Domain-Containing Protein 5
DMEM	Dulbecco's Modified Eagle's medium
EDA	Ethylenediamine
EDTA	Ethylenediaminetetraacetic acid
EEA1	Early Endosome Antigen 1
EGFR	Epidermal growth factor receptor
EGTA	Ethylene glycol tetraacetic acid
ER	Endoplasmic reticulum
Erk	Extracellular signal-regulated kinase
ESCRT	Endosomal sorting complexes required for transport
FACS	Flow cytometry
FasL	Fas Ligand
Fc	Immunoglobulin Fc portion
FDA	Food and drug Administration
FHL4	Familial hemophagocytic lymphohistiocytosis-4
FSC	Forward scatter
FW	Forward primer
GFP	Green fluorescent protein
GLUT4	Glucose transporter type 4
G_m	Membrane conductance
GM-CSF	Granulocyte-macrophage colony-stimulating factor
gRNA	Guide RNA
GTP	Guanosine triphosphate
GVAX	GM-CSF expressing B16.F10 melanoma
HEK	Human embryonic kidney cells
HEPES	4-(2-hydroxyethyl)-1-piperazineethanesulfonic acid

HIV	Human immunodeficiency virus
HLA	Human leukocyte antigen
ICAM-1	Intercellular Adhesion Molecule 1
IDO	Indoleamine-pyrrole 2,3-dioxygenase
IFN	Interferon
IL	Interleukin
I_m	Membrane current
IP_3	Inositol trisphosphate
ISRE	Interferon-stimulated response element
IST2	Increased sodium tolerance protein 2
ITIM	Immunoreceptor tyrosine-based inhibitory motif
ITSM	Immunoreceptor tyrosine-based switch motif
K^+	Potassium ions
K7-Rho	Heptalysine conjugated to rhodamine
Kd	Dissociation constant
LAMP1	Lysosomal-associated membrane protein 1
LAT	Linker for activation of T cells
LB	Luria-Bertani
LBPA	Lysobisphophatidic acid
Lck	Lymphocyte-specific protein tyrosine kinase
LCMV	Lymphocytic choriomeningitis
LFA-1	Lymphocyte function-associated antigen 1
MDSC	Myeloid-derived suppressor cells
MEND	Massive endocytosis
MHC	Major histocompatibility complex
mRNA	Messenger RNA
Munc18	Mammalian uncoordinated-18
MVB	Multivesicular body
Na^+	Sodium ions
NCX1	Sodium-calcium exchanger
NFATc1	Nuclear factor of activated T-cells, cytoplasmic 1
NFκB	Nuclear factor kappa-light-chain-enhancer of activated B cells

nh	*Nectria haematococca*
NK cells	Natural killer cell
NMDG	N-Methyl-D-glucamin
NSCLC	Non-Small Cell Lung Cancer
NSF	N-ethylmaleimide-sensitive factor
OE	Overlap extension
P2x7	P2X purinoceptor 7
PC	Phosphatidylcholines
PCR	Polymerase chain reaction
PD-1	Programmed cell death protein 1
PD-L1	Programmed cell death-ligand 1
PD-L2	Programmed cell death-ligand 2
PDCD1	Programmed cell death protein 1 encoding gene
PE	Phosphatidylethanolamines
PI3K	Phosphatidylinositol-4,5-bisphosphate 3-kinase
PIP_2	Phosphatidylinositol 4,5-bisphosphate
PKC	Protein kinase C
PLA2	Phospholipases A2
PLC	Phospholipase C
PLSCR1	Phospholipid scramblase 1
PM	Plasma membrane
PMCA ATPase	Plasma membrane Ca2+ ATPase
PP2A	Protein phosphatase 2
PS	Phosphatidylserine
PTEN	Phosphatase and tensin homolog
RBC	Red blood cell
RCC	Renal cell carcinoma
Rhod	Rhodamine
ROCK-1	Rho-associated, coiled-coil-containing protein kinase 1
ROS	Reactive oxygen species
RPMI	Roswell Park Memorial Institute medium
RS	Reverse primer

RTK	Receptor tyrosine kinase
SERCA ATPase	Sarco/endoplasmic reticulum Ca2+-ATPase
SFFV	Spleen focus-forming virus
SHP	Src homology 2 domain-containing phosphatase 1
shRNA	Short hairpin RNA
SLO	Streptolysin O
SM	Sphingomyelin
Smase	Sphingomyelinase
SNAP-25	Synaptosomal-Associated Protein, 25kDa
SNARE	Soluble NSF attachment protein receptor
SNX9	Sorting nexin-9
SR-SIM	Superresolution structured illumination microscopy
Src	Proto-oncogene tyrosine-protein kinase
SSC	Side scatter
STIM	Stromal interaction molecule
Syn	Synaptotagmin
T reg	Regulatory T lymphocyte
TAE	Tris -acetate EDTA
TBF	Transformation buffer
TCR	T cell receptor
TeNT	Tetanus toxin
TfR	Transferrin receptor
TGN	Trans-Golgi network
TILs	Tumour infiltrating lymphocyte
TIRFM	Total internal reflection fluorescence microscope
TM	Transmembrane domain
TNF	Tumor necrosis factors
VAMP	Vesicle associated membrane protein
WASp	Wiskott–Aldrich Syndrome protein
WT	Wild-type
Xkr8	Xk-related protein 8
Zap70	Zeta-chain-associated protein kinase 70

CHAPTER 1

INTRODUCTION

1.2 PD-1/PD-L1 Biology

1.2.1 Cancer Immunotherapy and the PD-1/PD-L1 pathway

The specific elimination of cancer cells without the parallel destruction of healthy tissues is the ultimate objective of cancer therapeutics. Conventional treatments have been limited in effectiveness by their lack of such specificity. Chemotherapeutic agents eliminate rapidly dividing cells while surgical resection and radiotherapy target the abnormal tumour mass, if it can be distinguished from normal structures. The need to balance tumour clearance with life threatening side effects often prevents successful treatment of cancer by these modalities (Vanneman and Dranoff, 2012). A greater understanding of the molecular basis of cancer has brought a new generation of targeted therapeutic approaches. Cancer genome sequencing has revealed common mutations or chromosomal translocations that lead to the activation of specific signalling pathways and promote uncontrolled cellular proliferation. Examples include inhibition of the constitutively activated BRAF pathway in melanoma and the BCR-Abl kinase in chronic myeloid leukaemia (CML) (Holderfield et al., 2014; Weisberg et al., 2007). A greater understanding of the relationship between tumours and the immune system has opened a new field of therapy, cancer immunotherapy, which is aimed at activating adaptive immune towards cancer cells.

The dysfunctional gene expression that leads to the uncontrolled proliferation of cancer cells also causes the expression of tumour antigens that can elicit cytotoxic T lymphocyte responses (Burnet, 1970; van der Bruggen et al., 1991). Since this discovery, the potential to direct an antigen-specific immune response towards cancer has been investigated as a potential therapeutic approach. The first attempts conducted in the 1980s employed vaccination protocols, delivering melanoma antigens along with immune adjuvants. These studies were almost uniformly unsuccessful (Rosenberg et al., 2004). One reason for this dispiriting beginning was a failure to address the causes of immune dysfunction in cancer. The tumour microenvironment has multiple direct and indirect mechanisms of immune suppression, including secreted immunosuppressive cytokines (Dranoff, 2004),

inhibitory co-stimulation (Pardoll, 2012), induction of tolerogenic dendritic cells (Seliger and Massa, 2013), the recruitment of inhibitory regulatory T cells (T regs) (Mougiakakos et al., 2010) and myeloid-derived suppressor cells (MDSCs) (Khaled et al., 2013) as well as metabolic interference (Wang et al., 2014). It has been as a result of an increasing understanding of these mechanisms that a new generation of effective immunotherapies has emerged.

T lymphocytes receive and integrate many signals through plasma membrane receptors that regulate their activity throughout cell activation and effector function. Initially, naïve cells recognise their cognate antigen peptide presented by MHC on an antigen-presenting cell (APC) (Signal 1) alongside signalling through co-stimulatory or co-inhibitory receptors (Signal 2) including CD28, CTLA-4 and PD-1. These signals together contribute to setting the activity and proliferative capacity of the cell. Cytokine signals (Signal 3), IL-12 and IL-10 for example, serve to structure the phenotype of the resulting T cell response (Chen and Flies, 2013). Later, when activated T cells encounter their antigen expressing target cells in the periphery, co-receptor signalling again regulates lymphocyte effector function. The diverse stimulatory and inhibitory co-receptor signals received by lymphocytes serve as immune checkpoints that work to maintain immune tolerance to self-tissues. Cancer cells evolve under an immune 'selection-pressure', and so are found to upregulate immunosuppressive factors that, under physiological conditions, maintain tolerance to healthy tissues (Dunn et al., 2004). Immune checkpoint therapies attempt to manipulate these auxiliary signals as a way to reverse immune dysfunction and break tolerance to cancer.

The CD28 family of co-stimulatory receptors are critical T lymphocyte regulators. They are characterised by a single extracellular immunoglobulin-like domain. Stimulatory CD28 signalling is essential for activation of naïve T cells while other family members, ICOS (stimulatory), CTLA-4, PD-1 and BTLA (inhibitory), serve to tune T cell activity (Riley and June, 2005). These pathways have emerged as crucial immune checkpoints and therefore targets for immunotherapeutic interventions.

The first checkpoint targeted was the inhibitory CTLA-4, a receptor only expressed on T lymphocytes, which shares its ligands with the stimulatory CD28 (Krummel and

Allison, 1995; Walunas et al., 1994). CTLA-4 signalling is influential at the early stage of antigen presentation to a naïve cell as its ligands CD80 and CD86 are only expressed on APCs (Walunas et al., 1996). Blocking antibodies that preclude ligand/receptor binding prevent inhibition by CTLA-4, and may also serve to downregulate regulatory T cell (Treg) function (Peggs et al., 2009). Work in mouse models demonstrated that CTLA-4 blockade promoted immune rejection of tumours (van Elsas et al., 1999). The humanised blocking antibody impilimumab produced clinical responses in patients with diverse tumour types including renal cell carcinoma (RCC) (Yang et al., 2007), melanoma (Weber et al., 2008) and ovarian cancer (Hodi et al., 2008) in early phase trials. A subsequent randomised trial combining a melanoma-specific vaccine with impilimumab showed a survival benefit of over three months in patients with metastatic melanoma (Hodi et al., 2010). Remarkably, in a subset of patients, treatment with impilimumab has been tentatively curative with remission seen for over 10 years (Schadendorf et al., 2015). Unfortunately, rates of adverse events were high in all studies with ~30% suffering autoimmune complications including severe colitis (Yang et al., 2007) (Weber et al., 2008) (Hodi et al., 2008). Impilimumab has now been approved by the US Food and Drug Administration (FDA) for use in metastatic melanoma.

In the last five years blockade of the PD-1/PD-L1 pathway has emerged as perhaps the most promising strategy for cancer immunotherapy. High PD-1 expression is a feature of the ineffective, 'exhausted' T cells found in tumours, while PD-L1 (the primary PD-1 ligand) is upregulated in multiple cancer types (discussed later). Early phase trials demonstrated efficacy of both anti-PD-1 and PD-L1 blocking antibodies with clinical responses in melanoma, RCC, bladder and non-small cell lung cancers (Brahmer et al., 2012; Powles et al., 2014; Topalian et al., 2012). Several anti-PD-1 antibodies have recently gained FDA approval for the treatment of metastatic melanoma. The antibody pembroluzimab (MK-3475) showed a 37% response rate in Phase I trials (Hamid et al., 2013), while Phase III trials testing the antibody nivolumab gave a survival rate of 72% vs. 42% in patients treated with the chemotherapeutic drug dacrabazine (Robert et al., 2015). A surprising outcome from these clinical studies is that PD-1/PD-L1 blockade has effects in classically non-immunogenic tumour types including NSCLC (Topalian et al., 2012). A recent Phase

III trial testing nivolumab for NSCLC was stopped early following a clear survival benefit over docetaxel. The rates of drug related adverse events were, however, consistently high across trials with ~10% rate of grade 3 or 4 adverse events (life threatening or requiring hospitalisation) and some fatalities from drug-induced pneumonitis, hepatitis, colitis and thyroiditis (Robert et al., 2015; Topalian et al., 2012). These side effects may limit these therapies to patient cohorts with severe, late stage metastatic disease and render them inappropriate treatments at earlier stages where curative and long-lasting interventions are more likely (Pardoll, 2012).

Immune checkpoint therapy is still at an early stage. Key questions remain, including how to predict which patients will respond to specific therapies, whether combinations of therapeutic blocking antibodies will have cumulative effects, and importantly how to limit the drug related adverse effects (Sharma and Allison, 2015). The PD-1/PD-L1 axis is clearly an important pathway in suppressing immune responses to cancer as well as a hugely promising target for therapeutics. There are many aspects of PD-1/PD-L1 biology that are still poorly understood, as will be discussed in this chapter. The molecular basis of PD-1 signalling, how expression at the cell surface is regulated, and the nature of the PD-1/PD-L1 interaction are yet to be completely understood. As with the field of cancer immunotherapy itself, a greater understanding of the underlying mechanisms will hopefully bring increasingly effective strategies to modulate this important pathway.

1.2.2 PD-1 Expression

PD-1 is expressed on T cells, B cells, NK cells and DCs (Keir et al., 2008). Expression is undetectable on naïve T cells but is induced upon cell activation (Agata et al., 1996). Expression is rapid, occurring within 6 - 24 hours after T cell receptor (TCR) stimulation *in vitro* and *in vivo* (Agata et al., 1996; Chikuma et al., 2009), but is transient, with levels returning to baseline within a week. During chronic viral infection however, T cells revert to a state of 'anergic' dysfunction, with low cytokine secretion, proliferation and cytotoxic function associated with clonal deletion and high expression of PD-1 (Brooks et al., 2005; Moskophidis et al., 1993; Wherry et al., 2005; Zajac et al., 1998). In this so-called 'exhausted' state, administration of PD-1 or PD-L1 blocking antibodies can recover T cell function (Barber et al., 2006; Wherry et al., 2007). Exhaustion may constitute a protective mechanism of peripheral tolerance, attenuating autoimmune responses to persistent 'self' antigens, but in turn leads to ineffective clearance of viruses and tumour cells (Barber et al., 2006; Velu et al., 2009). In the context of cancer, PD-1 expression is high on TILs in breast (Sun et al., 2014), melanoma (Ahmadzadeh et al., 2009; Chapon et al., 2011), renal cell carcinoma (Thompson et al., 2007), Ovarian (Matsuzaki et al., 2010), hepatocellular carcinoma (Shi et al., 2011), non-small cell lung (Zhang et al., 2010), prostate (Sfanos et al., 2009), thyroid (French et al., 2012) cancers. This expression acts as a biomarker for poor prognosis in many cases (Shi et al., 2011; Sun et al., 2014; Thompson et al., 2007).

Limited work has focused on understanding the transcriptional control of the *PDCD1* gene that transcribes PD-1. The Ca^{2+} dependent transcription factor NFATc1 induces PD-1 expression following TCR-activated Ca^{2+} influx, via a binding site in the PDCD1 promoter (Oestreich et al., 2008). This may explain the rapid, transient upregulation of PD-1 following activation but not the long-term sustained expression in exhaustion. A detailed interrogation of the *PDCD1* promoter by serial truncation studies found that an Interferon-Stimulated Response Element (ISRE) was present (Terawaki et al., 2011). Type I interferon IFN-α treatment led to sustained PD-1 expression reminiscent of exhaustion via the ISRE. The authors suggested that this may explain why IFN-α therapy, which is intended to enhance T cell responses, has

had limited success (Amato, 1999). *In vivo* studies showed that IFN-α therapy given alongside PD-1 blockade was synergistic in mouse-tumour models. Other cytokines including the γ-chain containing the cytokines IL-2, 7, 15 and 21 can also lead to PD-1 expression, but the mechanism for this is unclear.

Work directed towards understanding PD-1 transcriptional regulation has so far provided important insights that may help to guide future therapies. PD-1 expression constitutes a protective mechanism, preventing inappropriate immunity that may threaten important tissues. Adjuvants that promote immunity, such as cytokine-based therapies, will therefore likely be balanced by the application of immune 'brakes' such as PD-1. Better understanding of PD-1 regulation is therefore key to optimal manipulation of immune functions for therapeutic purposes.

1.2.3 PD-L1 and PD-L2 Expression

PD-L2 is only expressed on APCs whereas PD-L1 is inducible in the majority of cell types. PD-L1 is expressed in 'immune privileged' organs such as the eye, testes and placenta, where overzealous immune responses could damage important structures. IFN-γ and TNF-α rapidly upregulate PD-L1 expression in many cell types (Keir et al., 2008).

An immune-inhibitory tumour microenvironment is an important factor in tumour persistence and PD-L1 provides cells with protection from immune clearance. PD-L1 expression is found to be high on tumour cells in breast (Muenst et al., 2014), melanoma (Hino et al., 2010; Massi et al., 2014), RCC (Frigola et al., 2011), ovarian (Maine et al., 2014), HCC (Gao et al., 2009), NSCLC (Azuma et al., 2014), colon (Shi et al., 2013), cervical (Karim et al., 2009), and oesophageal (Ohigashi et al., 2005). In all these cases high PD-L1 expression is linked unfavourably to patient prognosis. It is unclear how this upregulation occurs in tumours. There is some evidence in glioblastoma that PD-L1 is upregulated by signalling downstream of dysfunctional PTEN (Parsa et al., 2007) but others have shown this is not the mechanism in melanoma (Atefi et al., 2014). Further work is needed to understand how this important prognostic factor is regulated in order to develop interventions aimed at modulating PD-L1 expression.

1.2.4 PD-1 Signalling

CTLA-4 knockout mice develop a catastrophic lymphoproliferative disorder soon after birth and die within 3-4 weeks (Tivol et al., 1995; Waterhouse et al., 1995). The phenotype in PD-1 knockout mice is less dramatic, with late development of an insidious lupus-like glomerulonephritis and arthritis (Nishimura et al., 1999) or inflammatory cardiomyopathy (Nishimura et al., 2001) depending on the mouse species. PD-1 is important in setting the threshold for adaptive immune activity, with knockout or blockade promoting autoimmune disease (Menke et al., 2007; Wang, 2005), while conferring resistance to viral infections (Iwai et al., 2003) and tumours (Iwai et al., 2002; Iwai et al., 2005) and promoting graft rejection (Ito et al., 2005).

The means by which PD-1 inhibits T cell effector function is complex, with new modalities still coming to light. The PD-1 intracellular domain does not possess any intrinsic inhibitory properties but instead functions as an adaptor for other inhibitory proteins. Two tyrosine-based motifs – an ITIM (V/I/LxYxxL) and ITSM (TxYxxL) – are present on its intracellular domain. The ITSM recruits the SHP-1 and SHP-2 phosphatases (Chemnitz et al., 2004). Ligation of PD-1 triggers the phosphorylation of both ITIM and ITSM, possibly by Lck and/or Src kinases (Sheppard et al., 2004). The recruited phosphatase is phosphorylated, changes conformation and becomes active. Following PD-1 engagement, de-phosphorylation events affect components of T cell signalling including CD3ζ, Zap70, and PKCtheta (Okazaki et al., 2001; Sheppard et al., 2004) and downstream PI3K and Akt (Parry et al., 2005). This simple picture of PD-1-induced phosphatase activation attenuating TCR signalling was added to by Yokosuka et al. who investigated the spatial requirements for PD-1 at the immune synapse(Yokosuka et al., 2012). They used TIRF Microscopy and planar bilayers to simulate antigen presentation and found that PD-1 is rapidly translocated to TCR-containing microclusters in the centre on the immune synapse (cSMAC), in a PD-L1 dependent manner. TCR microclusters have only been identified since the advent of TIRFM and constitute aggregates of TCRs and proximal signalling components. It is in these clusters that PD-1 recruits SHP-2. Disruption of clustering prevents PD-1-dependent de-phosphorylation of

TCR-associated signalling molecules. PD-1 signalling therefore relies on a dynamic spatial co-localisation with TCR for effective inhibition.

Due to the substantial inhibitory effects of PD-1 on T cell functions, Quigley and colleagues asked whether PD-1 stimulation resulted in a change in transcription factor expression (Quigley et al., 2010). They first compared the gene expression profiles of exhausted CD8+ T cells from HIV patients with PD-1 expressing Jurkat cells that had been stimulated with anti CD3CD28 and anti PD-1. They found an overlapping gene upregulation of 75 genes that included the inhibitory transcription factor BATF. Overexpression of BATF re-capitulated the phenotype of T cell exhaustion, with reduced proliferation and IL-2 production. Moreover, knockdown of BATF rescued effector functions in 'exhausted' HIV specific CD8+ cells. This work presents evidence that the inhibitory influence of PD-1 extends beyond TCR signal attenuation and involves the upregulation of an inhibitory gene profile. It is currently unclear how PD-1 can influence gene transcription in this way.

In work carried out in the Collins lab, which I contributed to during my BSc project, it was found that PD-1 signalling can also modulate the TCR downregulation that follows T cell activation (Karwacz et al., 2011). This incidental finding came out of work aimed at enhancing anti-tumour immune responses in mice via genetic modification of DCs. One of the strategies tested was the shRNA knockdown of PD-L1. The normal downregulation of the TCR that follows antigen presentation did not occur in T cells activated by PD-L1 knockout DCs. Independent work by Naramura et al. and others had demonstrated that the inhibitory E3 Ubiquitin ligase Cbl-b was involved in TCR downregulation following antigen presentation (Naramura et al., 2002; Shamim et al., 2007). This was mediated via ubiquitination of the CD3ζ leading to TCR internalisation. Indeed it was found that PD-1 signalling powerfully upregulates Cbl-b (Karwacz et al., 2011). This work presented a new mechanism by which PD-1 can inhibit effector function - by downregulating TCR expression, and thereby limiting 'Signal 1'. It is also likely that Cbl-b, known to be inhibitory to T cell function, could ubiquitinate other protein targets involved in T cell activation. Little is known about the transcriptional regulation of Cbl-b so it would also be

interesting to investigate whether the transcription factors identified in Quigley et al., shown to be upregulated by PD-1, are involved in Cbl-b regulation.

Lastly it was recently discovered that PD-1:PD-L1 engagement has profound effects on T cell motility. By employing Two Photon Microscopy (TPM), Zinselmeyer et al. demonstrated that exhausted T cells exposed to chronic LCMV infection localised to the splenic red pulp where they remained relatively immobile (Zinselmeyer et al., 2013). This paralysis is due to highly stable immune synapse formation mediated via PD-L1 that clusters in the cSMAC. Motility could be restored by PD-1 blockade. Interestingly, in the model of LCMV (C13) infection, this recovery was associated with an excessive immune response, mediated via IFN-γ, which was quickly fatal to mice. This demonstrates the important physiological role PD-1 plays in attenuating potentially damaging immune responses.

The PD-1 receptor seemingly has a very simple mechanism of inhibition; recruitment and activation of inhibitory phosphatases that limit stimulatory signalling. It has however become clear that PD-1 also has other effects on gene transcription as well influences on TCR regulation and cell behaviour. As interventions that aim to regulate this pathway in the context of cancer enter the clinic, evidence is of dramatic tumour rejection but high rates of adverse drug-related events. More needs to be understood about this promising pathway if we are to harness its full therapeutic potential.

1.2.5 PD-1 Membrane Regulation

The regulation of other members of the CD28 family has been a focus of considerable research but, to our knowledge, only one paper has attempted to understand the trafficking of PD-1. CTLA-4 is endocytosed via an AP-2 binding, tyrosine-based (YVKM) motif, leading to clathrin and dynamin-dependent endocytosis (Bradshaw et al., 1997; Qureshi et al., 2012). It is then either recycled to the plasma membrane or degraded in lysosomal compartments. The rate of this trafficking is increased during T cell activation (Qureshi et al., 2012) which likely enhances the trans-endocytosis of CTLA-4 ligands (discussed later). CD28

endocytosis appears to be more complicated, with evidence that a complex of WASp, SNX9 and p85 couple CD28 to the clathrin endocytic machinery (Badour et al., 2007).

Pentcheva-Hoang et al. investigated PD-1 trafficking using confocal microscopy – co-staining PD-1 and other organelle markers over a time course of OT-II T cell activation (Pentcheva-Hoang et al., 2007). At day three following activation, PD-1 could be seen on the plasma membrane as well as in Trans Golgi Network (TGN), demonstrated by co-localisation with TGN38, suggesting that it is sorted through this compartment on the way to the plasma membrane. PD-1 did not co-localise with trafficking endosomes (marked with anti-TfR and fluorescent transferrin) or lysosomes (marked with anti-LAMP1), which suggested to the authors that 'PD-1 is internalised via a different endocytic pathway'.

No further work has built on these insights or attempted to understand the mechanism of PD-1 endocytosis. PD-1 has no known internalisation motifs and it seems not to be trafficked through normal endocytic compartments. Nevertheless, despite no obvious leads, further investigation is warranted.

1.2.6 Intercellular Transmembrane Protein Transfer

In recent years, new mechanisms of intercellular communication have emerged beyond simple membrane-bound or secreted ligand-receptor interactions. It has been discovered that membrane proteins can be captured and transferred from one cell to another during cell contact. This transfer can take different forms, with proteins either being recycled or degraded by the recipient cell. CD28 family members have been found to take part in two forms of this protein exchange: Trans-endocytosis and Trogocytosis.

CTLA-4 is another inhibitory member of the CD28 family with both intrinsic and extrinsic mechanisms of T cell inhibition. A salient feature of CTLA-4 is that it shares the ligands CD80 and CD86 with the stimulatory receptor CD28. CTLA-4 has been shown to indirectly recruit SHP-2 and PP2A phosphatases that dephosphorylate factors downstream of TCR in a similar way to PD-1 though with distinct targets. This model does not seem to fully explain the inhibitory effects of

CTLA-4 as it can still be inhibitory without phosphatase recruitment, and in other cases is not inhibitory when associated with phosphatases (Alegre et al., 2001). CTLA-4 can disrupt lipid raft and microcluster formation (Schneider et al., 2007) (Chikuma et al., 2003) and therefore normal TCR signalling. Affinity studies have demonstrated that CTLA-4 has a much higher binding affinity for its ligands (especially CD80) than CD28 (Collins et al., 2002). This suggests that CTLA-4 can compete favourably with CD28 for ligands and therefore reduce stimulatory signalling through CD28. CTLA-4 can also inhibit by cell extrinsic mechanisms including secretion of soluble CTLA-4 and induction of the enzyme indoleamine 2,3-dioxy-genase (IDO) in APCs (Rudd, 2008).

In 2011, Qureshi and colleagues discovered an exciting new modality for cell extrinsic CTLA-4 inhibition (Qureshi et al., 2011). In experiments using fluorescently tagged CD80 and CD86 expressed on DCs, they discovered that these ligands were transferred onto CTLA-4 expressing T regulatory cells (Tregs) in co-culture. This transfer was enhanced when TCR stimulation was applied in parallel. Using a membrane dye the authors showed that small amounts of membrane were also transferred with the ligands. Crucially, ligands were swiftly degraded in the T cell, a process that could be blocked using the lysosome inhibitor bafilomycin A. These experiments suggested that complete ligands, still associated with membrane fragments, were depleted from DC surface and degraded by CTLA-4 expressing T cells. This process of ligand removal and degradation is named Trans-endocytosis and was first observed in the context of early development, occurring during Notch receptor signalling (Klueg and Muskavitch, 1999) and EPH-Ephrin interactions (Marston et al., 2003). In the case of CTLA-4, it constitutes a novel means of immune inhibition, by depleting the pool of CD28 ligands available. This may have effects on the cell undergoing trans-endocytosis, as well as on other cells that subsequently come into contact with that DC. The strong affinity CTLA-4 possesses for its ligands is thought to be crucial in allowing Trans-endocytosis to occur, although the mechanism behind trans-endocytosis is still unclear.

Following this discovery, it was important to ask whether PD-1 could also engage in ligand capture. Using surface plasmon resonance and isothermal titration calimetry,

Cheng et al. conducted a comprehensive interrogation of PD-1-ligand binding properties (Cheng et al., 2013). They found that PD-1 has a surprisingly weak interaction with its ligands. The half lives of human PD-1:PDL1 (Kd=8μM) and PD-1:PD-L2 (Kd=2μM) were between 1000-5000 shorter than for CTLA-4:CD80 and even more short-lived for mouse PD-1:PD-L (Kd = 30-35μM). PD-1 takes part in monovalent interactions with its ligands, unlike CTLA-4 which can form very stable bivalent interactions (Zhang et al., 2004). PD-1:PD-L1 interactions were shown to be entropically driven and three-fold weaker than PD-1:PD-L2 interactions, which are enthapically driven. Due to this very weak affinity, the authors concluded that PD-1 would be incapable of trans-endocytosis. They also raised the important question as to what the functional role of trans-endocytosis would be in the case of PD-1 that does not compete for ligands with other receptors. Despite this, in 2012 Gary et al. found that it was possible for PD-L1 to be transferred to PD-1 expressing T cells via trogocytosis (Gary et al., 2012).

In trogocytosis, the transfer of membrane protein with membrane patch results in the expression of that protein on the plasma membrane of the recipient cell rather than intracellular retention and degradation as in the case of trans-endocytosis. Trogocytosis has been shown to occur in mouse and human T lymphocytes where peptide -MHC and co-stimulatory receptors, ligands and receptors are transferred from DC to T cell (Game et al., 2005; Huang et al., 1999) or visa versa (Busch et al., 2008) *in vitro* and *in vivo* (Riond et al., 2007). There is also evidence of transfer of proteins from endothelial cells to T cells during migration (Brezinschek et al., 1999). Gary et al. found that in co-culture experiments, PD-L1 could be transferred from DCs and tumour cells onto CD8+ T cells in a cell-cell contact dependent and antigen-specific manner (Gary et al., 2012). They also showed that functional actin cytoskeletion was necessary as well as vATPases. They also presented some evidence that once the PD-L1 had been transferred onto the T cell, those cells were able to induce apoptosis in other T cells. This effect was abolished by PD-L1 blocking antibodies, implying that the transferred PD-L1 was functionally active. The authors concluded that this process might serve to spread the inhibitory influence beyond the original PD-L1 expressing DC/tumour cell. No further studies have investigated the role that this protein transfer may play on immune responses *in vivo*.

An apparent conflict appears here, in that affinity studies demonstrate that the PD-1:PD-L1 interaction is very weak and transient, whilst *in vitro* cellular studies show that it is capable of transferring ligands, which presumably requires a more stable interaction.

1.3 Ca^{2+}-activated plasma membrane responses

Signal transduction across cell membranes is essential for life. The ability of cells to receive extracellular signals and convert them to an intracellular response allows multicellular organisms to coordinate the actions of billions of cells under ever-changing environmental pressures. These signals can take many forms – crosslinking of transmembrane proteins can lead to phosphorylation events, while activation of pumps and channels can change the intracellular makeup of ions and molecules. These changes may later lead to the upregulation of new proteins with functions able to subtly or dramatically change cell behaviour. Calcium ions (Ca^{2+}) and phosphate are perhaps the most ubiquitous messengers in cell biology and the majority of cell signalling constitutes changes in concentration of these messengers over time.

Cells use ion gradients as a stored signal that can rapidly be triggered by plasma membrane channel opening; for example the gradients of sodium and potassium in the neuron are used to transmit depolarisation signals across large distances in milliseconds. The normal ion gradients between cellular cytoplasm and the extracellular space for human cells are shown in Figure 1.X.

The size of the Ca^{2+} gradient is striking, with ~20,000 calcium ions outside the cell for every one ion in the cytosol. The Ca^{2+} ATPase pump maintains this steep gradient by pumping Ca^{2+} out of the cell (PMCA ATPase) or into the endoplasmic or sarcoplasmic reticulum (SERCA ATPase). The reason for such a significant exclusion of Ca^{2+} from the cell arises from its chemical properties, which can be both beneficial and highly toxic to the cell. The major hazard of Ca^{2+} is its ability to precipitate phosphate, unlike other bivalent cations such as magnesium. Despite this danger, Ca^{2+} is also essential to many cell processes including cell activation, exocytosis, and apoptosis, and is further essential in its capacity as an indicator of plasma membrane integrity.

Conc. (mM)

	Extra	Intra
Na^+	145	12
K^+	4	140
Cl^-	100	2.5
Ca^{2+}	2	0.0001

Ratio

	Extra	Intra
Na^+	12	1
K^+	1	35
Cl^-	40	1
Ca^{2+}	20,000	1

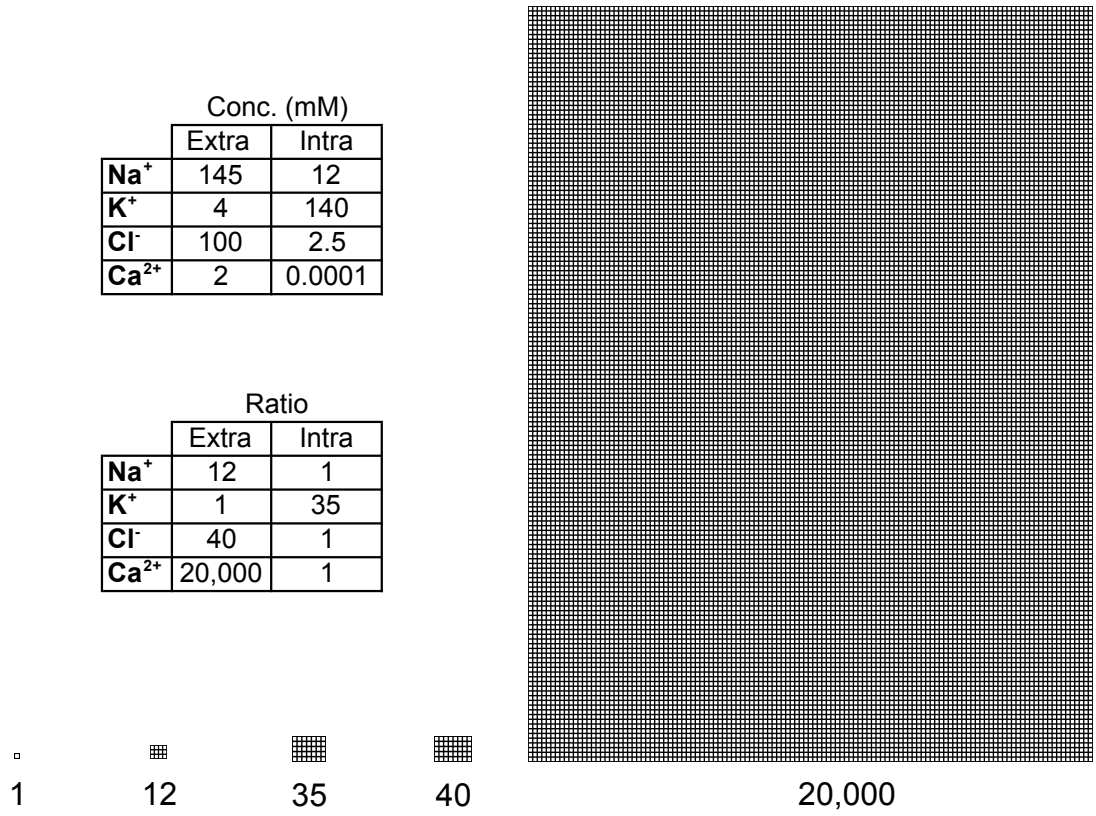

Figure 1.1 **Ion gradients across the eukaryotic plasma membrane**. Approximate intracellular and extracellular concentrations (mM) and ratios of key ions across the plasma membrane as well as a pictorial representation of the ion ratios with one square equivalent to one ion.

The properties of proteins depend on their structure and charge. Whilst phosphorylation links anionic phosphate to certain amino acid hydroxyl groups, Ca^{2+} acts like a portable cation, able to rapidly provide proteins new functions. Ca^{2+} sensing domains such as EF hands and C2 domains possess structures of anionic amino acids that accommodate Ca^{2+} binding. In the case of C2 domains, once in complex with Ca^{2+}, these newly cationic structures are able to bind anionic phospholipids on the inner leaflet of the plasma membranes like PS and PIP_2. Ca^{2+} binding domains have varying affinities to Ca^{2+} that provide distinct thresholds for different Ca^{2+} dependent cellular responses.

Cell activation often involves the influx of Ca^{2+} ions through the Ca^{2+} -release activated current (CRAC) channel. Activation of PLCs leads to the release of IP_3, which triggers rapid release of Ca^{2+} from the endoplasmic reticulum via IP_3 receptors. ER Ca^{2+} depletion causes the aggregation of ER STIM proteins that activate the PM Orai 1 CRAC channel. This is the basis for T cell Ca^{2+} influx following TCR stimulation and is essential for T cell activation (Clapham, 2007).

This section will provide an overview of some of the changes that occur to the cellular plasma membranes following Ca^{2+} influx, and highlight the important questions that remain unanswered.

1.3.1 Regulated Exocytosis

Exocytosis is the process by which intracellular membranes fuse with the plasma membrane. It is a ubiquitous activity across eukaryotic cells and can serve many diverse purposes. Secretory cells eject the contents of cytoplasmic vesicles into the extracellular environment via exocytosis whilst other cells use them to bring internal membrane and associated proteins to the cell surface to participate in signalling or to patch damaged plasma membrane. Both secretory and non-secretory exocytosis are highly regulated events and intense research has focused on understanding the protein machinery that orchestrates this important cellular function (Chieregatti and Meldolesi, 2005). The uniting feature of many types of regulated exocytosis, across cell types and species, is the trigger – calcium ions.

1.3.1.1 Secretory Exocytosis

Regulated secretion is a pathway for intercellular communication. The majority of exocytosis research has focused on its role in the brain. The basic functional unit of the brain is the neuronal synapse where communication between nerve cells occurs. There are over 1000 trillion of these synapses in a human brain. Depolarisation of the presynaptic neuron leads to the opening of voltage-gated Ca^{2+} channels on the presynaptic membrane. Ca^{2+} influx triggers the secretion of neurotransmitter into the synapse by exocytosis, leading to the opening of ligand-gated ion channels on

the postsynaptic plasma membrane, transferring the depolarising signal from one nerve cell to the other. Neurotransmitter release occurs on a millisecond time scale in a discrete area of the synapse, known as the active zone. Bernard Katz at UCL was the first to show that neurotransmitters were released in 'quanta' (Del Castillo and Katz, 1954; Fatt and Katz, 1952) and that these corresponded to the fusion of individual vesicles. He was awarded the Nobel Prize in 1970 for this discovery. One of Katz's post-doctoral fellows John Heuser went on to pioneer the technique of quick-freeze deep-etch electron microscopy which later allowed vesicular fusion to be visualised (Heuser et al., 1979).

Exocytosis in neurons is the key step in communicating signals between adjacent cells. More long-range communication in the brain is achieved by neurosecretory cells that exocytose dense-core vesicles (containing neuropeptides, hormones and neurotransmitters) uniformly into the pericellular space, which can have effects both on the brain and peripherally if they enter the blood stream (Chieregatti and Meldolesi, 2005). Non-excitatory cells of exocrine and endocrine glands undergo regulated secretory exocytosis, an example being the pancreatic acinar cells that secrete the hormone insulin.

Exocytosis by cells of the immune system is important to their ability to communicate and orchestrate an effective immune response. The release of cytokines, chemokines and effector molecules by different cell types, at specific times, following specific stimuli, is key in regulating an appropriate response to diverse pathogens. This can occur at short range in the immune synapse by T lymphocytes (discussed later), or in bulk for example by mast cells.

1.3.1.2 Non-secretory exocytosis

Non-secretory exocytosis can be separated into two main types – protein exposing and membrane expanding. Channels, transporters, pumps and receptors can all be brought to the plasma membrane following cell activation. For example, regulated expression of aquaporins on the surface of kidney duct cells occurs by exocytosis triggered by cAMP (Brown, 2003; Lorenz et al., 2003) a failure of which results in diabetes insipidus. In response to insulin, adipocytes and muscle cells translocate

GLUT4 transporter to their surface by exocytosis for glucose uptake, a failure of which leads to diabetes mellitus (Stöckli et al., 2011).

Non-secretory exocytosis can also be employed to expand the plasma membrane. This is important during phagocytosis when large amounts of plasma membrane are donated to the phagosome. This loss is compensated for by membrane exocytosis (Di et al., 2003; Holevinsky and Nelson, 1998). During the final stages of cell division there is exocytosis adjacent to the cleavage furrow that provides sufficient membrane for cytokinesis (Danilchik et al., 2003). Large exocytosis is also an important mechanism of cell membrane repair and is discussed in detail later.

1.3.1.3 Exocytosis machinery

The role of exocytosis machinery is to bring two membranes into close proximity, overcome the energy barrier to fusion posed by the electrostatic and elastic properties of the membranes, induce merger of the membrane bilayers and thus open a 'fusion pore' connecting the lumen of the vesicle with the extracellular space. All this must occur while maintaining the continuity of the plasma membrane.

The 2013 Nobel Prize in Physiology or Medicine was awarded to Randy Schekman, James Rothman and Thomas Südhof for their work on vesicle traffic and the machinery of exocytosis. Schekman screened for mutants in yeast (sec mutants) that displayed defective vesicular transport and consequently accumulated vesicles in different cellular compartments (Novick et al., 1980). Rothman meanwhile found and purified N-ethylmaleimide-sensitive factor (NSF) and soluble NSF-attachment protein (SNAP) through studies using a cell-free system that was able to mimic the movement of vesicles through the Golgi stack (Block et al., 1988; Malhotra et al., 1988). These proteins were necessary for vesicular fusion and later a collaboration showed that Schekman's *sec18* mutant corresponded to NSF (Wilson et al., 1989) and *sec17* to SNAP (Griff et al., 1992) demonstrating that the machinery for exocytosis is ancient and highly conserved. Rothman went on to discover more proteins, which he named soluble NSF-attachment protein receptors (SNAREs), that formed a complex necessary for fusion (Söllner et al., 1993).

Südhof was interested in how Ca^{2+} controlled vesicular exocytosis in the synapse and he demonstrated the role of synaptotagmin I as the Ca^{2+} sensor (Geppert et al., 1994; Perin et al., 1990). He also showed that the protein Munc 18-1 is necessary for vesicular fusion in neurons and that it corresponds to Schekman's *sec1* (Rizo and Südhof, 2012). Together the work of these three and many others has provided a model for vesicular fusion, although much is yet unknown. The model of SNARE machinery in neurons is detailed below.

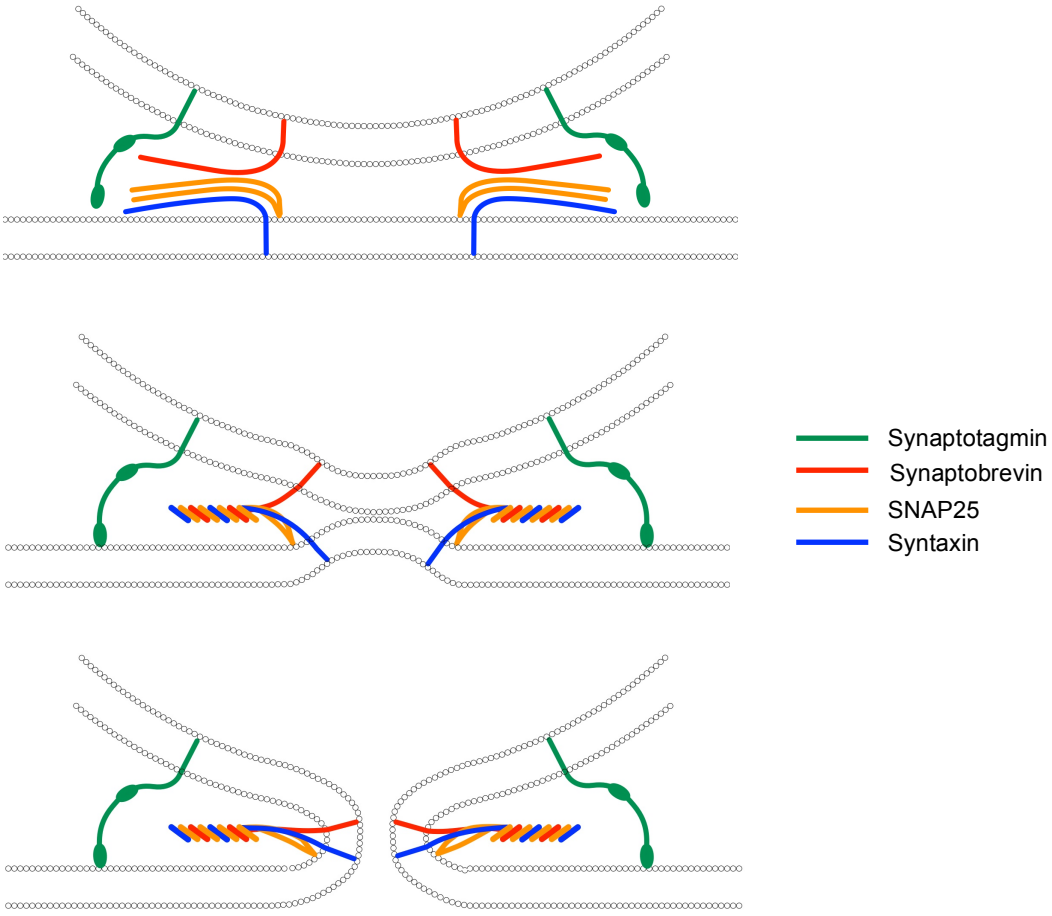

Figure 1.2 **SNARE machinery of exocytosis.**

The SNARE machinery (Figure 1.2) is made up of proteins with attachments to either the vesicular or plasma membrane. Synaptobrevin (or VAMP) is inserted on the vesicle membrane whilst SNAP25 and syntaxin are attached to the plasma membrane. These proteins have similar coiled-coil stretches known as SNARE motifs. SNAP25 contributes two of these SNARE motifs to the complex and is

attached to the plasma membrane by a palmitoylated linker rather than a transmembrane region. During the complex association, the four alpha helices form a tight bundle, known as zippering, that brings the membranes into close proximity.

The Ca^{2+} sensor for fusion, synaptotagmin, is present on the vesicle membrane and possesses two C2 domains. C2 domains are formed of B sandwiches that contain Ca^{2+} binding loops. These C2 domains are able to bind to phospholipids on the inner leaflet of the plasma membrane only once they are in complex with Ca^{2+}. It has also been found that the synaptotagmin C2 domains can also bind syntaxin (Jahn and Fasshauer, 2012).

The mechanism by which Ca^{2+} binding to synaptotagmins initiates the final steps of fusion is unclear. The accepted models either have synaptotagmins interacting with SNARE proteins or with the plasma membrane. In the former case, Ca^{2+} binding either releases a synaptotagmin clamp on fusion (Chicka et al., 2008), or does the opposite and displaces a clamp to SNARE-zippering and fusion (Yang et al., 2010). Alternatively, it might bind the membrane through the C2 domains, overcoming the energy barrier to fusion either by disrupting the phospholipids close to the fusion site (Stein et al., 2007), or by increasing the membrane curvature stress (Hui et al., 2009; Martens et al., 2007).

Botulinum toxin and tetanus toxin both act by cleaving components of the SNARE machinery. BotNT cleaves SNAP-25 whilst TeNT cleaves synaptobrevin (VAMP2). In both cases the inhibition of exocytosis in the brain is typically fatal. These toxins have provided valuable research tools for uncovering the roles of SNARE proteins in different exocytic events.

Though the SNARE-synaptotagmin model goes a long way to explaining exocytosis in neurons, this model does not account for a large range of Ca^{2+} activated fusion events occurring in cells. After deletion of multiple synaptotagmin isoforms, extensive Ca^{2+} activated exocytic processes still occur in classical secretory cells over seconds (Schonn et al., 2008), and Ca^{2+} activated exocytosis that doubles the surface membrane area in non-secretory cells is entirely unaffected by the deletion of synaptotagmins(Wang and Hilgemann, 2008). No other mechanisms for exocytosis have so far been proposed.

1.3.1.4 Exocytosis in T lymphocytes

Regulated exocytosis triggered by Ca^{2+} influx in T lymphocytes is crucial for their effector function. A key focal point for these events is the immune synapse. In this space the membranes of the lymphocyte and APC/target cell come into close contact and signals are sent and received both by transmembrane and secreted proteins. Polarised secretion of lytic granules by CD8+ CTLs is the primary mechanism of target-cell killing. These granules contain two major effector proteins – the pore-forming protein perforin that facilitates the entry of the other, granzyme, which in turn initiates apoptosis of the target cell (Stinchcombe and Griffiths, 2007).

Several SNARE proteins have been associated with lytic granule exocytosis although there is uncertainty about the exact machinery involved. Syntaxin 11 is strongly implicated as its congenital deficiency gives rise to familial hemophagocytic lymphohitiocytosis type 4 (FHL4) in which CTLs lose their cytotoxic function (zur Stadt et al., 2005). This may be due to defects in vesicular traffic upstream of lytic granule exocytosis (Valdez et al., 1999). However there is evidence of Syn11 accumulation at the immune synapse, co-localised with lytic granules, implying a direct role (Halimani et al., 2014). Knockdown of VAMP 7 and 8 does inhibit but does not block granule exocytosis (Loo et al., 2009; Marcet-Palacios et al., 2008). There is recent evidence that synaptobrevin 2 (VAMP2) may be the v-SNARE for lytic granule exocytosis in cytotoxic T cells, with both expression of tetanus toxin and knockdown of VAMP2 preventing lytic granule fusion (Matti et al., 2013).

Lytic granules are also known as secretory lysosomes; this is because their exocytosis is also associated with the expression of Lysosomal Associated Membrane Proteins 1 and 2 (LAMP 1/2)(Betts and Koup, 2004). These are not the only proteins to be trafficked to the synapse by non-secretory exocytosis. In Soares et. al. it was demonstrated that Lck, TCR-ζ chain and LAT are all trafficked to the immune synapse in vesicles and exocytosed in distinct nano-territories (Soares et al., 2013). This was shown to be important for TCR signalling and downstream Erk activation, CD69 expression and IL-2 and IFN-g production. The Ca^{2+} sensor for LAT and TCR-ζ chain vesicular fusion is Syn7 with knockdown leading to deficient T cell activation.

1.3.1.5 Cell Membrane Repair by Exocytosis

So far much of the regulated exocytosis discussed has involved small cargos exocytosed in a targeted manner into defined areas such as the immune or neuronal synapse in response to localised increases in Ca^{2+} through gated-channels. Another form of large, bulk exocytosis occurs following cell membrane injury when the cell is flooded with Ca^{2+}.

Plasma membrane injury can have rapid and catastrophic implications for the cell, so mechanisms are therefore in place for rapid resealing. Physiologically, certain cell types are constantly subject to mechanical disruptions of the plasma membrane, including skeletal muscle and fibroblasts. Other cell types are subject to the effects of pore forming toxins (McNeil and Kirchhausen, 2005). Ca^{2+} influx through the disrupted plasma membrane is the trigger for membrane resealing. Though necessary for repair, Ca^{2+} can also be highly toxic to cells, so speed of responses is crucial to cell survival. Membrane fusion events have been shown to be essential for the timely repair of plasma membranes. The Ca^{2+} threshold for this type of exocytosis is significantly higher than that needed for other forms of regulated exocytosis, in the range of 10-30μM or higher (Coorssen et al., 1996; Yaradanakul et al., 2008). This raises several important questions: how does exocytosis promote repair? What is the membrane lipid exocytosed? How is Ca^{2+} influx sensed? What is the machinery for cell repair by exocytosis?

It is widely accepted that the exocytosis of membranes serves to form a membrane patch that restores the continuity of the plasma membrane. It is also known that a decrease in membrane tension promotes membrane repair and that exocytosis of new membrane can facilitate this loss in tension (Togo et al., 2000). The patch hypothesis has been confirmed by multiple studies that have shown the accumulation of internal membranes at the site of disruption. The identity of these membranes is, however, a matter of controversy.

In 1995 it was discovered that lysosomal membranes localise and fuse to the site of *Trypanosoma cruzi* invasion (Andrews, 1995) and later the same group discovered that lysosomal fusion occurs at the site of plasma membrane injury in a Ca^{2+} dependent manner (Reddy et al., 2001). Cell injury was rapidly followed by the

appearance of lysosomal associated proteins on the plasma membrane, reinforcing this hypothesis. However subsequent work has found that normal membrane repair can occur in cells with defective lysosomal exocytosis, and in the presence of the small molecule vacuolin that blocks lysosomal exocytosis (Cerny et al., 2004). There is no current evidence that other organelles such as the endoplasmic reticulum or the Golgi donate membranes for repair. There has, however, emerged a new organelle named the "enlargesome" which may provide the source membrane. This poorly characterised pool of membranes is ubiquitous and can patch damaged plasma membrane in a Ca^{2+} dependent manner (Cerny et al., 2004; Cocucci et al., 2004). The requirement for lysosomes and enlargesomes for membrane repair in different cell types remains unclear.

A key question that arose following the discovery that lysosomes could fuse and repair damaged membranes was as to the identity of the Ca^{2+} sensor. Work from the original lysosomal repair group implicated synaptotagmin VII. Using blocking antibodies against SynVII, that were micro-injected into cells, lysosomal fusion and membrane repair could be inhibited (Andrews, 2002; Chakrabarti et al., 2003; Martinez et al., 2000). Subsequent SynVII knockout studies showed no inhibition of lysosomal fusion or membrane repair (Jaiswal et al., 2004; Wang and Hilgemann, 2008). SynIII blocking peptide has been shown to inhibit membrane repair in giant squid axons (Detrait et al., 2000), but no further follow-up studies have confirmed this in other cell types.

Following membrane damage, intracellular Ca^{2+} levels may reach levels sufficient for direct binding of Ca^{2+} to anionic phospholipids on the inner leaflet of the membrane. High Ca^{2+} has been found to induce fusion of artificial membrane vesicles (Wilschut et al., 1981). However, magnesium is not able to induce membrane repair responses despite binding to anionic lipids with equal affinity (Steinhardt et al., 1994).

As discussed above, the protein complex necessary for regulated exocytosis in many cell types is the SNARE machinery. Tetanus toxin blocks cell repair in 3T3 cell (Togo et al., 1999) and sea urchin eggs (Bi et al., 1995) indicating that at least synaptobrevin is important in exocytosis based repair, but no further work has identified which SNARE proteins are involved (for example by knockout studies) or

shown consistency across cell types. A new class of proteins that may be important in the fusion machinery is the dysferlins. Dysferlin localises to sites of membrane injury and dysferlin-null mice show defects in membrane repair (Bansal et al., 2003). Moreover, lack of dysferlin in humans leads to a profound muscular dystrophy that is thought to be due to defective muscular repair (Liu et al., 1998). However no role for dysferlins in regulated exocytosis has yet been demonstrated. Other proteins implicated in repair are the Ca^{2+} dependent membrane binding proteins annexins, but despite observed binding of annexins to sites of membrane damage, no functional role or link to exocytosis has been shown (McNeil and Kirchhausen, 2005).

Despite considerable work directed towards understanding the mechanisms and protein players involved in membrane repair by exocytosis, few answers have emerged. Research so far has failed to demonstrate consistently that either lysosomal membranes or SynVII are necessary for plasma membrane repair or to uncover alternative mechanisms for Ca^{2+} sensing. Contradictory studies demonstrate that this process may be more complex than initially thought and that answers may lie outside the existing paradigms of the proteins and membranes thought to be involved.

1.3.2 Endocytosis

Endocytosis is the process by which areas of surface plasma membrane, with associated transmembrane proteins or extracellular cargos, are taken inside the cell. This can rapidly change the way in which cells interact with their environment by remodelling the array of functional proteins able to signal across the membrane. This is especially important in lymphocytes whose function is to detect and respond appropriately to extracellular signals transmitted by other cells. Endocytosis can be highly selective, with mechanisms initiated by single transmembrane proteins, or non-selective, with large areas of membrane internalised, as in the case of phagocytosis and macropinocytosis.

For endocytosis to occur the plasma membrane must curve inwards to the point at which it can be split and resealed, a process known as fission, thereby detaching the newly formed endocytic vesicle from the plasma membrane. There are multiple forms of endocytosis employed by different cells with many mechanisms that carry out curvature and fission.

A classical and extensively researched form is clathrin-mediated endocytosis in which protein adapters coordinate the polymerisation of clathrin into a curved basket structure. Once the membrane has been curved sufficiently to produce a constricted neck, the protein GTPase dynamin completes membrane fission. The primary adapter for clathrin-mediated endocytosis is adapter protein-2 (AP2) that binds to specific di-leucine or tyrosine-based motifs on the intracellular domains of transmembrane receptors.

1.3.2.1 Ca^{2+} and endocytosis

Many studies have shown that raised intracellular Ca^{2+} is linked to the rapid internalisation of membrane. This endocytosis results in the generation of large non-acidified intracellular vesicles, and has been described as ‘massive’, ‘excessive’ and ‘bulk’. Though these studies agree on the extent and speed of membrane intake, they differ on the machinery involved. Some have found dynamins are necessary (Clayton and Cousin, 2009), others found it to act independently of clarthrin

(Thomas et al., 1994), and Larricia et al. found it to be independent of all classical endocytic machinery (Lariccia et al., 2011). What is clear is that this Ca^{2+} induced endocytosis is very different to other forms of endocytosis and warrants further investigation.

The Ca^{2+} threshold and mechanism of Ca^{2+} entry is likely to be key to understanding the role of this endocytosis. In Oocytes endocytosis can be triggered following influx through Ca^{2+} channels (Vogel et al., 1999), but in most cell types the Ca^{2+} threshold for endocytosis is high, suggesting a role in cell membrane repair. Indeed Idone et al. observe that a rapid Ca^{2+} activated endocytosis is necessary for membrane repair of SLO toxin pores in NRK cells (Idone et al., 2008).

As described earlier, exocytosis has been shown to be a general mechanism for membrane repair where internal membranes are used to patch wounds. Lariccia et al. found exocytosis to precede large Ca^{2+} induced endocytosis in BHK and HEK293 cells. This was an observation also made by Tam et al. who then proposed that exocytosis was necessary for subsequent endocytosis (Tam et al., 2010). They presented evidence that lysosomal exocytosis secreted acid sphingomyelinases onto the outer leaftlet of the plasma membrane. These enzymes break down sphingomyelin to ceramide and phosphitidylcholine. Production of ceramide domains on one leaflet of the membrane causes inward membrane curvature, budding and fission of artificial membrane liposomes (Bollinger et al., 2005; Goñi and Alonso, 2009; Holopainen et al., 2000).

This was an attractive model, uniting exocytosis and endocytosis and providing a mechanism that is independent of internal protein machinery. However subsequent work by the Hilgemann lab has cast this model into question. Lariccia et al. found that endocytosis could indeed be induced by the extracellular application of SMases, but that this was not linked to Ca^{2+} activated endocytosis. Firstly, endocytosis was unaffected by application of high concentrations of the SMase inhibitor desipramine (reported to be effective in Tam et al.). Secondly, exocytosis and endocytosis could be uncoupled completely by addition of intracellular polyamines. Both these findings are incompatible with the idea that endocytosis is triggered by secreted acid sphingomyelinases. No further lines of evidence have emerged to support the

hypothesis proposed by Tam et al. but no alternative models have been proposed either.

Larricia et al. describe a form of Ca^{2+} activated endocytosis they call 'Massive endocytosis' (MEND) which was demonstrated in BHK and HEK293 as well as in mouse myocytes. The Hilgemann lab are able to track membrane movements in real-time using measurements of cell capacitance via whole cell patch clamp. As well as being a very accurate method for measuring exocytosis and endocytosis, this technique also provides access to the cytoplasm of the cell, allowing for the use of cell-impermeable proteins and inhibitors that facilitate the manipulation of multiple signalling pathways. MEND comes in both immediate (fast) and delayed forms. The mechanism for the 'delayed' form of MEND involves the palmitoylation of surface proteins by DHHC5, following release of CoA from mitochondria (Hilgemann et al., 2013).

In fast MEND, up to 50% of the plasma membrane can be taken up in a matter of seconds. Lariccia et al. directed a lot of effort towards understanding which proteins were involved in both Ca^{2+} sensing and endocytosis, and what was remarkable is that they found no answers. Fast MEND is independent of ATP, GTP, actin, microtubules, dynamin, clathrin, calmodulin, Ca^{2+} activated phosphatases and proteases. Having been unable to implicate any classical structural or adapter proteins in the mechanism, they next looked to constituents of the plasma membrane. PIP2 was an attractive candidate as it is a substrate for adapters and G proteins that possess PH domains but also there was evidence that reagents affecting membrane composition such as cholesterol loading or depletion had an effect on endocytosis. Unfortunately PIP2 depletion was unable to block fast endocytosis. Parallel work in Fine et al. found that the application, or application and then washing, of amphipaths on the outer leaflet of the plasma membrane led to rapid MEND (Fine et al., 2011). This presented the possibility that Ca^{2+} activated MEND was triggered by rapid changes in plasma membrane composition with generation of new lipids causing membrane curvature. The only positive result in this direction was the potent inhibition of MEND by the phospholipase (PLA2) inhibitor BEL. Perhaps Ca^{2+} activation of PLA2 induces endocytosis in a similar way to internally applied lysolipids. As BEL is a

reasonably non-specific reagent, further work will be necessary, involving knockdown studies of phospholipases, in order to further investigate this hypothesis.

1.3.3 Microvesicles

It was previously thought that cells communicated only by secreted factors or through the interactions of plasma membrane-bound proteins. However, a new form of intercellular communication has become the focus of much research in recent years. It is now known that cells can release portions of their plasma and internal membranes as vesicles, bearing protein messengers. These vesicles come in a variety of sizes and are formed by different mechanisms. Microvesicles are sized up to 1μm and are shed directly from the plasma membrane, whilst exosomes are less than 200nm in size and are released via the exocytosis of multi-vesicular bodies (MVB) in which they are produced. Exosomes will not be discussed in detail here but instead the focus will be on the lesser-characterised plasma membrane-derived microvesicles.

As the study of these novel signalling effectors is still at an early stage, with many labs characterising them in different cell types, microvesicles have been christened with many names: ectosomes (Lee et al., 1993), microparticles (Cauwenberghs et al., 2006) and shedding bodies (Cocucci et al., 2007) to name a few. They play a diverse role in many biological processes from blood coagulation to signalling in the brain. The specific study of microvesicles has proved challenging, as discriminating between microvesicles and exosomes in cellular supernatants is problematic. Nevertheless insights are emerging as to how they are produced and which proteins are sorted with them.

1.3.3.1 Biogenesis

Microvesicles derive from plasma membrane protrusions that have detached by fission. This process is poorly understood but has been linked to cell activation, and more specifically to increases in intracellular Ca^{2+}. In multiple cell types, activation

of purinergic receptors or treatment with Ca^{2+} ionophores is quickly followed by extensive release of microvesicles (Heijnen et al., 1999; MacKenzie et al., 2001). Others have implicated protein kinase C activation (Pilzer et al., 2005) and recently the ESCRT machinery in microvesicle production (discussed later).

Inherent in the process of microvesicle release is the loss of plasma membrane from the cell. This might be compensated for by compensatory exocytosis of internal membranes (Cocucci et al., 2007). The relationship between exocytosis and vesicle release is unclear. Whether one is necessary for the other or whether one precedes the other is unknown. One consistent observation, with special relevance to this study, is a delay of seconds to minutes between the onset of Ca^{2+} influx and microvesicle release (Cocucci et al., 2007; Lee et al., 1993; MacKenzie et al., 2001; Moskovich and Fishelson, 2007; Stein and Luzio, 1991). It has been hypothesised that this delay may be due to the need for preceding exocytosis (Cocucci et al., 2009).

1.3.3.2 Protein sorting

As microvesicles play an important role in cellular communication it is important to understand which proteins are sorted onto their membranes. It has been demonstrated that specific molecules are both included and excluded in released microvesicle membranes with a variety of microscopic techniques (Cocucci et al., 2007; Moskovich and Fishelson, 2007). Some studies have implicated membrane-intrinsic factors in this sorting of proteins as the disruption of cholesterol metabolism has been found to have an impact on protein inclusion, suggesting the role of lipid domains (Del Conde et al., 2005; Stein and Luzio, 1991). The role of exocytosis is also an important factor in this sorting as microvesicles have also been found to be enriched in exocytic proteins such as annexins and desmoyokin whilst plasma membrane proteins such as Ka/K/ ATPase are excluded (Cocucci et al., 2007).

1.3.3.3 Physiological roles

Microvesicles are shed from the surface of activated platelets following contact with collagen. These vesicles are thought to provide a surface upon which different stages of the clotting cascade can initiate (Sims et al., 1988).

Microvesicles have been implicated in both pro-inflammatory and anti-inflammatory responses and have been linked to inflammatory diseases including arthritis (Distler et al., 2005; Köppler et al., 2006). Inflammatory mediators can be located both in vesicle membranes and contained within shed in vesicles. Microvesicles have been found to constitute a novel secretory pathway, for example in the case of interleukin-1β, which cannot be secreted as it lacks the relevant secretory leader sequences. MacKenzie and colleagues found that IL-1β was contained within the lumen of shed microvesicles that were released following Ca^{2+} influx through purinergic receptors, stimulated by ATP. This secretory pathway operates by release of protein containing vesicles rather than direct secretion.

Microvesicles are highly enriched in the tumour microenvironment and have been found to play a number of roles. These vesicles can be coated in matrix proteases that can digest the extracellular matrix, aiding metastasis and angiogeneisis (Ginestra et al., 1998; Giusti et al., 2008; Mochizuki and Okada, 2007). Vesicles can also absorb chemotherapeutic drugs, diluting the drugs' ability to directly target cancer cells (Shedden et al., 2003). Lastly there is evidence that FasL bearing tumour-derived microvesicles can inhibit TILs, suppressing anti-tumour immune responses (Albanese et al., 1998; Kim et al., 2005).

1.3.3.4 Microvesicles at antigen presentation

As discussed previously, the immune synapse is the site at which T cells and APCs exchange and integrate signals that dictate the magnitude and characteristics of the following adaptive immune response. Recent work by Choudhuri and colleagues has changed the way in which we view the immune synapse (Choudhuri et al., 2014). It had previously been observed that a diffusion barrier exists at the centre of the immune synapse where TCRs and cytoplasm seem confined (Varma et al., 2006).

This is in contrast to the borders of the synapse where protein movement is highly dynamic. In elegant work using planar bilayers that reconstitute APC membranes the authors imaged the immune synapse using a combination of transmission electron microscopy and TIRF microscopy. In this way they constructed a three-dimensional model of the synapse and found a centrally located cavity in which TCR-enriched microvesicles were formed in an antigen-dependent manner. These microvesicles were fully detached from the plasma membrane and served to explain the diffusion barrier that existed at the IS centre. Interestingly the majority of these vesicles remained on the planar bilayer after the termination of antigen presentation. These remaining vesicles were able to induce Ca^{2+} signalling via TCR-pMHC in primary B-cells. The authors next sought to understand the mechanism underlying microvesicle release in the synapse. They looked to the endosomal ESCRT protein complex known to cause budding and scission of vesicles into MVBs and viral particles from the cell membrane. They found that the ESCRT-I protein TSG101 is necessary for TCR enrichment into microvesicles and that the ESCRT-III protein VSP4 was necessary for vesicle scission. Questions remain as to how these proteins are recruited to the immune synapse and what factors drive membrane protrusion.

In this way, vesicles may serve to regulate the two-way nature of antigen presentation in the IS. TCR downregulation, through sequestering receptors into microvesicles rather than by internalisation, might serve to terminate TCR signalling, whilst vesicle TCR-pMHC signalling persists. This could provide a form of T cell help – reinforcing B cell activity directed at a common target whilst limiting TCR signalling. The insights gained into the mechanism underlying vesicle formation provide clear avenues for future work directed towards understanding how vesicle release is important in regulating outcomes after antigen presentation.

1.3.3.5 Cell membrane repair

Patching of damaged membrane by exocytosis was discussed earlier, but another form of protective pathway exists. It has been demonstrated that pore-forming toxins induce budding and release of membrane microvesicles; presumably in order

to quickly remove small patches of damaged membrane(Atanassoff et al., 2014; Babiychuk et al., 2009; Keyel et al., 2011). Given this, Jimenez et al investigated the role of the ESCRT machinery in this process(Jimenez et al., 2014). They found a co-localisation of the ESCRT protein CHMP proteins and ALIX at the sites of cell injury just preceding cell repair, and that this occurred in a Ca^{2+} dependent manner. Knockdown studies confirmed the role of these proteins in the rapid repair of small membrane holes. They also found that ESCRT recruitment to sites of damage was ATP independent, but microvesicle shedding was not.

A key question that arises is as to the mechanism of Ca^{2+} dependent ESCRT recruitment to the plasma membrane. This has generally only been seen when ESCRT-III is overexpressed, lacks inhibitory domains or in the case of viral budding(Bodon et al., 2011; Hanson et al., 2008). It remains possible that exocytosis of endosomal membranes bearing ESCRT machinery could be involved in recruitment. The ESCRT component ALIX is localised to endosomes owing to a LBPA-binding domain. This phospholipid is found on endosomes but not on the plasma membrane. Their data ALIX can bind the plasma membrane suggests that either ALIX is able to bind other plasma membrane phospholipids, or that LBPA appears at sites of plasma membrane damage. Could this then be due to membrane exocytosis? The authors think not for two reasons. Firstly, because co-staining of endosomal and lysosomal markers LBPA, Lamp1 and EEA1 with ESCRT protein CHMP4 showed no co-localisation at sites of membrane injury, and secondly because the recruitment was energy independent. Recent work also implicates the EF-hand containing ALG-2 in the Ca^{2+} dependent accumulation of the ESCRT complex at sites of injury (Scheffer et al., 2014). Recruitment of soluble ESCRT-III proteins may therefore be a plausible alternative to vesicular transport. It should however be noted that in the absence of clarity surrounding the internal membranes or protein machinery (whether ATP dependent or independent) involved in exocytic membrane repair, vesicular transport may not be rejected as a possible mechanism for ESCRT-III recruitment to the plasma membrane.

1.3.4 Phospholipid Scrambling

1.3.4.1 Plasma Membrane Phospholipid Structure and Distribution

Segregation, concentration and compartmentalisation are necessities of living cells. Life cannot occur without a barrier to enclose, protect and define biochemical reactions. The 30Å thick membranes that provide these boundaries are complex structures composed mainly of lipids on which proteins can be organised.

The plasma membrane is composed of amphipathic phospholipids that form a continuous bilayer, defining the cell boundaries and providing a diffusion barrier. Proteins are able to move, cluster and be organised in membrane territories. Membrane lipids can themselves act as signalling messengers, with changes in plasma membrane phospholipid distribution providing apoptotic 'eat me' signals (Miyanishi et al., 2007; Park et al., 2007) and surface to initiate coagulation.

The plasma membrane is composed mainly of the glycerophospholipids: Phophatidylcholine (PC), Phosphatidylethanolamine (PE), and Phosphatidylserine (PS), which have diacylglycerol (DAG) backbones, and Sphingomyelin (SM) which has a ceramide backbone. Phosphatidylinositides are also present at low concentrations that serve as important signalling molecules in different phosphorylation states. Cholesterol provides important stability and flexibility to the membrane and forms high-density domains in complex with sphingolipids (van Meer et al., 2008).

A striking feature of the plasma membrane phospholipids is their asymmetric distribution across outer and inner monolayer. PC and SM are found mostly on the outer monolayer and PS and PE on the inner. This is maintained by ATP dependent flippases and floppases that pump phospholipids to their respective leaflet. The 'flippase' protein responsible for translocating PS and PE to the inner monolayer is ATP11C and is well characterised whereas the identity of the 'floppase' is unknown (Paulusma and Elferink, 2010).

From studies on model membranes, it is believed that spontaneous movement of phospholipids from one leaflet to the other is very slow – taking from hours to days

(Pomorski and Menon, 2006). Under certain physiological conditions, very rapid 'scrambling' of membrane phospholipids occurs.

1.3.4.2 Functions of Phospholipid Scrambling

It was discovered in 1992 that PS appearance on the outer leaflet of the plasma membrane is a hallmark of apoptotic cells. The PS binding protein Annexin V is therefore widely used as a maker of cell death. It has also been found that PS exposure can be non-apoptotic in B cells, platelets, macrophages, skeletal muscle cells, red blood cells, sperm cell capacitation mast cells, and T lymphocytes, a process linked to Ca^{2+} influx and cell activation (Bevers and Williamson, 2010; Fischer et al., 2006).

Functionally, membrane scrambling during apoptosis is thought to tag dead cells with an 'eat-me' signal, helping phagocytes to recognise and clear dead cells (Miyanishi et al., 2007; Park et al., 2007). Non-apoptotic functions of PS exposure are best characterised in the platelet, where membrane PS serves as binding sites for clotting factors. In erythrocytes it is thought to promote adhesion to endothelial cells (Manodori et al., 2000) and in muscle development aid myotube formation(van den Eijnde et al., 2001). In immune cells it has been linked to mast cell degranulation (Demo et al., 1999), and microvesicle shedding in both T lymphocytes and macrophages (Elliott et al., 2005; MacKenzie et al., 2001). It is unclear whether scrambling is a cause or consequence of these processes.

Elliot et al. were the first to notice non-apoptotic PS exposure in T lymphocytes, on a subset of activated memory CD4+ mouse T cells (Elliot Nat cell biology 2005). They found an inverse correlation between PS exposure and CD45 expression as well as purinergic P2X7 receptor activity. There was an association also with CD62L shedding in microvesicles. Furthermore PS exposure caused both a reversal in multidrug transporter P-glycoprotein and supported cell migration. The authors concluded that these wide-ranging effects of PS distribution constituted a novel signalling modality in T lymphocytes.

Independent work by Fischer et al demonstrated that PS exposure occurred in Melan-A-specific human T cells when activated with antigen or antiCD3CD28

antibodies. This exposure was rapid, not associated with apoptosis and reversible over three days following activation. Interestingly, following imaging studies on the activated primary T cells, the authors found the distribution of PS was non-homogenous and appeared in patches. These patches were colocalised to lipid rafts when cells were stimulated with anti-CD3CD28. When imaging CTLs in association with antigen-loaded T2 cells, they found PS exposure was restricted to the immune synapse. Further work is needed to confirm and clarify the roles of membrane scrambling in T lymphocyte biology. It will be important to establish whether membrane scrambling is itself functional or whether it is a consequence of other processes occurring at the plasma membrane.

Without an understanding of the identity of the protein responsible for scrambling, further insights into the physiological significance of PS exposure in other tissues were not forthcoming.

1.3.4.3 The Search for a Scramblase

With the discovery that normal asymmetric phospholipid redistribution on the plasma membrane can be rapidly scrambled in the response to certain stimuli, the search began for a protein responsible. Work in this area had a confused beginning as initially it was unclear whether there was one or several scramblases. The first protein to be isolated and cloned from a fraction of platelet and red blood cell lysate that scrambled membranes in reconstitution experiments was named Phospholipid Scramblase 1 (PLSCR1). Cell scrambling seemed to correlate well with mRNA and protein levels in different cell types (Zhao et al., 1998; Zhou et al., 1997) and expression of PLSCR1 in low-scrambling cells seemed to activate scrambling(Zhao et al., 1998). However later knockout and knockdown studies showed no impact on scrambling, indicating that the wrongly named PLSCR1 is not the membrane scramblase (Fadeel et al., 1999; Zhou et al., 2000). Other proteins - ABC1 (Hamon et al., 2000) and Tat-1 (Züllig et al., 2007) have been implicated but that implication later disputed. The Ca^{2+} threshold for scrambling is reasonably high at around Ca^{2+} 25-100μM (Williamson et al., 2001; Woon et al., 1999).

Work on cells from patients with Scott Syndrome (discussed below), which do not scramble their membranes in response to Ca^{2+}, showed that apoptotic scrambling was maintained whilst Ca^{2+}-induced was abolished (Williamson et al., 2001). This suggested that there are two scramblases, one Ca^{2+} and one apoptosis induced. Work in the last five years has confirmed this assertion by identifying the 'scramblases' involved.

1.3.4.4 TMEM16F

In 1979 a case report was published describing a severe bleeding disorder in a 34-year-old woman named Mrs MA Scott. The authors speculated that this was due to a deficiency in factor Xa binding sites on platelets (Weiss et al., 1979). In 1985 it was found that these binding sites were phosphatidylserine molecules on the outer leaflet of activated platelet cell membranes (Rosing et al., 1985). Ca^{2+} activated translocation of phosphatidylserine from the inner to the outer leaflet of the plasma membrane is seen in the majority of cell types and is known as membrane scrambling. The search for the protein responsible has been a focus of much research since.

In 2010 Suzuki and colleagues adopted a methodical approach to identifying the Ca^{2+} activated scramblase (Suzuki et al., 2010). Using multiple rounds of cell sorting they were able to isolate a clone of Ba/F3 cells that had constitutively scrambled membranes with low Ca^{2+} activation. They then constructed a cDNA library from that clone and transformed the cDNA back into the parental Ba/F3 cell line. They then sorted transformed cells that now constitutively scrambled their membranes and by sequencing the introduced cDNA identified TMEM16F as the gene responsible. An A-G nucleotide mutation caused a mutation (D409G) in TMEM16F which confers constitutive scrambling capacity. The authors went on to sequence the TMEM16F gene in immortalised B-cell from a patient with Scott syndrome as well as the patient's parents. They found a homozygous G-to-T mutation at the splice-accepter site in intron 12 in the patient and the heterozygous mutation in both parents' genes. Analysis of the patient TMEM16F mRNA demonstrated that Exon 13 was skipped in the transcripts, causing a frame shift that resulted in premature

termination at exon 14. Subsequent studies by other groups have since confirmed that mutations in TMEM16F are the cause of Scott syndrome (Castoldi et al., 2011). Attention then turned to the phenotype of the knockout mouse. These mice indeed have a clotting disorder very similar to that of Scott syndrome, with increased bleeding time and impaired thrombus formation (Yang et al., 2012). In addition these mice have impaired bone mineralisation, a phenotype not present in patients with Scott syndrome, and potentially more subtle phenotypes yet to be identified. Remarkably researchers had correctly predicted that the location of the 'scramblase' gene would be on chromosome 12 earlier in 2010. An inbred strain of German shepherd dogs possess a clotting and scrambling defect identical to Scott Syndrome and genome-wide studies had revealed causative defect of the canine Ch27, equivalent to human chromosome 12 (Brooks et al., 2010; Brooks et al., 2002).

TMEM16F is a member of the anoctamin family of Ca^{2+} activated ion channels. Every member possesses eight transmembrane domains. TMEM16A and B are Ca^{2+} activated chloride channels. It was thought that the whole family were anion channels hence the name Ano- (anion) –octamin (eight transmembrane domains) but this has slowly come into question, hence the reversion to the TMEM16 name. A striking feature of the family is the wide variation in Ca^{2+} sensitivity and the unconventional site of Ca^{2+} sensing. None of the family possesses classical Ca^{2+} binding domains but the family thought to bind Ca^{2+} with motifs in one of their membrane spanning domains.

There are conflicting reports concerning the function of TMEM16F as an ion channel. Different groups have reported it as a Ca^{2+} activated chloride channel (Tian et al., 2012), a volume activated chloride channel (Almaça et al., 2009), and others as a hyperpolarisation activated chloride channel (Martins et al., 2011). TMEM16F has been demonstrated to be a delayed activation channel in multiple studies (Grubb et al., 2013; Kim et al., 2015). This means that the channel can delay activation even having reached its Ca^{2+} threshold for firing – a delay that decreases with increasing intracellular Ca^{2+}.

Yang et al carried out considerable work directed towards resolving the issue of ion conduction by TMEM16F. Surprisingly they found TMEM16F to be a non-selective

cation channel capable of conducting large ions including Ca^{2+}. The authors concluded that the channel resembled a large 6Å pore able to non-selectively conduct cations when activated by Ca^{2+}. They found that in multiple cell lines, including HEK293 cells, heterologous expression of TMEM16F was not able to induce Ca^{2+} activated phospholipid scrambling – a result also found by Suzuki et al. The authors concluded that the channel is necessary but not sufficient for membrane scrambling and that it is the cation current induced by TMEM16F that operates alongside an unknown scramblase. The findings that supported this hypothesis were that megakaryocytes (precursors to platelets) possessed a Ca^{2+} activated cation current similar to that of TMEM16F and that the D409G mutation had a significant impact on the thresholds of the ion current.

Other groups however have drawn different conclusions. Some have shown that heterologous expression of TMEM16F is capable of enhancing phospholipid scrambling, arguing for direct scrambling by TMEM16F (Yu et al., 2015), and others have found that TMEM16F induced ion currents and phospholipid scrambling could be separated (Kmit et al., 2013) using channel inhibitors, whereas another study showed that channel blockers could inhibit phospholipid scrambling (Taylor et al., 2008b).

With many conflicting and incompatible findings and conclusions being made by multiple groups adopting different approaches, the need for some structural insights was clear. This came at the end of 2014 when Brunner and colleagues published the crystal structure of an ancestral TMEM16F from *Nectria haematococca* (Brunner et al., 2014). Firstly, having purified large amounts of protein, the authors used a liposome-based assay to assess the ability of the protein to translocate phospholipids. They demonstrated that there was phospholipid translocation in liposome that bore nhTMEM16 and that this was non-selective to phospholipids and enhanced by the addition of Ca^{2+}. This was backed up by work carried out by Malvezzi and colleagues who had reconstituted TMEM protein from *Aspergillus fumigatus* and reported similar results in liposome-based assays (Malvezzi et al., 2013). They also were able to detect non-selective anion and cation currents in afTMEM containing vesicles.

Brunner et al next solved the crystal structure and found there to be a hydrophilic cleft that the authors concluded might be capable of translocating phospholipids as well as conducting ions. Yu et al. were also able to afford TMEM16A with scrambling capacity by transferring this domain from TMEM16F. These lines of evidence point towards the fact that TMEM16 is indeed a protein with the dual ability to conduct ions and phospholipids mediated through a protein intrinsic domain.

There are however a number of factors to consider that add uncertainty to these conclusions. Firstly, it was found that considerable scrambling could occur even in the absence of Ca^{2+} in liposomes containing the ancestral TMEM proteins. Other proteins have previously been implicated as phospholipid scramblases using similar cell-free reconstitution assays (Acharya et al., 2006; Bevers and Williamson, 2010; Fadeel and Xue, 2009; Ory et al., 2013). This calls into question the validity of a liposome based assay as a surrogate for the plasma membrane. Also experiments directed towards characterising the ion conduction through afTMEM16 may be unreliable as the channel activity was shown to be very low. Although the hypothesis that a hydrophilic cleft is able to translocate phospholipid is compelling no direct evidence of this exists beyond reconstitution assays. Finally conclusions drawn from fungal homologues may not be transferable to mammalian or indeed human TMEM16F.

1.3.4.5 An Alternative Model to a 'Scramblase'

Though the popular model for membrane scrambling is the activation of a protein 'scramblase', work by a number of labs has suggested an alternative hypothesis.

It has long been observed that mast cells expose PS following exocytosis of their granules. This degranulation is triggered by Ca^{2+} influx so may just be concurrent activation of a protein scramblase. However, studies have shown that PS exposure (measured by AnxV binding) appears in distinct punctae on the plasma membrane, which coincide with sites of vesicle fusion (Demo et al., 1999). The link is so strong that AnXV binding is even used as a read out for mast cell degranulation by many labs (Martin et al., 2000).

Given that Ca^{2+} influx is known to cause both membrane scrambling and trigger cell repair by the exocytosis of lysosomes (or other internal membranes), Mirnikjoo and colleagues investigated the possibility that the two events were linked. The authors loaded cells with Rhodamine conjugated PE at 37°C until it was internalised into endosomal membranes, then the PM was washed of Rhod-PE and cells treated with Ca^{2+} ionophore. What they found was a rapid redistribution of the fluorescent lipid back to the plasma membrane and concurrent membrane scrambling. They observed the same phenomenon when triggering apoptosis in the cells using STS. Furthermore they could block both membrane scrambling and Rho-PE redistribution using the lysosomotropic chloroquine. This suggested that fusion of internal membranes with the plasma membrane was the origin of scrambled membrane. The authors concluded that membrane scrambling constituted a suicidal 'pseudo-membrane repair' mechanism.

Follow-up work to this study was carried out by Lee et al., prompted by the observation that some cells scramble their membranes more than others (Lee et al., 2013). Having gathered cell lines with both high and low membrane scrambling in response to Ca^{2+} ionophore and apoptosis the authors asked some simple questions. Do cells that scramble their membrane contain more phosphatidylserine? They carried out total cell AnxV staining and found no difference. Do some cells contain intrinsic scramblase inhibitors? Fusing T98G cells that do not scramble with Jurkat cells that do did not inhibit membrane scrambling. Can overexpression of TMEM16F convert the phenotype? Overexpression of TMEM16F did nothing. Further work carried out in the paper implicated the fusion of internal membrane vesicles with the PM as the trigger for PS exposure. This study will be reviewed in further detail and has relevance to Chapter 5 as the internal membranes implicated were a pool that only appear during apoptosis. These two studies are however not entirely in agreement. Lee et al found no decrease in lysosomal bulk or inhibition of PS exposure by chloroquine.

Taken together, though the model of a protein 'scramblase' is generally accepted and recent work has even suggested there to be a 'scrambling domain' in the structure of TMEM16F that may be the active site for phospholipid translocation,

certain factors in the model do not make sense. An alternative hypothesis that the fusion of internal membranes is the trigger linked to PM scrambling has recently been proposed. This also raises many questions such as: what is the machinery for this exocytosis? How is it linked to TMEM16F? How does membrane fusion cause membrane scrambling? How do red blood cells, that have no internal membranes, still scramble membranes? Further work is needed to reconcile these opposing models.

CHAPTER 2

MATERIALS AND METHODS

2.1 Materials

2.1.1 Buffers and Reagents

Table 2.1 Buffers and Gels

Buffers	**Recipe**
Phosphate Buffered Saline (PBS)	137 mM NaCl 2 mM KCl 10 mM Sodium Hydrogen Phosphate 2 mM Potassium Hydrogen Phosphate
Blocking Buffer	PBS 10% Goat Serum
LB Broth	10% NaCl 1% bacto-trptone 0.5% bacto-yeast extract
LB Agar	LB Broth w/bacto-agar 15g/L
Agarose Gel	1% Agrose 1X TAE Buffer 5ug/ml Ethidium Bromide
Tris -acetate EDTA (TAE Buffer)	40 mM Tris HCl 1 mM EDTA 20 mM Sodium Acetate
Transformation Buffer (TBF)-I	100 mM rubidium chloride 50 mM magnesium chloride 30 mM potassium acetate 10 mM calcium chloride 15% glycerol to pH 5.5 with acetic acid
TBF-II	75 mM calcium chloride 10 mM MOPS 10 mM rubidium chloride 15% glycerol to pH 6.5 with KOH

Table 2.2 Solutions for Electrophysiology

Buffers	pH	Recipe
Standard Ringer Solution	7	145 mM NaCl 10 mM HEPES 2 mM $CaCl_2$ 2 mM $MgCl_2$
Standard Cytoplasmic Solution (KCl)	7.4	145 mM KCl 10 mM HEPES 0.5 mM EGTA 0.25 mM $CaCl_2$ 8 mM MgATP 2 mM Tris ATP 0.2 mM GTP
NMDG Aspartate *when intracellular* *when extracellular*	7	145 mM N-Methyl-D-glucamin 145 mM Aspartic Acid 10 mM HEPES + 8 mM MgATP + 2 mM Tris ATP + 0.2 mM GTP + 2 mM $CaCl_2$ + $MgCl_2$
Sucrose Solution *when intracellular* *when extracellular*	7	240 mM sucrose 5 mM KCl + 8 mM MgATP + 2 mM Tris ATP + 0.2 mM GTP + 2 mM $CaCl_2$ +2 mM $MgCl_2$
NCX1 Cytoplasmic	7	80 mM LiOH 20 mM TEA-OH 15 mM HEPES 40 mM NaOH 0.5 mM $MgCl_2$ 0.5 mM EGTA 0.25 mM CaCl2 to pH with aspartate
NCX1 Extracellular	7	120 mM LiOH 4 mM $MgCl_2$ or 4 mM $CaCl_2$ 20 mM TEA-OH 10 mM HEPES 0.5 mM EGTA to pH with aspartate

Table 2.3 Reagents, Dyes and Proteins

Reagent	Conc.	Manufacturer
Ionomycin Free Acid	2-20 µM	Carbiochem
Tetanus Toxin L-chain	400 nM	Alpha Universe LLC
Latrunculin A	3 µM	Sigma-Aldrich
Phillоidin	10 µM	Tocris
Myristoylated Dynamin inhibitory peptide	3 µM	Tocris
Spermine	50 - 500 µM	Sigma-Aldrich
FM 4-64	5 µM	Life Technologies
Fluo 4 AM	1 µM	Life Technologies
K7 - Rhodamine	3 µM	NeoMPS, Inc.
PD-L1-Fc Chimera	1-2 µg/ml	R&D Systems
Etoposide	2 µM	Sigma-Aldrich

Table 2.4 FACS Antibodies and Reagents

Target	Species	Clone	Fluorophore	Manufacturer	Dilution
PD-1	Human	MIH4	APC / PE	BD Biosciences	1:100
PDL1	Human	MIH5	APC	BD Biosciences	1:100
CD28	Human	CD28.2	PE	Biolegend	1:100
ICAM-1	Human	HA58	PE	BD Biosciences	1:100
LFA-1	Human	HI111	PE	Biolegend	1:100
CD4	Human	OKT4	PE	Biolegend	1:100
CD3	Human	UCHT1	PECy7	Biolegend	1:200
TfR	Human	M-A712	PE	BD Biosciences	1:100
HLA ABC	Human	W6/32	PE	Biolegend	1:200
PD-1	Mouse	29F.1A12	PerCP-Cy5.5	Biolegend	1:100
CD4	Mouse	RM4-5	v500	BD Biosciences	1:100
CD8	Mouse	53-6.7	v450	eBioscience	1:100
Viability Dye			eFluor® 780	eBioscience	1:1000
Annexin V			PE	Biolegend	9ng/ml

2.1.2 Plasmids

Table 2.5 Plasmids produced for this study

Plasmid	pSFFV	Species	pUbiquitin
pDUAL	PD1WT	Human	GFP
pDUAL	PD1WT	Human	Cherry
pDUAL	PD1Δ223	Human	GFP
pDUAL	PD1Δ217	Human	GFP
pDUAL	PD1Δ211	Human	GFP
pDUAL	PD1Δ205	Human	GFP
pDUAL	PD1Δ199	Human	GFP
pDUAL	PD1Δ193	Human	GFP
pDUAL	PD1Δ187	Human	GFP
pDUAL	PD1Tm	Human	GFP
pDUAL	HLATm	Human	GFP
pDUAL	HLA-A2	Human	GFP
pDUAL	PD-L1	Human	GFP
pSIN	PD1-GFP	Human	
pSIN	PD1-Cherry	Human	
pSIN	PDL1-Cherry	Mouse	

2.1.3 Primers

Table 2.6 Cloning Primers

Amplicon	Dir.	Enzyme	Primer sequence (5'--3')
PD1WT	FW	BamHI	GGGGGGATCCGCCACCATGCAGATCCCACAGGCGCC
	RS	NotI	CCCCGCGGCCGCTCAGATCAGACCCAGACTAGCAGCACCAG
PD1Δ223	RS	NotI	CCCCGCGGCCGCTCAGATCAATAGTCCACAGAGAACACAGGC
PD1Δ217	RS	NotI	CCCCGCGGCCGCTCAGATCAAGGCACGGCTGAGGGGTCCTCCT
PD1Δ211	RS	NotI	CCCCGCGGCCGCTCAGATCACTCCTTCAGGGGCTGGCCGGTG
PD1Δ205	RS	NotI	CCCCGCGGCCGCTCAGATCAGGTGCGCCTGGCTCCTATTGTC
PD1Δ199	RS	NotI	CCCCGCGGCCGCTCAGATCATGTCCCTCGTGCGGCCCGGGAG
PD1Δ193	RS	NotI	CCCCGCGGCCGCTCAGATCAGGAGCAGATGACGGCCAGG
PD1Δ187	RS	NotI	CCCCGCGGCCGCTCAGATCAGACCCAGACTAGCAGCACCAG
HLA-A2	FW	BamHI	GGGGGGATCCGCCACCATGACAAGAGTTACTAACAGCCCCTCT
	RS	NotI	CCCCGCGGCCGCTCACACTTTACAAGCTGTGAGAGACACATCAG
hPD-L1	FW	BglII	GGGGAGATCTGCCACCATGAGGATATTTGCTGTCTTTATATTCATGA
	RS	NotI	CCCCGCGGCCGCTTACGTCTCCTCCAAATGTGTATCA
mPD-L1	FW	BglII	GGGGAGATCTGCCACCATGAGGATATTTGCTGGCATTATATTCA
	RS	NotI	CCCCGCGGCCGCTTACGTCTCCTCGAATTGTGTATCA
GFP	RS	NotI	CCCCGCGGCCGCTTTACTTGTACAGCTCGTCCATGCCGAGAGTGATCCC
Cherry	RS	NotI	CCCCGCGGCCGCTTACTTGTACAGCTCGTCCATGCCGCC

Table 2.7 Chimeric Protein Primers

Amplicon	Direction	Primer sequence (5'--3')
PD1-GFP	Sense	GGCTCCGGCTCCGGCTCCGTGAGCAAGGGCGAGGAGCT
	Antisense	GGAGCCGGAGCCGGAGCCGAGGGGCCAAGAGCAGTGTC
PD1-Cherry	Sense	GGCTCCGGCTCCGGCTCCGTGAGCAAGGGCGAGGAGGA
	Antisense	GACACTGCTCTTGGCCCCTCGGCTCCGGCTCCGGCTCC
mPDL1-Cherry	Sense	GGCTCCGGCTCCGGCTCCGTGAGCAAGGGCGAGGAGGATA
	Antisense	GGAGCCGGAGCCGGAGCCCGTCTCCTCGAATTGTGTATCA
PD1Tm	Sense	TCTGGGTCCTGGCCGTCATCAGGAGGAAGAGCTCAGATAG
	Antisense	CTATCTGAGCTCTTCCTCCTGATGACGGCCAGGACCCAGA
HLATm	Sense	CAGCCGGCCAGTTCCAAACCATCGTGGGCATCATTGCTGG
	Antisense	CCAGCAATGATGCCCACGATGGTTTGGAACTGGCCGGCTG

Table 2.8 Sequencing Primers

Gene	Direction	Primer sequence (5'--3')
pDUAL /pSIN	FW	CGAGCTCTATAAAAGAGCTCA
	RS	TAAAGCAGCGTATCCACATAGCGTAAAAGGA
PJET	FW	CGACTCACTATAGGGAGAGCGGC
	RS	AAGAACATCGATTTTCCATGGCAG
TMEM16F Set 1	FW	GTGCAGGTTCATGCTTCATTT
	RS	GCACAGTCCCTGCAATAAGA
TMEM16F Set 2	FW	CCCGGTGCTGCTGATTTA
	RS	GGATCTACAGCCATTGAAGGAA
TMEM16F Set 3	FW	AGTGGTGGTCTCTGTATTGTTT
	RS	AAACAGCAGGTTCCAAATTACC
CRISPR gRNA	FW	GAGGGCCTATTTCCCATGATT

2.2 Molecular Biology

2.2.1 Polymerase Chain Reaction (PCR)

PCR reactions were performed using a Hybriad thermal cycler. The proof-reading Phusion® Polymerase (NEB) was used to generate DNA amplicons for cloning into lentiviral transfer vectors (pSIN or pDUAL). The Phusion® PCR reaction mixture is shown in Table 2.9 and the cycling parameters are described in Table 2.12. GoTaq® polymerase (Promega) was used for bacterial colony screening. The GoTaq® PCR reaction mixture is shown in Table 2.10 and cycling parameters in Table 2.13. HotStar Taq Plus® was used for amplification of genomic DNA for verification of CRISPR gene editing. HotStar Taq Plus ® PCR reaction mixture is shown in Table 2.11 and cycling parameters in Table 2.14. Genomic DNA PCRs were performed in collaboration with Julia Sung at the National Institute for Biological Standards and Control.

Table 2.9 Phusion Reaction Mix

Reagent	**Stock Conc.**	**Volume**
HF or GC Buffer*	5X	1X
dNTP	10 mM	1 µl
FW Primer	10 µM	1 µl
RS Primer	10 µM	1 µl
DNA Template	100 ng	1 µl
Phusion Polymerase	2 units/µl	0.5 µl
Nuclease-free H_2O		to 50 µl
Total Volume		**50 µl**

*High Fidelity (HF) Buffer used unless amplicon was GC rich or PCR failed, in which case GC Buffer was used

Table 2.10 GoTaq Reaction Mix

Reagent	Stock Conc.	Volume
GoTaq Green Mastermix	2X	1X
FW Primer	10 µM	1 µl
RS Primer	10 µM	1 µl
DNA Template	E. coli scraping from colony	
Nuclease-free H_2O		to 50 µl
Total Volume		**50 µl**

Table 2.11 HotStar Taq Plus Reaction Mix

Reagent	Stock Conc.	Volume
Qiagen's HotStar Taq Plus MM	2X	20 µl
Forward primer	10 µM	1 µl
Reverse primer	10 µM	1 µl
Coral Load concentrate	10X	4 µl
DNA Template		1 µl
Nuclease-free H_2O		13 µl
Total Volume		**40 µl**

Table 2.12 Phusion PCR Cycling Parameters

Phase	Cycles	Temperature.	Time (s)
Activation	1	98°C	30
Denaturation		98°C	10
Primer annealing	25-30	5°C below primer T_m	20
Extension		72°C	30/kb
Final Extension	1	72°C	10 min
Hold	1	4°C	∞

Table 2.13 GoTaq PCR Cycling Parameters

Phase	Cycles	Temperature.	Time (s)
Activation	1	95°C	2 min
Denaturation		95°C	30
Primer annealing	25-30	5°C below primer T_m	30
Extension		72°C	1min/kb
Final Extension	1	72°C	10 min
Hold	1	4°C	∞

Table 2.14 HotStar Taq Plus PCR Cycling Parameters

Phase	Cycles	Temperature.	Time (s)
Activation	1	95°C	15 min
Denaturation		94°C	30
Primer annealing	36	57°C	30
Extension		72°C	1 min
Final Extension	1	72°C	10 min
Hold	1	8°C	∞

2.2.2 Overlap Extension (OE) PCR

Chimeric proteins were produced by OE PCR using the Phusion® proof-reading polymerase (Figure 2.1). Three PCRs were carried out in two stages as described in Figure 2.1. Both genes were amplified with a complimentary primer pair (Sense and Antisense). This produces two amplicons which overlap at the 3' end of Gene A and the 5' end of Gene B. These two PCR products were then combined in a third PCR with the Gene A FW and Gene B RS primers. The PCR product of this reaction is a fusion of the two genes (Heckman and Pease, 2007).

Sequencing of the DNA fragment was performed before cloning into an expression vector.

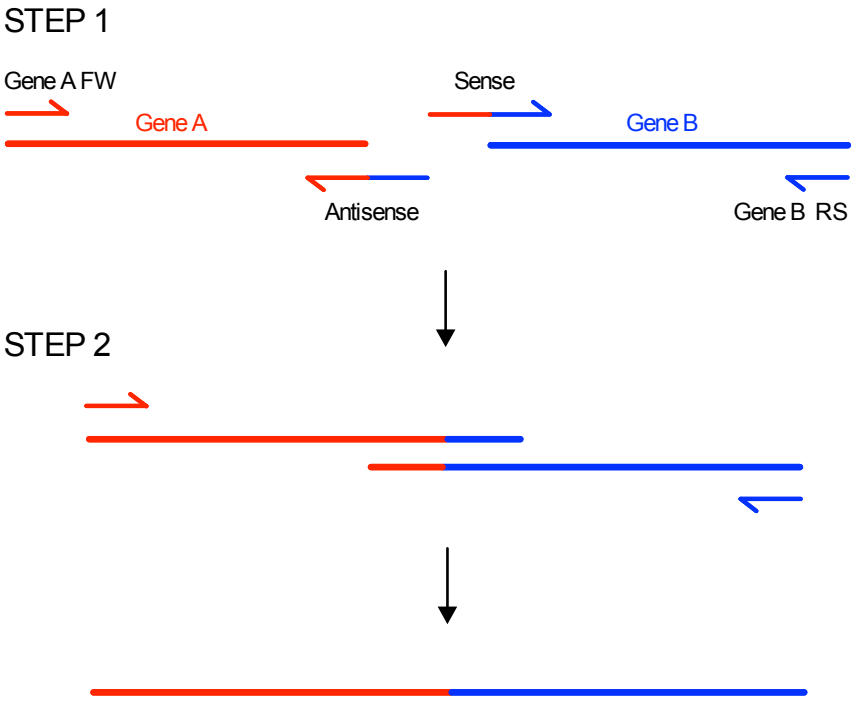

Figure 2.1 **Overlap extension PCR.** Three PCRs are needed to create a chimeric protein composed of Gene A fused to Gene B. A set of complimentary primers (Sense and Antisense) are synthesised consisting of the last 20 base pairs at the 3'end of Gene A and the first 20 base pairs at the 5' end of Gene B. Gene A is then amplified with the FW primer of Gene A and the Antisense primer. Gene B is amplified with the RS primer of Gene B and the Sense primer. These two PCR products are then combined in a third PCR with the Gene A FW primer and the Gene B reverse primer. The product of this PCR will transcribe the GeneA-GeneB fusion protein.

2.2.3 Restriction digestion and ligation

Double restriction digestions to isolate the plasmid backbone and an insert were carried out with appropriate buffers as directed by NEB. Digestions were performed at 37°C in a final volume of 30ul consisting of 3ul DNA, 3ul 10X Buffer, 1ul of each enzyme and 23ul of water for 1 hour. For diagnostic digestions a final volume of 10ul was used.

Plasmid- insert ligations were performed with the Rapid DNA Ligation Kit (Thermo Scientific). Reactions were performed at room temperature for 5 minutes with a total volume of 20ul consisting of 4ul 5X Ligation Buffer and 1ul T4 Ligase (5U/ul).

2.2.4 Agrose gel electrophoresis

To isolate DNA fragments, DNA samples were mixed with 6X TriTrack Loading Buffer (Thermo Scientific) and loaded into 1% Agarose gel containing 5ug/ml ethidium bromide (Sigma Aldrich). The sample was run alongside a 1kb Plus DNA Ladder (Invitrogen) to allow DNA band identification by size. A UV light box was used to visualise and excise the DNA bands. DNA was purified from the agarose using the QIAquick Gel Extraction Kit (Qiagen).

2.2.5 Preparation and transformation of competent bacteria

XL10 Gold (Agilent) bacteria were expanded using the following method: cells were plated onto a Tetracycline (10ug/ml) LB Agar plate and incubated overnight. The next day a colony was picked and grown overnight in 10ml LB buffer containing 10ug/ml Tetracycline. The following day 1ml of this solution was added to 100ml of antibiotic-free LB Buffer for 1 – 2 hours until an OD600 of 0.5-0.6 was reached. The solution was then cooled on ice for 10 min and spun at 3000 rpm at 4°C for 10 min. The bacteria were resuspended and incubated in TFB-I buffer for 5 mins on ice and then spun again. The pellet was resuspended in TBF-II buffer and incubated for a further 15 mins on ice. Competent cells were then aliquoted and stored at -80°C.

Transformation of competent bacteria was performed after bacteria were thawed slowly on ice. Plasmid (~500ng) was added to the bacterial suspension and heat shocked at 37°C for 2 minutes before being returned to ice for a further 2 mins. Bacteria were then plated on an antibiotic impregnated LB agar plate (Ampicillin used at 50ug/ml, Kanamycin at 30ug/ml) and placed at 37°C overnight.

2.2.6 DNA purification and quantification

For the purification of plasmid DNA, bacterial colonies were picked and grown overnight in LB Broth (5ml for miniprep and 100ml for midiprep) containing antibiotic (Ampicillin 50ug/ml, Kanamycin 30ug/ml). Bacteria were isolated by centrifugation at 3000rpm for 30mins at 4°C before DNA purification was performed with either a Miniprep or Midiprep kit (Qiagen), following the manufacturer's protocol. DNA was eluted in either EB Buffer (Qiagen) or nuclease free water. DNA concentration and purity were assessed using a NanoDrop 3300 spectrophotometer (Thermo Scientific).

2.2.7 DNA sequencing

Sequencing primers are shown in Table 2.8. DNA was sequenced either by the UCL Cancer Institute Sequencing Service or Beckman Coulter.

2.3 Tissue Culture

Jurkat T cells (E6.1) were acquired from ECACC. THP-1 cells were a gift from Dr Mahdad Noursadeghi, UCL. These suspension cells were grown in Roswell Park Memorial Institute (RPMI) medium (Sigma) supplemented with 10% Foetal Calf Serum (FCS)(Gibco), 2mM L-glutamine, 100U/ml Penicillin and 100ug/ml Streptomycin (Gibco) in a 5% CO_2 incubator. Cells were maintained in upright T25 flasks (Nunc) and passaged 1:10 every other day.

HEK 293T (Collins lab), HEK 293 TRex cells (Life Technologies), B16.F10 and GM-CSF expressing B16.F10 cells (GVAX) (Quezada lab) were grown in Dulbecco's

Modified Eagle's Medium (DMEM) (Sigma) supplemented with 10% Foetal Calf Serum (FCS), 2mM L-glutamine, 100U/ml Penicillin and 100ug/ml Streptomycin in a 10% CO_2 incubator. Cells were maintained in T75 flasks (Nunc) and passaged 1:10 every other day.

Cell counting was performed with Neubauer chamber slide. Cells were frozen in FCS with 10% dimethyl sulfoxide (DMSO).

2.4 Lentiviral vectors

2.4.1 Packaging cells

HEK 293T cells were used for lentiviral vector packaging and viral titrations. These are derived from human embryonic kidney cells and express the simian virus 40 large T antigen. This antigen promotes episomal maintenance and increases the replication of vectors that contain the SV40 promoter (Pear PNAS 1993).

2.4.2 Plasmids

The single promoter (pSIN) and dual promoter (pDUAL) lentiviral transfer vectors used in this study are shown in Figure 2.2. The use of these plasmids has been described by this lab and others (Rowe et al., 2009). pSIN has an SFFV promoter whilst pDUAL has both an SFFV and Ubiquitin promoter. With pDUAL, the SFFV promoter drives target gene expression whilst the ubiquitin promoter drives expression of either GFP or mCherry.

Cloning of target genes into these vectors is a four step process. Firstly the chosen sequence is amplified by Phusion® polymerase PCR with a forward primer that introduces a 5' BamHI site (GGATCC) with a Kozak sequence (GCCACC) and a reverse primer that introduces a 3' NotI site. In cases where the target gene has an internal BamHI site, a Bglll site was instead introduced (AGATCT) as the cut site is compatible with BamHI. This PCR product was then blunt ligated into the PJET cloning vector (Thermo Scientific) with 2ul PCR product, 10ul 2X ligation buffer, 1ul

T4 ligase and 1ul PJET vector 6ul water incubated for 10 minutes at room temperature. Bacteria were then transformed with the ligation mixture. Colony PCR was conducted to confirm the presence of the insert and positive colonies were grown. DNA was purified and digested with the relevant enzymes. Cut vector and insert were then ligated as described above.

For lentiviral production the 2nd generation packaging plasmid p8.91 expressing HIV proteins gag, pol, tat and rev was used along with the pMD.G plasmid expressing the envelope of vesicular stomatitis virus (VSV-G). These plasmids originate from the Naldini lab (Zufferey et al., 1998) and were synthesised by Plasmid Factory.

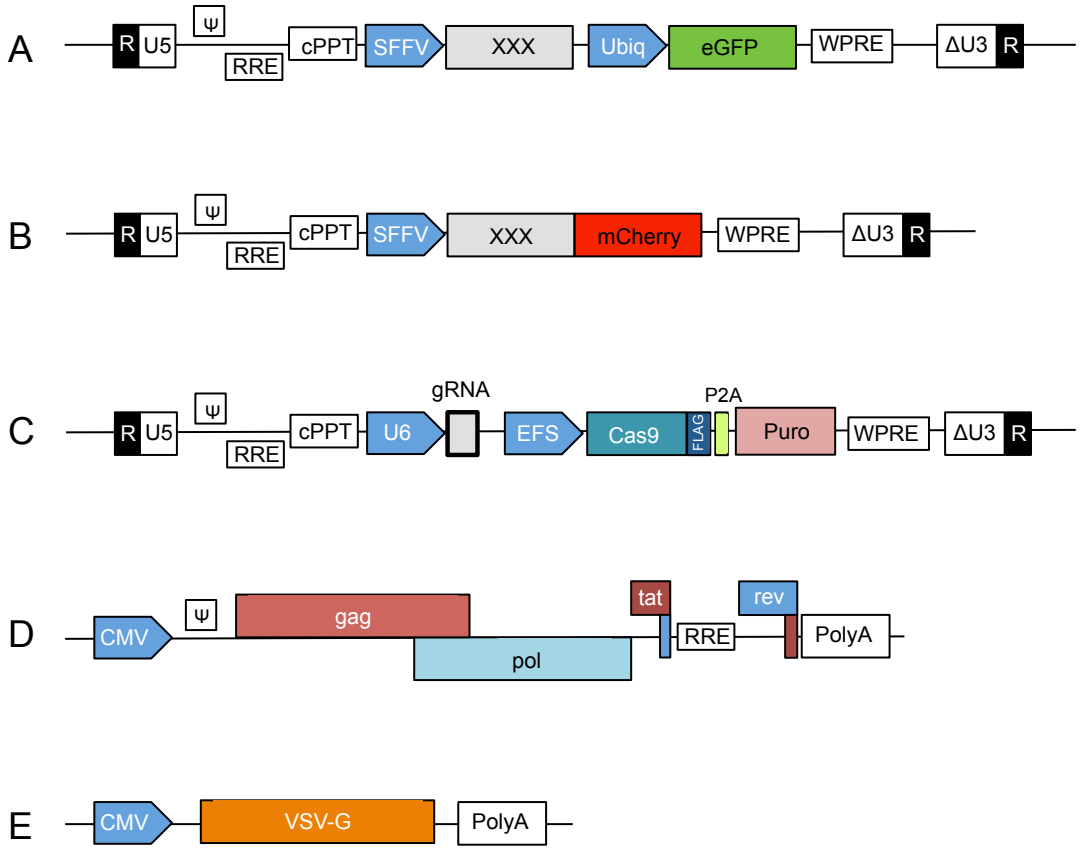

Figure 2.2 **Lentiviral vector Plasmids**. A pDUAL B pSIN C CRISPRlenti v2 D p8.91 E pMD.G . RRE: Rev response element. cPPT: central poly purine tract. SFFV: spleen focus-forming virus promoter. Ubiq: Ubiquitin promoter. WPRE: woodchuck hepatitis virus post-transcriptional regulatory element. U6: human RNA polymerase III U6 promoter. EFS: elongation factor 1α promoter. P2A: self-cleaving 2A peptide. VSV-G: vesicular stomatitis virus glycoprotein.

2.4.3 Lentiviral vector Production

$1x10^7$ HEK 293 T cells were seeded in a 15cm plate and by the end of the following day the plate was ~80% confluent. Cells were transfected with the transfer vector (pSIN or pDUAL), packaging plasmid (p8.91) and envelope plasmid (pMD.G) using Fugene 6 transfection reagent in the proportions given in Table 2.15. The transfection mixture was combined 20 minutes prior to transfection and then added dropwise over the cells. The following day the cell media was collected, discarded and replaced. Cell media was then collected on days 2 and 3 after transfection and kept at 4°C.

To concentrate the lentiviral vectors, collected cell media was first filtered through a 0.45µm filter to remove cells and debris and then loaded into sterile ultracentrifuge tubes (Beckman Coulter). A 2ml 20% sucrose cushion was loaded at the base of the tube before the tubes were spun at 20,000 rpm for 2 hours at 4°C in a Sorvall ultra-centrifuge (Beckman Coulter). Following centrifugation supernatant was discarded, viral pellets were resuspended in normal media, kept on ice for 30 minutes, and then resuspended again before being aliquoted and stored at -80°C.

Table 2.15 Lentivector Transfection Mix

Reagent	Amount
p8.91	2.5 µg
pMD.G	2.5 µg
Transfer Plasmid	3.75 µg
Fugene 6	45 µl
Opti-MEM	500 µl

2.4.4 Lentiviral vector Titration

Concentrated lentiviral vectors were titrated to establish the infectious units per ml (IU/ml). 0.5ml of complete DMEM containing $2x10^5$ HEK 293T cells were seeded per well in a 24 well plate. Once cells had adhered (~4 hours later), serial dilutions of 1 in 5, 25, 125, 625, 3125 of virus were added to the cells. The following day a further 1

ml of DMEM was added to each well. Three days after transduction, cells were collected and the percentage of cells expressing fluorescent protein measured by FACS (described later). These values were plotted and dilutions that that fell within the linear phase (10-30% transduced) were applied to the following formula:

$$\frac{\text{No. of Cells x \% Transduced x Dilution Factor}}{\text{Volume of Virus}} \text{ x 1000 = Infectious units / ml}$$

2.5 CRISPR-Cas9 Genome Editing

CRISPR is a new and revolutionary method of genome editing. The process employs the machinery of a prokaryotic adaptive immune pathway. CRISPR loci in bacterial genomes contain Clustered Regularly Interspaced Short Palindromic Repeats (CRISPR) along with short DNA sequences derived from pathogenic bacteriophages that have previously infected the prokaryotic cell line. These short non-coding sequences guide nuclease enzymes to pathogenic DNA sequences if the bacteriophage reinfects the cell (Marraffini and Sontheimer, 2010).

Heterologous expression of the Cas9 nuclease from *Streptococcus pyogenes* with a guide RNA (gRNA) specific for the target gene of interest in eukaryotic cells leads to gene disruption and knockout. Cas9 introduces a double stranded break that is repaired by 'non-homologous end joining'. Small insertions or deletions introduced by this form of DNA repair lead to frame shift mutations and therefore block protein expression (Sander and Joung, 2014).

The lentiCRISPR v2 plasmid was used as described previously (Sanjana et al., 2014) and is shown in Figure 2.2. The gRNA sequence targeting TMEM16F Exon 2 was 5'-TCAGCATGATTTTCGAACCC-3' and TMEM16F Exon 5 was 5'-TGTAAAAGTACACGCACCAT-3'. The primers that contain these sequences, shown in Table 2.16, were annealed in a PCR thermocycler with a 30 minute hold at 37°C, then a 5 min step at 95°C followed by a ramp down to 25°C over 14 minutes. The annealed primers were then ligated into the lentiCRISPR plasmid that had been cut

with BsmBI (Fermentas) according to the Zhang Lab protocol. The plasmid was then sequenced to confirm the presence of the gRNA using the primers shown in Table 2.8.

Transient transfection of the lentiCRISPR plasmid is preferred as this reduces the risk of accrued off-target genome editing. TREx-293 cells were transiently transfected with the plasmid using Lipofectamine (Life Technologies). Jurkat T cells cannot be transfected so virus was produced as described in 2.4.3 and cells were transduced. 48 hours after transfection/transduction cells were selected in 0.5ug/ml Puromycin for Jurkat and 5ug/ml Puromycin for TREx-293 for 24 hours before single-cell clones were isolated. Jurkat T cells stably expressing Cas9 and gRNA after transduction were frozen following initial expansion and aliquots thawed as needed to avoid off-target effects resulting from long-term culture. Gene editing was confirmed by sequencing (Beckman Coulter) (Figure 3.5). Genomic DNA for sequencing of the edited region of interest was extracted from $1x10^6$ cells using the DNeasy Blood and Tissue kit (Qiagen). Two different primer sets were used to amplify Exon 2 (Set 1 and 2) and one for Exon 5 (Set 3). Amplicons were sequenced using the same primers (Table 2.8).

Table 2.16 CRISPR gRNA sequences

Gene	Exon	Side	Primer sequence (5'--3')
TMEM16F	2	Top	CACCGTCAGCATGATTTTCGAACCC
		Bottom	AAACGGGTTCGAAAATCATGCTGAC
	5	Top	CACCGTGTAAAAGTACACGCACCAT
		Bottom	AAACATGGTGCGTGTACTTTTACAC

2.6 Flow cytometry (FACS)

Cells were collected, transferred into a 96-well plate (Helena Biosciences) and washed twice with ice cold PBS. Cells were centrifuged at 1500rpm for 5 minutes in all steps unless otherwise stated. All steps subsequent to initial washed were carried out in blocking buffer (Table 2.1). Cells were incubated in blocking buffer for 30 mins prior to antibody staining. Changes in intracellular Ca^{2+} concentration were measured with 1μM Fluo 4 AM (Life Technologies) loaded into cells for 30 mins at 37°C prior to the experiment. Surface phosphatidylserine was detected with 9ng/ml Annexin V applied in Annexin binding buffer (BioLegend). Microvesicles were distinguished from apoptotic bodies using the DNA (Viability) eFluor® 780 dye (eBioscience). This dye was also used to gate for viable cells in all experiments. Surface staining for receptors was carried out for 30 mins on ice using the antibodies detailed in Table 2.4. Flow cytometry was performed using a BD Fortessa (BD Bioscience) with FACS Diva software (BD Biosciences) and data was analysed with FlowJo (Treestar).

2.7 Electrophysiology

Whole cell patch clamp recording of cells was performed to simultaneously measure membrane capacitance, conductance and current in real-time.

Glass electrode tips were pulled with a Narishige PP-830 microelectrode puller, dipped in molten wax (Kerr Corp.) before being cut and polished on a forge. These were made with an opening of appropriate size to minimize access resistance and allow for stable patch formation. Tips were filled with intracellular solution before being mounted on a micromanipulator. Cells were kept in a microscope-mounted bath containing extracellular solution. All experiments were conducted within a faraday cage to remove electromagnetic interference. One silver chloride electrode was present in the tip and one in the cell bath paired to a Nation Instruments digital acquisition board and an Axopatch 200b patch clamp amplifier connected to Capmeter 6v3 software running in MATLAB (Wang and Hilgemann, 2008). Suction

was used to bring the cell onto the electrode tip and the cell was opened with further suction or a high voltage pulse.

Parameters were measured using the Lindau-Neher method (Lindau and Neher, 1988) in Capmeter (Figure 2.3). Square-wave voltage perturbation (20 mV; 0.5 kHz) was controlled using the Capmeter software. Like an electrical capacitor, the capacitance of a cellular membrane is directly proportional to its surface area (membrane area), with 1mF equal to 1cm^2 of cell membrane. Initial input resistances were generally between 2-10 MΩ and apparent cell resistance was 0.1-2 GΩ.

External solutions were water-bath heated to 35-37°C in a multi-chamber gravity fed solution switcher set to a flow rate of approximately 200 µl/min. To switch solutions, the microscope platform and solution switcher were moved to position the cell in the middle of the appropriate solution stream.

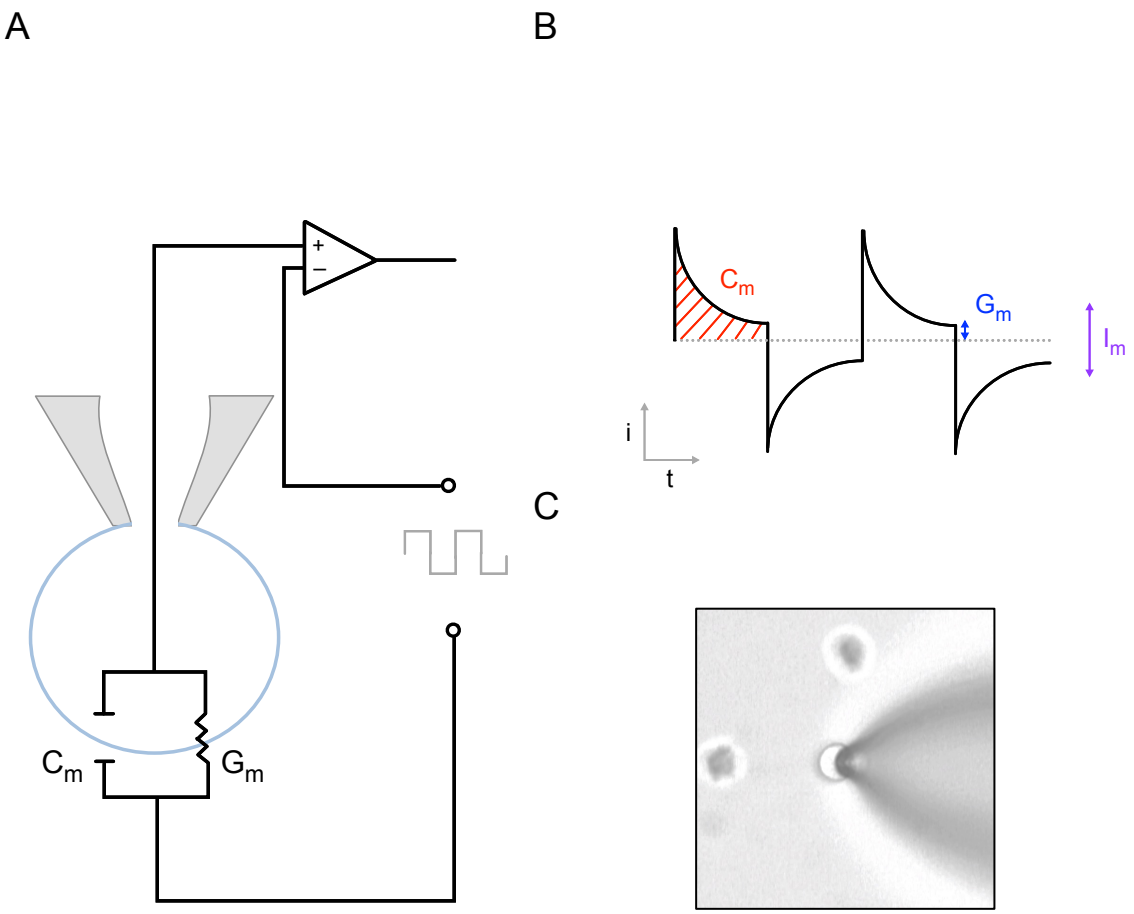

Figure 2.3 **Whole cell patch clamp recording**.

A The minimum equivalent circuit of the whole cell patch clamp configuration. A square wave voltage pulse is applied across the membrane with one terminal in the patch pipette and the other in the cell bath. When a cell is in this configuration, the current trace in response to the voltage pulse is shown in **B**. Capacitance is proportional to the rate of current relaxation in response to a voltage step (area under the curve). The conductance is proportional to the difference between the asymptote of the curve and the origin. **C** The view from above a Jurkat T cell in whole cell patch clamp configuration as seen through a Nikon Eclipse Ti-U light microscope with a 40X lens.

2.8 Confocal Microscopy

Confocal imaging was performed by a Nikon TE2000-U microscope; 60× oil immersion, 1.45-NA objective paired with the EZ-C1 confocal system (Nikon) containing a 40-mW 163-Argon laser (Spectra Physics; Newport Corporation) operating at 488 nm at 7.5% maximum capacity for FM4-64 recordings and a 1.5 mW Melles Griot cylindrical HeNe laser at 543 nm at 55% of maximum capacity for K7-Rhodamine. Emission filters were set to either 500-540 nm or 580LP respectively. Typically resolution was 512 x 512, set with a pixel dwell time yielding <1-s exposure times per frame and a pinhole of 150µm. Image analysis was performed using either the EZ-C1 v3.9 (Nikon Instruments) or ImageJ (NIH). Photobleaching was negligible for these experiments. For experiments where confocal imaging and electrophysiology were combined, a RC-26 recording chamber (Warner Instruments) was used. For independent confocal imaging of intact cells, 800µl of media containing Jurkat cells was placed in a glass bottom 4-chamber dish (Nunc). 200µl of warmed ionomycin solution was rapidly added manually and cells imaged using the same conditions as above.

2.9 Super-resolution Structured Illumination Microscopy

The resolution of conventional light microscopy is limited by the diffraction limit of visible light, to approximately 300nm. Super-resolution (SR) microscopy techniques allow for image resolution above the diffraction limit. Many SR techniques such as PALM and STORM rely on stochastically activated fluorophores which facilitate the detection of single emitting molecules. Structured illumination microscopy is a SR approach that permits the use of conventional fluorophores (e.g. GFP and mCherry). Images are taken through a series of rotating optical gratings. By analysing the fringes of light that appear through the Moire pattern produced through the grating, and combining this information over the different rotations, spatial resolution can be increased by a factor of two (Kner et al., 2009).

SR-SIM was used in this case to resolve the membranes of individual microvesicles and endocytic vesicles bearing fluorescently conjugated PD-1.

SR-SIM imaging was performed using Plan-Apochromat 63x/1.4 oil DIC M27 objective in an Elyra PS.1 microscope (Zeiss). Images were acquired using 5 phase shifts and 3 grid rotations, with 34µm grating period for the 561nm laser and filter set 4 (1851-248, Zeiss). SR-SIM Images were acquired using an sCMOS camera and processed using ZEN software (2012, version 8.1.6.484, Zeiss).

2.10 *In vivo* Tumour Experiment

At Day 0, Female C57BL/6 mice (three per group) were injected subcutaneously on the flank with $2x10^5$ WT or PDL1-Cherry expressing B16.F10 mouse melanoma cells. At day 6 and day 8 $1x10^6$ irradiated (150 Gy) GM-CSF-expressing B16 cells (GVAX) were injected on the contralateral flank. At Day 13 mice were sacrificed and the blood, lymph nodes and spleen were collected. Cells from lymph nodes, spleen and tumours were mashed through a 70µm nylon mesh filter (BD Falcon). Cells from spleen and blood were treated for 5 mins in red blood cell lysis buffer (Sigma Aldrich) for 5 minutes at room temperature. TILs were isolated from tumours by Ficoll (GE) gradient. Cells were then stained for FACS as described above. Mice were kept and bred by UCL Biological Services and used at 6 - 8 weeks of age. This experiement was performed under supervision from Dr Dana Briesmeister from the Quezada lab.

2.11 Statistical Analysis

Data analysis was performed in Prism 6 (GraphPad). Unless stated otherwise, error bars represent standard error with significance assessed by Student's t-tests.

CHAPTER 3

Ca^{2+} ACTIVATED PLASMA MEMBRANE CHANGES REGULATED BY TMEM16F

3.1 Introduction

It has long been recognised that increases in intracellular Ca^{2+} have profound and wide-ranging effects on the plasma membrane of cells. Ca^{2+} activated fusion of intracellular vesicles allows secretion of effector molecules, the rapid expression of transmembrane proteins and the addition of new membranes to the plasma membrane. This exocytosis is fundamental to cellular functions ranging from endocrine signalling to membrane repair. Ca^{2+} activated microvesicle shedding constitutes a pathway for intercellular signalling while Ca^{2+} activated changes in plasma membrane phospholipid distribution can catalyse the coagulation cascade and facilitate the phagocytosis of dead cells. Endocytosis of large volumes of membrane can also follow large Ca^{2+} influx. Though many of these events have been extensively studied and well characterised, the mechanisms that underlie them remain unclear.

As well as sharing the common trigger of Ca^{2+} influx, these events can often coincide. This has led researchers to question whether these events are mechanistically linked. Does phospholipid scrambling cause microvesicle release (Elliott, 2006; MacKenzie et al., 2001)? Does exocytosis cause phospholipid scrambling (Lee et al., 2013; Mirnikjoo et al., 2009)? Does exocytosis have to precede endocytosis, through secretion of membrane-altering enzymes (Tam et al., 2010)? Though evidence has emerged to support many of these hypotheses, few firm conclusions can be drawn from the fragmented and often contradictory literature.

Key to solving these mysteries is identifying the protein machinery involved and the mechanisms by which they operate. The synaptotagmins have emerged as the Ca^{2+} sensors for exocytosis in many cell types (Südhof, 2013), though exocytosis still occurs in the absence of multiple synaptotagmins in secretory (Schonn et al., 2008) and non-secretory (Wang and Hilgemann, 2008) cells. No Ca^{2+} sensor has yet been identified for the large exocytosis necessary for membrane repair (McNeil and Kirchhausen, 2005).

There may be multiple mechanisms for microvesicle release, some of which are Ca^{2+} dependent and some of which are Ca^{2+} independent. The endosomal ESCRT

machinery has recently been implicated in microvesicle release in a number of contexts including Ca^{2+} activated membrane repair, but the mechanism of ESCRT Ca^{2+} dependence and recruitment to the plasma membrane is uncertain (Jimenez et al., 2014; Scheffer et al., 2014).

The Ca^{2+} activated phospholipid scramblase has recently been identified as TMEM16F and its deletion has been shown to cause of the rare bleeding disorder Scott Syndrome. Controversy surrounds how a Ca^{2+} activated ion channel can translocate phospholipids, with some reports concluding that TMEM16F is not sufficient for membrane scrambling (Yang et al., 2012) while other contradictory reports showing that TMEM16F alone can scramble artificial membrane liposomes (Brunner et al., 2014; Malvezzi et al., 2013).

These events have wide-ranging effects in multiple cell types, though they have all been investigated in T lymphocytes. Exocytosis, phospholipid scrambling and microvesicle release are seen during T cell activation (Choudhuri et al., 2014; Fischer et al., 2006; Soares et al., 2013).

We began to be interested in the response of cells to large Ca^{2+} influx following the discovery that the important T cell regulator PD-1 is specifically downregulated following Ca^{2+} influx in lymphocytes (Chapter 4). We found there to be much confusion and contradiction in the literature. Several events were seen to coincide with Ca^{2+} influx: exocytosis, MEND, microvesicle shedding and phospholipid scrambling. How these are linked and whether they accounted for the downregulation of PD-1 was unclear. Prof. Hilgemann has worked extensively on these problems and first demonstrated and characterised Ca^{2+}-activated MEND.

We set out to methodically investigate Ca^{2+} triggered membrane changes in T lymphocytes. In order to best achieve this we had to employ a diverse array of techniques, from lentiviral vector-based genome manipulation to flow cytometry to whole cell patch clamp electrophysiology. This work was performed between Prof. Collins' lab in London, UK and Prof. Hilgemann's lab in Dallas, US where I spent five months on a Bogue research fellowship.

The model upon which we based much of this research is the human Jurkat leukaemic T cell line. These cells are of great historic importance in T cell biology,

with many of the key discoveries in T cell signalling having been first demonstrated in Jurkats. The discoveries that TCR ligation leads to an increase in cytoplasmic Ca^{2+} (Imboden et al., 1985) and protein tyrosine phosphorylation activation (Veillette et al., 1988), the discovery and characterisation of ZAP70 (Chan et al., 1992), the identification of PLCγ1 as a TCR signalling molecule (Weiss et al., 1991), and the identities and significance of many ion channels (Lewis and Cahalan, 1995), were all discoveries first made in Jurkat T cells (Abraham and Weiss, 2004). Importantly in our case, Jurkat T cells are a suitable size for patchclamp experiments, are amenable to genetic manipulation using lentiviral vectors, while behaving similarly to primary human T cells in plasma membrane protein expression.

This chapter presents our findings, which draw connections between many of these Ca^{2+}-activated plasma membrane changes, and implicate one protein as their master regulator.

3.1.1 Research questions

- What is the response of T lymphocytes to large Ca^{2+} influx?

- What is the mechanism underlying:

- Ca^{2+} activated large exocytosis?

- Ca^{2+} activated microvesicle shedding?

- Ca^{2+} induced phospholipid scrambling?

- Ca^{2+} activated massive endocytosis (MEND)?

3.2 Results

3.2.1 Ca^{2+} activated exocytosis in Jurkat T cells is associated with ion conduction through a Ca^{2+} activated ion channel

In order to study Ca^{2+} activated membrane responses we employed real-time capacitance recording via whole-cell patch clamp. As detailed in chapter 2, this assay allows very accurate measurement of plasma membrane area as well as of movement of ions across the plasma membrane over time. Capacitance data alone, however, only provides information on net membrane area changes, not directionality, so if exocytosis and endocytosis occur at the same time, this will not be obvious. In order to gain information about the directionality of membrane movements, we employed concurrent confocal imaging with the membrane tracer dye FM4-64. This dye is highly suited for these experiments as it is cell-impermeable, it rapidly binds and can be completely and rapidly washed from the membrane. Endocytosis in the presence of FM dye leads to the irreversible retention of dye in endocytic vesicles whilst exocytosis leads to an increase in bound dye which can be completely washed.

Figure 3.1 shows the response of WT Jurkat T cells to Ca^{2+} influx facilitated by the ionophore ionomycin. Following Ca^{2+} influx cell plasma membrane area doubles in ~30 seconds. FM dye binding to the plasma membrane increases with identical kinetics to capacitance increase and this binding is entirely reversible by washing (Images 1-4), demonstrating that there is no contemporaneous endocytosis. Exocytosis is accompanied by a large membrane conductance of ~60nS that activates within five seconds and inactivates over approximately one minute.

Next we analysed the relationship between exocytosis and conductance. As Figure 3.2A shows, the rate of change of capacitance (dC_m/dt) closely matches the rate of change in ion movement i.e. the conductance. Crucially when a +20mV membrane potential is applied to the cell (Figure 3.2B), the conductance is associated with a persistent transmembrane current. This indicates that ions are flowing between the cytoplasm and the extracellular space.

As this large membrane exocytosis is always associated with a flow of ions across the plasma membrane through a Ca^{2+} activated ion channel, we next investigated whether this ion movement was necessary for exocytosis. When normal intracellular and extracellular ions were replaced with NMDG aspartate, the level of Ca^{2+} activated exocytosis was reduced, as was the case when cytoplasmic ions were replaced with sucrose solution. Interestingly, replacing all ions with symmetrical sucrose solution facilitated a complete block in exocytosis. These data suggest that ion conduction through the channel is necessary in the mechanism of exocytosis.

Next we asked whether the same SNARE machinery necessary for regulated exocytosis in many cell types, including neurons and lytic granule exocytosis in cytotoxic T cells (Matti et al., 2013; Südhof, 2013), was involved in this large Ca^{2+} activated exocytosis. These types of membrane fusion employ synaptobrevin (VAMP2) that is rapidly degraded by tetanus toxin. Inclusion of 400nM tetanus toxin in the cytoplasmic solution did not block exocytosis. We also confirmed that neither cellular ATP nor GTP were necessary as exocytosis was unaffected in their absence.

Together these data demonstrate a form of Ca^{2+} activated exocytosis that relies on ion flux through a Ca^{2+} activated ion channel by a mechanism independent of ATP and classical SNARE machinery.

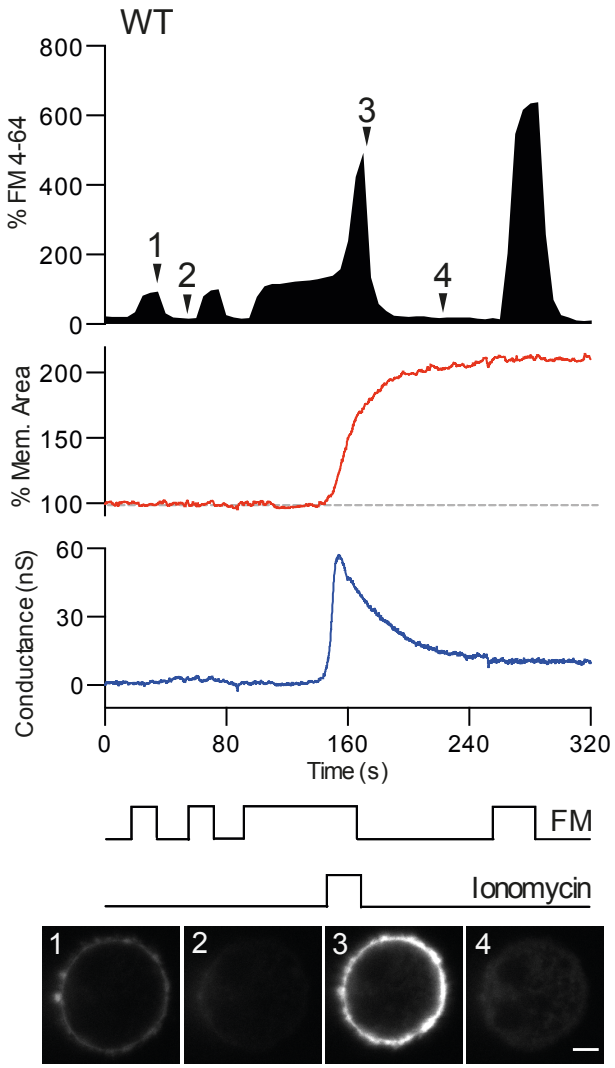

Figure 3.1 **Ca^{2+}-activated exocytosis and channel opening.** Real-time membrane area (capacitance) and transmembrane ion movement (conductance) of WT Jurkat T cells were measured by whole-cell patch-clamp with concurrent confocal imaging using standard Ringer and cytoplasmic solutions. FM4-64 and ionomycin were applied and washed as shown. Membrane area and FM4-64 fluorescence are shown as percentage of baseline values. Images are of FM4-64 binding to the cell at indicated time points with a scale bar of 5μm.

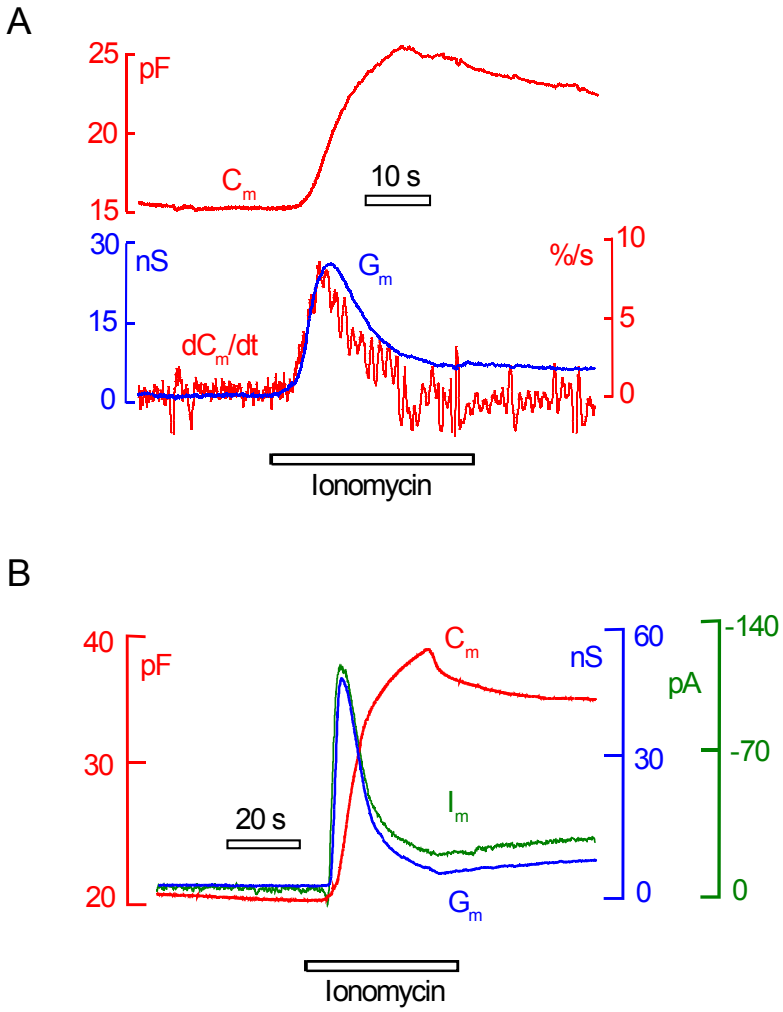

Figure 3.2 **Kinetics of Ca^{2+}-activated exocytosis, conductance and current. A** Membrane capacitance and conductance following treatment with 5µM ionomycin with standard extracellular and cytoplasmic solutions. The rate of change of membrane area (dCm/dt), was calculated from capacitance records (Cm) and filtered at 1 Hz. In 8 experiments analyzed, the peak of conductance occurred within 3 s of the maximal rate of exocytosis. **B,** Membrane capacitance, current and conductance changes following treatment with 5µM ionomycin in standard Ringer solution. A membrane potential of +20mV was applied across the membrane.

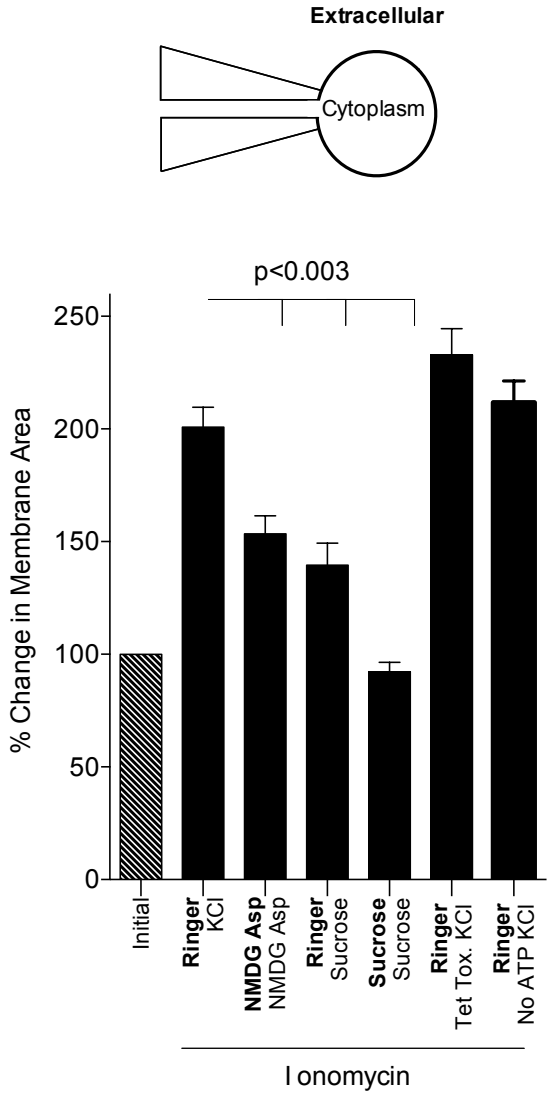

Figure 3.3 **Exocytosis is dependent on ion movement but is not tetanus toxin sensitive nor ATP dependent.** Percentage of initial membrane area at 30s after ionomycin treatment of WT Jurkat cells. Cells were perfused with given cytoplasmic solutions for more than 200s before ionomycin treatment. Conditions were extracellular Ringer and standard cytoplasmic solution (KCl), symmetrical NMDG Aspartate, extracellular Ringer with cytoplasmic sucrose, symmetrical sucrose, extracellular Ringer with 400nM Tetanus Toxin L chain in standard cytoplasmic solution and extracellular Ringer with standard cytoplasmic solution containing no ATP or GTP.

3.2.2 Ca^{2+} activated exocytosis is followed by the shedding of plasma membrane microvesicles

We were next interested in the fate of the plasma membrane following this large exocytosis. Figure 3.4A shows long-term capacitance recording of WT Jurkat cells stimulated with ionomycin. Following exocytosis there is a gradual loss in plasma membrane area over approximately 10 minutes plateauing at approximately 80% of baseline.

In Figure 3.4B and Supplementary Video 3.1, confocal imaging of whole cells incubated in FM4-64 membrane dye, revealed a dramatic shedding of plasma membrane microvesicles following exocytosis. From these images there appears to be no concurrent endocytosis.

These data confirm findings made by others that Ca^{2+} influx leads to plasma membrane microvesicle shedding. However, it demonstrates for the first time that large exocytosis precedes microvesicle shedding.

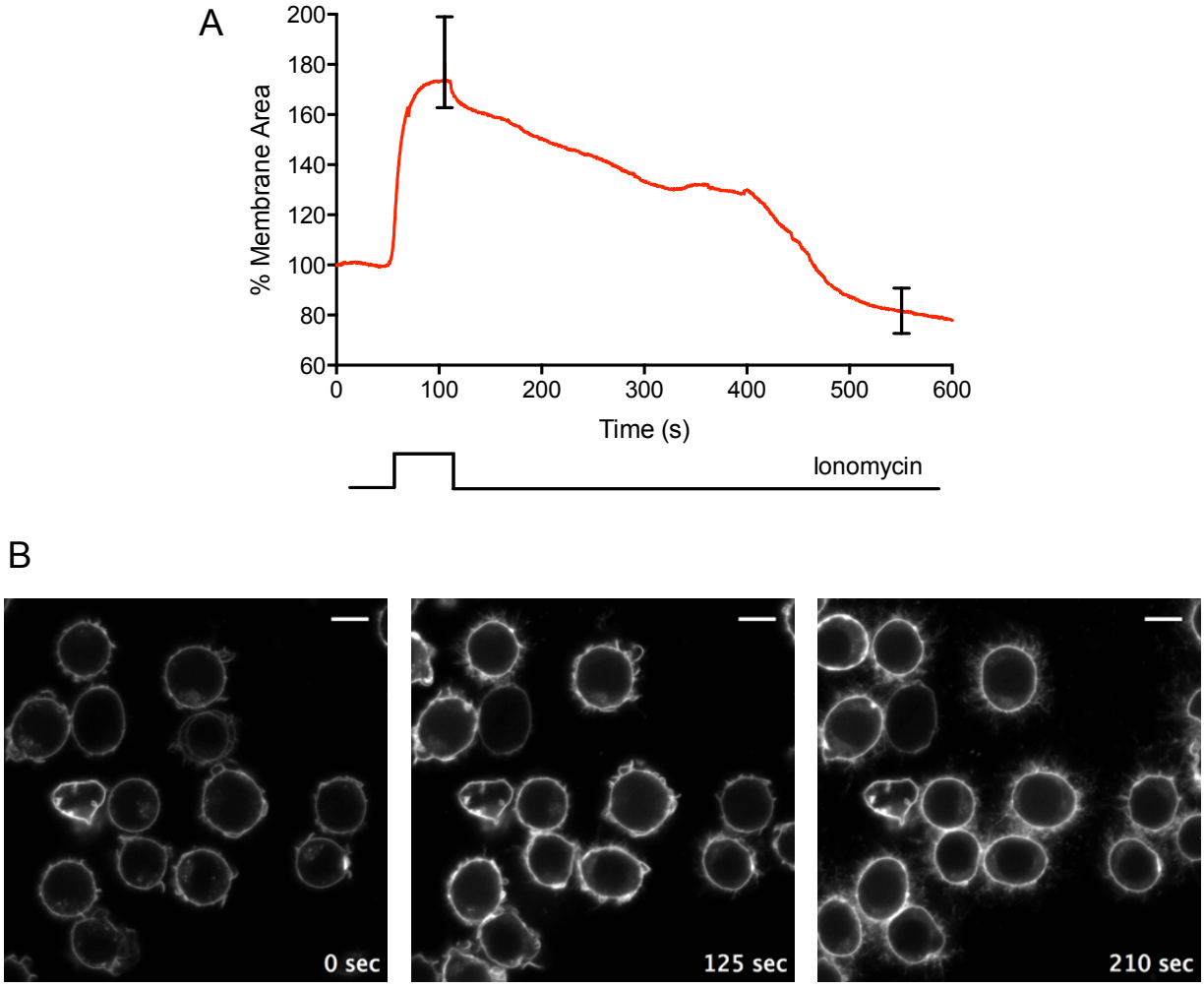

Figure 3.4 **Slow loss of plasma membrane area following exocytosis is due to microvesicle shedding. A** Capacitance recording of WT Jurkat T cell treated with 5μM ionomycin with standard Ringer extracellular and cytoplasmic solutions. **B** Confocal imaging of whole cells in a bath containing FM4-64 dye. 5μM ionomycin was added to the dish at 60 seconds. The scale bar equates to 10μm.

3.2.3 Loss of TMEM16F converts Ca^{2+} activated exocytosis to massive endocytosis (MEND)

Data presented so far implicates a Ca^{2+} activated ion channel as the trigger for large exocytosis. We next aimed to establish the identity of this channel. The phenotype of the channel we observed had many of the features of TMEM16F. The channel was Ca^{2+} activated (Picollo et al., 2015), had a high Ca^{2+} threshold for activation (Grubb et al., 2013; Yang et al., 2012), was often delayed in activation by seconds to minutes at low ionomycin concentrations (data not shown) (Grubb et al., 2013; Kim et al., 2015), and was still able to conduct large ions such as NMDG (Yang et al., 2012).

The recent emergence of CRISPR-Cas9 gene editing has provided researchers with the ability for total gene knockout rather than knockdown by techniques such as RNA interference. In this case we suspected that the channel might still function at low expression levels so a gene knockout strategy was preferable.

Figure 3.5 shows the strategy for CRISPR-Cas9 targeting of the TMEM16F gene. As transfection of Jurkat T cells is not possible, we used the lentiviral vector-based approach pioneered by the Zhang lab at MIT (Sanjana et al., 2014). We separately targeted both Exon 2 and 5 of the gene (Figure 3.5A and 3.5E) to ensure the knockout phenotypes were consistent and not due to off-target deletion of other genes. Single cell clones were isolated and genomic DNA was sequenced to confirm gene editing. PCRs were performed with two different primer sets and both amplicons were sequenced. The sequence of control cell TMEM16F Exon 2 is shown in Figure 3.5B. In the Exon 2-targeted clone, a single base insertion across alleles has led to a frame shift mutation and early termination of the gene (Figure 3.5C).

CRISPR vector transduced cells targeting Exon 5 of TMEM16F as well as control cells were sequenced (Figure 3.5F and 3.5G). In this case, gene editing was not consistent across alleles and so it is hard to establish the exact mutations in each allele by sanger sequencing, however it is clear from Figure 3.5G that profound gene disruption had occurred at the targeted site. At several sites there is no WT nucleotide present indicating that no WT transcripts are present. It was not possible to carry out western blots to confirm knockdown due to a lack of commercially

available antibodies to TMEM16F. Experiments were performed on both Exon 2 and 5 targeted clones to confirm that responses corresponded. Unless otherwise stated, all electrophysiology data appearing in this thesis was performed on the Exon 2 targeted clone.

Figure 3.6 shows whole cell patch clamp experiments with concurrent confocal imaging performed on TMEM16F-null cells following the same protocol described for Figure 3.1. In striking contrast to WT cell responses, Ca^{2+} influx triggers massive endocytosis, with ~50% of the plasma membrane taken in over ~20 seconds. Endocytosis is confirmed by retention of FM4-64 tracer dye which can no longer be washed. As expected, no Ca^{2+} activated membrane conductance is seen in the absence of TMEM16F.

These data confirm the identity of the channel necessary for exocytosis as TMEM16F. They also reveal a pathway of massive endocytosis that operates, in the absence of TMEM16F-induced exocytosis, in response to large Ca^{2+} influx.

This Ca^{2+} activated endocytosis appeared similar to that described previously in BHK, HEK 293 and mouse cardiomyocytes (Lariccia et al., 2011), and which was found to be independent of all endocytic and cytoskeletal protein machinery. To confirm this phenotype, we carried out patch-clamp experiments on the TMEM16F-null Jurkat T cells using targeted inhibitors (Figure 3.7). Endocytosis was not blocked by cytoskeletal disruption by Latrunculin A or Phalloidin. Latrunculin A inhibits actin polymerisation while Phalloidin crosslinks actin filaments. Clathrin-dependent endocytosis does not occur in the absence of intracellular potassium (K^+) (Ivanov, 2008) and K^+ free cytoplasmic solutions had no effect on this endocytosis. Neither did the dynamin inhibitory peptide, which prevents amphiphysin-dynamin binding and therefore CCP formation (Grabs et al., 1997). Lastly absence of ATP and GTP had no effect on endocytosis. This marked independence from conventional endocytic proteins strongly suggests the endocytosis seen in TMEM16F-null cells is that described previously as MEND.

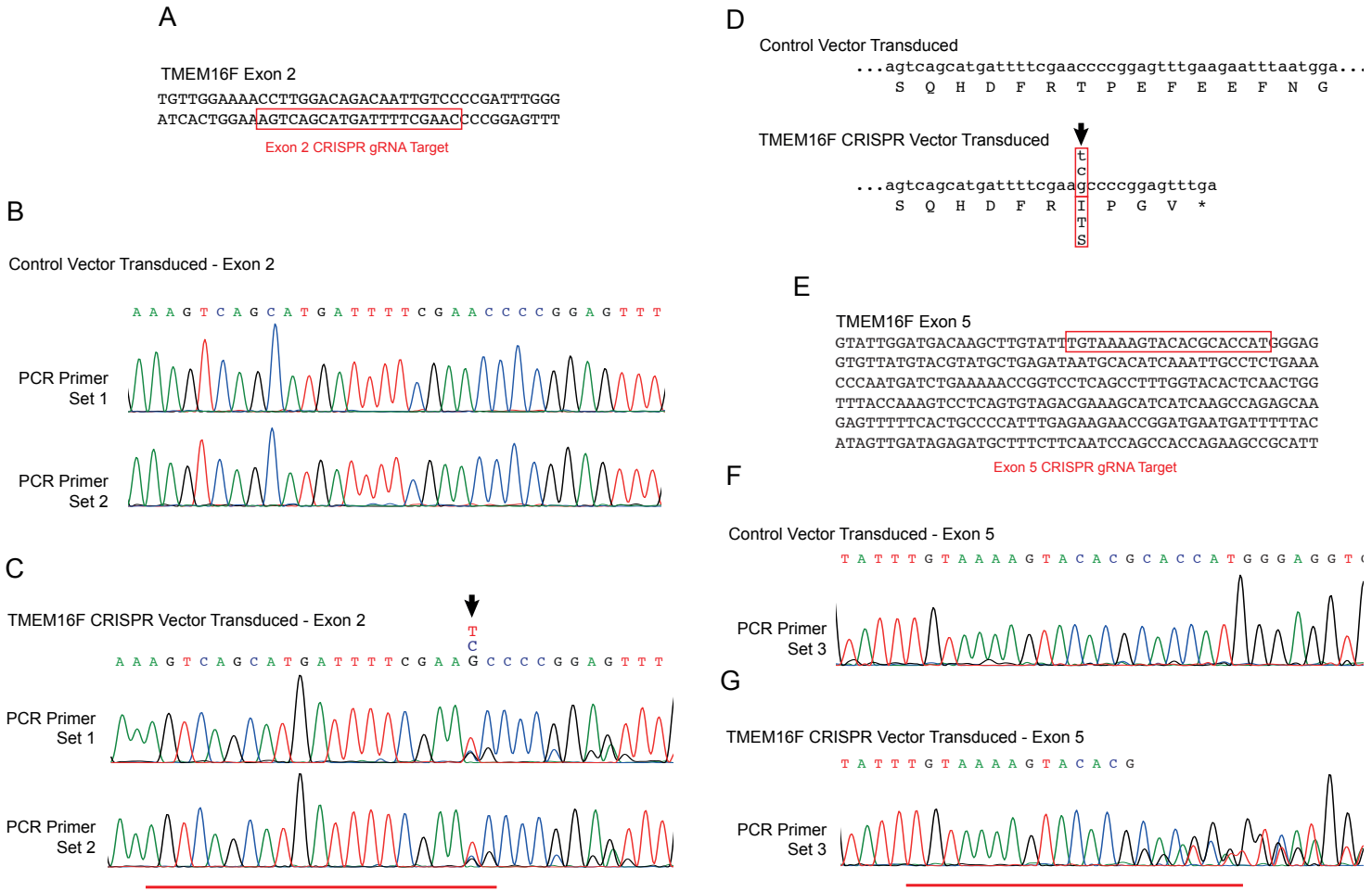

Figure 3.5 **CRISPR-Cas9 mediated TMEM16F deletion in Jurkat T cells.** TMEM16F was edited using the lentiviral vector-based CRISPR-Cas9 system as described (PubMed 25075903). **A** TMEM16F Exon 2 and target sequence is shown. **B** Two sets of primers were used to amplify TMEM16F Exon 2 from vector-only transduced Jurkat T cell genomic DNA. The two amplicons were then sequenced. **C** The same amplicons were sequenced from a clone transduced with TMEM16F Exon 2-targeted CRISPR-Cas9 lentiviral vector. **D** the result of the single nucleotide insertion in Exon 2 on the amino acid sequence. A stop codon results 10 nucleotides downstream of the insertion that truncates TMEM16F from 910 to 50 amino acids. **E** TMEM16F Exon 5 and target sequence. **F** One primer set were used to amplify TMEM16F Exon 5 from vector-only transduced Jurkat T cell genomic DNA and sequenced G The same amplicon was sequenced from a clone transduced with TMEM16F Exon 5-targeted CRISPR-Cas9 lentiviral vector.

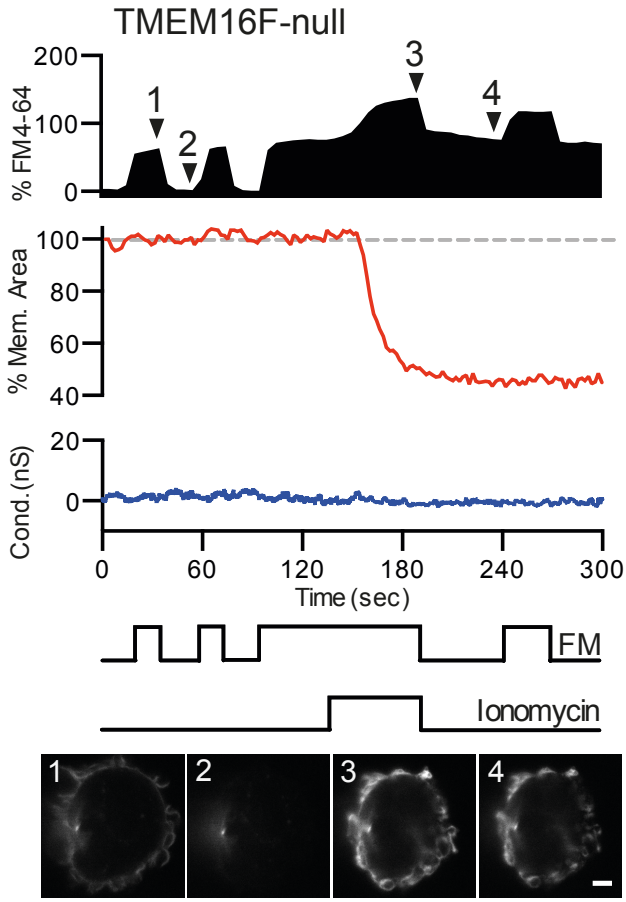

Figure 3.6 **Ca^{2+} triggers massive endocytosis in the absence of TMEM16F.** Real-time membrane area (capacitance) and transmembrane ion movement (conductance) of TMEM16F-null Jurkat T cells were measured by whole-cell patch-clamp with concurrent confocal imaging using standard Ringer and cytoplasmic solutions. FM4-64 and ionomycin were applied and washed as shown. Membrane area and FM4-64 fluorescence are shown as percentage of baseline values. Images are of FM4-64 binding to the cell at indicated time points with a scale bar of 5μm.

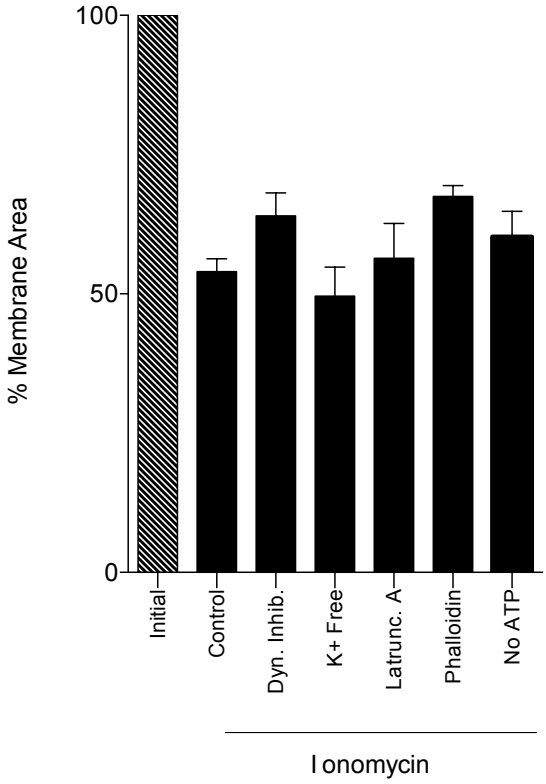

Figure 3.7 Massive endocytosis is independent of classical endocytic machinery. Percentage of initial membrane area at 30s after ionomycin treatment of TMEM16F-null Jurkat cells is shown as compared to initial value. Conditions were standard extracellular Ringer and cytoplasmic solution (Control); standard solutions with added 3μM cytoplasmic dynamin inhibitory peptide, symmetrical 3μM Latrunculin A or cytoplasmic 10μM Phalloidin, K^+-free symmetrical NMDG Aspartate solutions and standard extracellular Ringer with cytoplasmic solution lacking ATP and GTP.

3.2.4 Intracellular Spermine blocks TMEM16F function in a dose-dependent manner

Introduction of intracellular polyamines such as spermidine, spermine and ethalenediamine (EDA) is able to convert cellular responses from exocytosis to endocytosis (Lariccia et al., 2011).

Following our findings that TMEM16F is the Ca^{2+} sensor for large exocytosis and that in the absence of TMEM16F MEND occurs, we hypothesised that intracellular polyamines were able to block TMEM16F.

Figure 3.9 shows the effect of intracellular spermine on Ca^{2+} activated membrane movements and TMEM16F channel activity in WT Jurkat T cells. At 250μM spermine, cells underwent an intermediate phenotype of partial endocytosis followed by exocytosis as shown in Figure 3.9A. At 500μM all WT cells underwent endocytosis (Figure 3.9B). This change in phenotype was matched by a dose-dependent decrease in peak membrane conductance through TMEM16F.

These data demonstrate that intracellular spermine inhibits both TMEM16F-induced exocytosis and ion conduction.

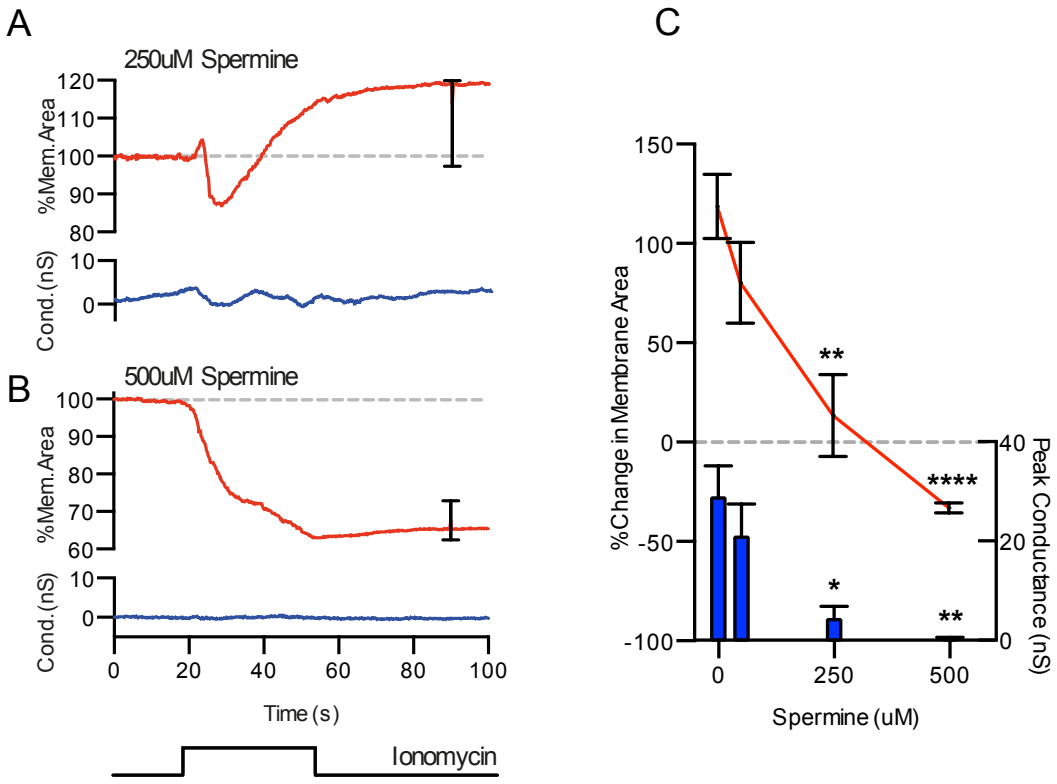

Figure 3.8 **Spermine blocks TMEM16F function in a dose-dependent manner. A,B,C** WT Jurkat cells were patch-clamped with spermine added to cytoplasmic solutions at given concentrations and held for at least 200s before recordings began.

3.2.5 TMEM16F-regulated membrane movements are conserved across cell types

TMEM16F is ubiquitously expressed across cell types (Tian et al., 2012). We next wanted to establish whether TMEM16F-induced exocytosis is also ubiquitous across cell types. We therefore conducted whole-cell patch clamp experiments on THP-1 macrophages and NCX1-expressing HEK293 cells. Ca^{2+} activates a large exocytosis and membrane conductance in THP-1 cells (Figure 9A). Membrane area decrease following exocytosis is likely to be due to microvesicle shedding (MacKenzie et al., 2001).

Next we tested WT HEK293 cell responses with Ca^{2+} transients produced by NCX1 reverse exchange. The NCX1 sodium-calcium exchanger is physiologically important in removing Ca^{2+} from the cytoplasm by employing the normal sodium gradient. By loading cells with sodium in whole-cell patch-clamp experiments, and then placing cells in Ca^{2+} -containing extracellular solution, this 'reverses' the exchanger leading to a Ca^{2+} transient. This produces a membrane conductance and also an outward current, as three sodium ions are exchanged for every one Ca^{2+} ion.

TMEM16F was deleted in HEK293 cells employing the same strategy outlined in Figure 3.5, targeting Exon 5 on TMEM16F. Figures 3.8B and 3.8C show Ca^{2+} activated membrane movements in HEK293 WT and TMEM16F-null cells. Ca^{2+} influx via NCX1 induces a ~20% increase in plasma membrane area in WT cells which is converted to MEND of ~50% plasma membrane in TMEM16F-null cells. Membrane conductance is not significantly changed between WT and TMEM16F-null cells. Though responses closely correspond to those shown in Jurkat T cells, it is of note that quantity of exocytosed membrane is significantly smaller in HEK293 cells.

These data indicate that the findings detailed so far in this chapter are broadly applicable across cell types, occurring irrespective of whether Ca^{2+} influx is transient (via NCX1 reverse exchange) or sustained (via ionophore).

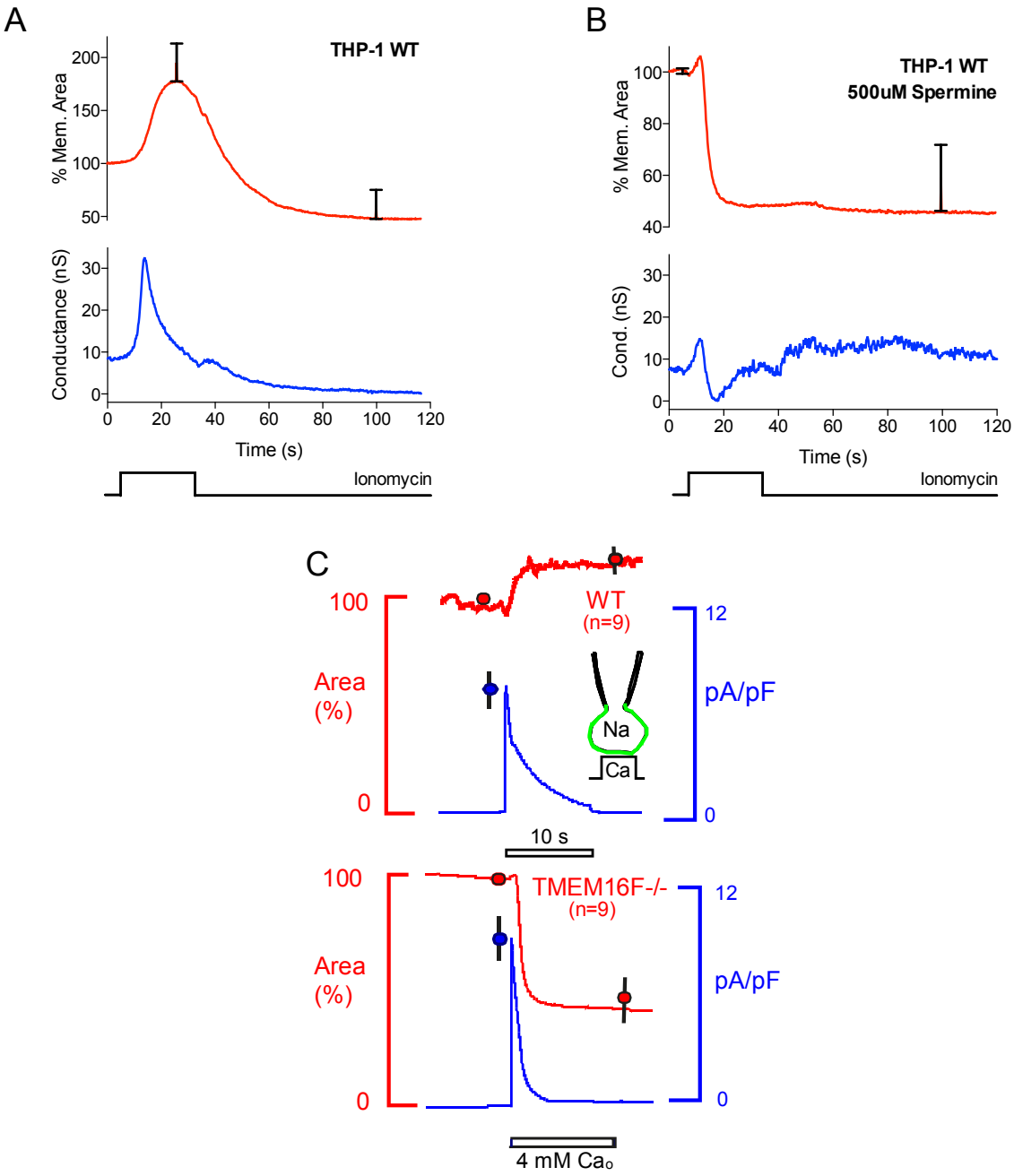

Figure 3.9 **TMEM16F regulated membrane movements occur across cell types and with Ca^{2+} influx initiated by NCX1 reverse exchange.**

WT THP-1 cells were treated with 5μM ionomycin either with standard cytoplasmic solutions (**A**) or cytoplasmic solutions containing 500μM spermine (**B**). **C** WT and TMEM16F-null TREx cells that express the cardiac Na/Ca^{2+} exchanger, NCX1, were patch clamped using solutions that maximize Ca^{2+} influx via outward $3Na^{+}$:$1Ca^{2+}$ exchange current when extracellular Ca^{2+} is applied. TMEM16F-deficient TreX cell line was produced by CRISPR Cas9 targeting to Exon 5.

3.2.6 TMEM16F-induced phospholipid scrambling and microvesicle shedding are coupled to exocytosis

In 2010 it was discovered that TMEM16F is the Ca^{2+} activated phospholipid scramblase and that it is the loss of TMEM16F that leads to the bleeding disorder Scott syndrome (Suzuki et al., 2010). Here we have demonstrated that TMEM16F regulates a large exocytosis of internal membranes. We therefore next examined the relationship between exocytosis and phospholipid scrambling.

Figure 3.10A shows the phenotype of WT and TMEM16F-null cells before and after treatment with ionomycin. Cells were probed with the fluorochrome-labelled PS binding protein Annexin V, as well as with the Ca^{2+} sensitive dye Fluo-4 AM. In WT cells, Ca^{2+} influx, confirmed by increased Fluo-4 fluorescence, leads to AnxV binding to PS on the outer leaflet of the plasma membrane (Figure 3.10A). In TMEM16F-null cells AnxV does not bind to cells following Ca^{2+} influx, indicating that membrane scrambling has not occurred. This data confirms that TMEM16F is necessary for Ca^{2+} activated plasma membrane phospholipid scrambling.

Next we aimed to establish how the kinetic of phospholipid scrambling related to that of TMEM16F induced exocytosis. It was not possible to use AnxV for this experiment due to the slow binding kinetic of AnxV to PS. Prof. Hilgemann has developed a probe for real-time analysis of phospholipid scrambling, which consists of the cationic peptide Heptalysine, composed of seven Lysines conjugated to Rhodamine (K7-Rho). This cationic peptide binds quickly to anionic PS and so is suitable for real-time microscopy. K7-Rho is also readily washed in the same way as FM4-64 dye, which allows for insights into the directionality of membrane movements. As Figure 3.10B Image 1 shows, in resting cells that have PS only on the inner leaflet of their plasma membrane, no K7-Rho binds to the membrane.

The kinetic of TMEM16F-induced exocytosis and that of plasma membrane phospholipid scrambling is identical (Figure 3.10B). As discussed for Figure 3.4, a slow shedding of plasma membrane microvesicles follows TMEM16F- induced exocytosis. In a similar approach to that used in Figures 3.1 and 3.6, K7-Rho was periodically washed from the membrane throughout the experiment. Complete

reversibility of K7-Rho binding throughout the decrease in capacitance corroborates the findings of Figure 3.4, namely that the slow loss in plasma membrane area is due to shedding of membrane and not endocytosis. Whole WT Jurkat T cells stimulated with ionomycin in Ringer containing K7-Rho showed similar responses (Video 3.2).

Phospholipid scrambling also occurs during apoptosis. Figure 3.11 shows experiments on WT and TMEM16F-null Jurkat T cells, where gene expression was deleted by targeting either Exon 2 or Exon 5. Cells were stimulated with ionomycin for 15 minutes or treated overnight with Etoposide, a topoisomerase inhibitor that triggers apoptosis via the DNA damage pathway (Karpinich et al., 2002). Though Ca^{2+}-activated scrambling is blocked in TMEM16F-null cells, apoptotic scrambling is unaffected. This concurs with recent data from others that implicate other 'scramblase' machinery involved in apoptosis-induced scrambling (Segawa et al., 2014; Suzuki et al., 2013).

Finally, as demonstrated in Figures 3.4 and 3.10, microvesicle shedding follows TMEM16F-induced exocytosis in WT cells. The mechanism for Ca^{2+} induced microvesicle shedding, which occurs in a wide variety of cell types, remains unknown. Following our previous finding that microvesicle shedding follows TMEM16F-induced exocytosis, we hypothesised that TMEM16F was necessary for Ca^{2+} activated microvesicle shedding. We quantified shed microvesicles using a FACS-based assay. Cells and vesicles were pelleted at high speed (3000 rpm for 10 mins) and subcellular events gated by FSC/SSC (Figure 3.12). Apoptotic bodies and microvesicles were separated using a cell-permeable DNA dye that stained DNA fragments present only in apoptotic bodies. Figure 3.12 shows shed microvesicles only in WT cells and not in TMEM16F-null cells. This indicates that TMEM16F is necessary for Ca^{2+} activated microvesicle release in Jurkat T cells.

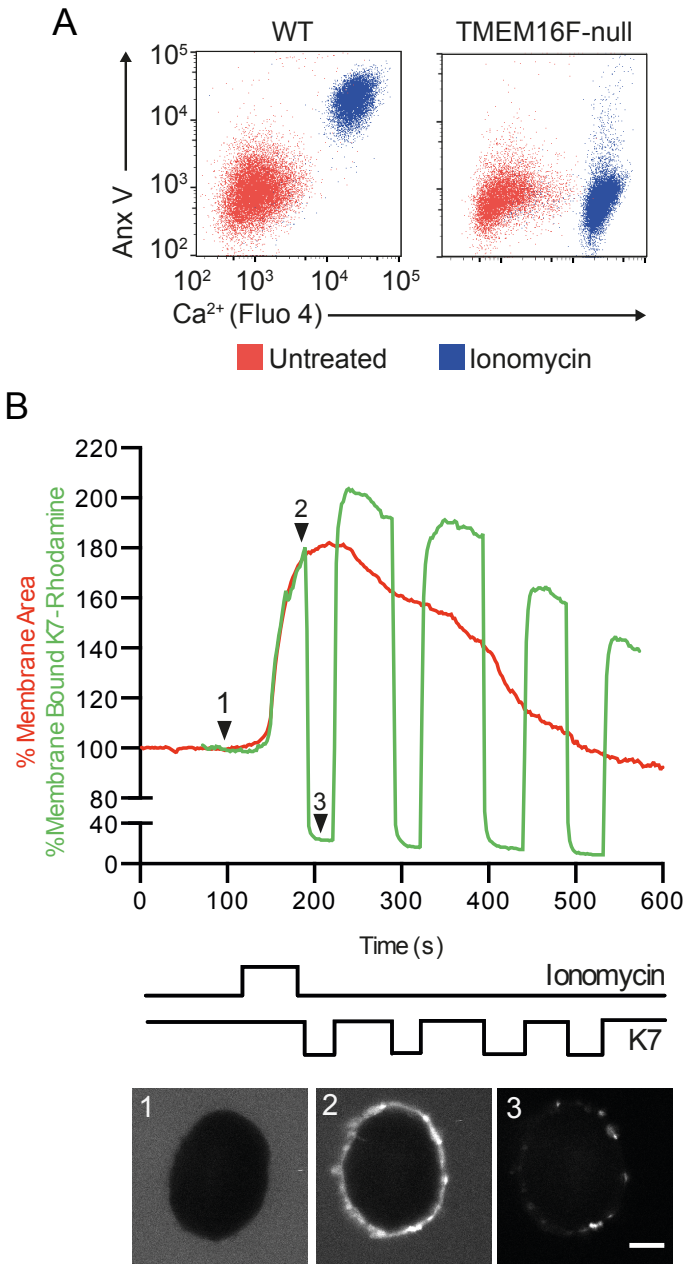

Figure 3.10 **TMEM16F-induced phospholipid scrambling and membrane exocytosis proceed with identical kinetics. A** Fluo4-AM loaded WT and TMEM16F-null Jurkat T cells were treated with 5μM Ionomycin for 15 min and stained with Annexin V. **B** Real-time membrane scrambling and membrane area were measured with Polylysine-Rhodamine (K7) membrane binding with concurrent whole-cell patch-clamp of WT Jurkat T cells using standard solutions following ionomycin treatment. Images are of K7 binding to the cell at indicated time points with scale bar representing 10μm.

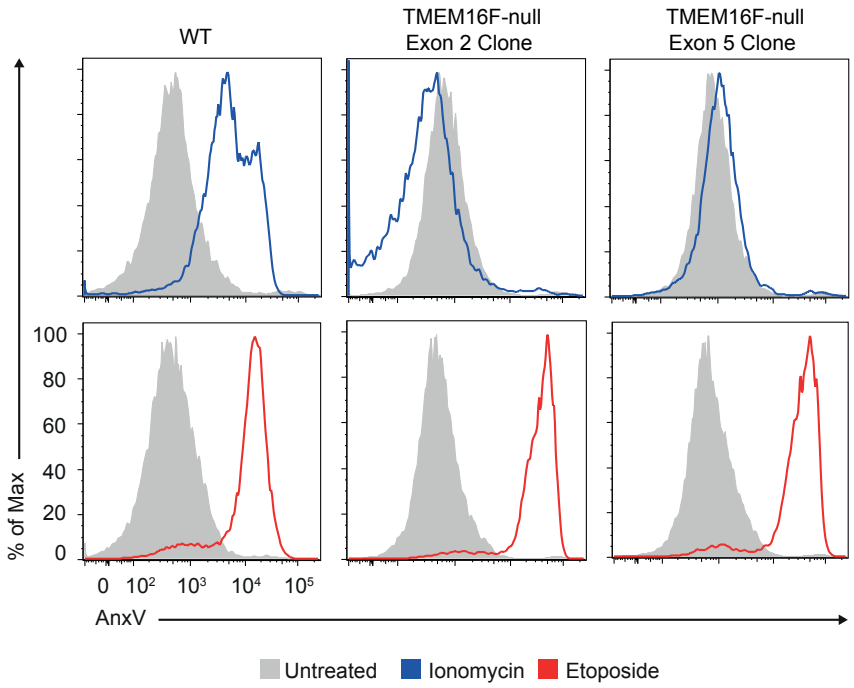

Figure 3.11 **TMEM16F deletion abolishes Ca^{2+} activated but not apoptotic plasma membrane scrambling.** WT and TMEM16F-null Jurkat T cells CRISPR-targeted to either Exon 2 or Exon 5 were treated with 5μM ionomycin for 15 mins or 2μM Etoposide overnight and stained with Annexin V and compared to untreated cells.

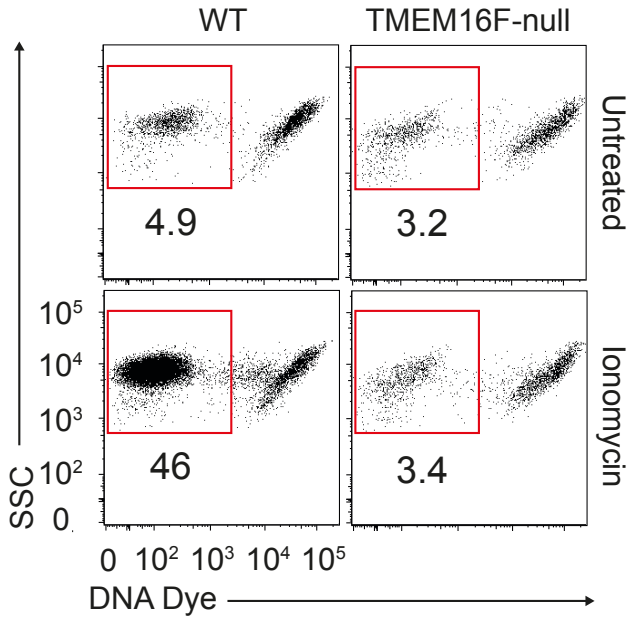

Figure 3.12 **TMEM16F is necessary for Ca^{2+} activated microvesicle shedding.** WT Jurkat T cells were treated for 15 min with ionomycin in Ringer and stained with DNA dye. Subcellular sized events were gated and apoptotic bodies distinguished from microvesicles by DNA dye uptake. Numbers are percentage of total events.

3.3 Discussion

3.3.1 TMEM16F is a Ca^{2+} sensor for exocytosis

The fusion of intracellular vesicles to the plasma membrane is a key function of living cells, from yeast to sea urchins to neurons. Regulation of exocytosis is necessary to pair specific stimuli with vesicle fusion. This is important for the timely secretion of molecules (e.g. cytotoxic granzyme and perforin by T lymphocyte effectors), expression of transmembrane proteins (e.g. aquaporin 2 in the kidney duct cells) and addition of new membrane to the plasma membrane (e.g. during membrane repair). The key controller of regulated exocytosis is intracellular Ca^{2+}.

The last 20 years have seen significant advances in the understanding of the only known mechanism of Ca^{2+} activated membrane fusion. Those awarded the Nobel Prize in 2013 pioneered the discovery of the SNARE/synaptotagmin model of vesicular trafficking that has been extensively studied in the context of neurotransmitter release into the neuronal synapse. The proteins involved also regulate fusion in other tissues including T lymphocyte lytic granule exocytosis (Matti et al., 2013). The Ca^{2+} sensors for this type of exocytosis are the synaptotagmins, proteins that sit in the vesicular membrane and possess two Ca^{2+} binding C2 domains.

Though the protein players in the SNARE/Syn model have been identified and characterised, there are many mysteries yet to be solved in the field of regulated exocytosis. Important questions in the SNARE/synaptogamin model remain unanswered, not least how synaptotagmin-Ca^{2+} binding catalyses vesicular fusion. There is also growing uncertainty as to whether this model describes the only mechanism of Ca^{2+} activated exocytosis. Knockout of multiple synaptotagmin isoforms fails to block Ca^{2+} activated exocytosis in secretory (Schonn et al., 2008) and non-secretory cells (Wang and Hilgemann, 2008). No Ca^{2+} sensors have been identified that account for the large exocytosis seen during membrane repair.

We first set out to establish how plasma membrane area changes with Ca^{2+} influx in WT Jurkat T cells. Treatment with 5μM ionomycin in physiological 2mM extracellular Ca^{2+} triggers ~100% increase in plasma membrane area over ~30 seconds (Figure 3.1). Ionomycin concentrations down to 2.5μM elicit the same response, but with a delay of up to several minutes (data not shown). This response is conserved across cell types with large exocytosis also occurring in THP-1 macrophages and a smaller exocytosis in HEK293 cells (Figure 3.9). This exocytosis has a high Ca^{2+} threshold and so appears alike to that described in RBL and BHK cells by Wang et al. and Yaradanakul et al. also suggesting it is a common response across species (Wang and Hilgemann, 2008; Yaradanakul et al., 2008). Others have described exocytosis in response to large Ca^{2+} influx triggered by membrane injury (McNeil and Kirchhausen, 2005). Though different protocols were used in those experiments, with none of them employing real time capacitance recording, it is likely that the large exocytosis we see here is the same as that triggered in membrane repair. This will need to be investigated in further work.

We next looked for clues as to the mechanism of this large exocytosis. Whole-cell patch clamp of cells allows for the detection of conductance and current as well as capacitance. A conductance peak always accompanies exocytosis in WT Jurkat T cells (Figure 3.1). Importantly, the rate of change of membrane area (dCm/dt), calculated from capacitance records (Cm) and filtered at 1 Hz, matches the time course of conductance with the peak of conductance occurring within 3 seconds of the maximal rate of exocytosis. Others have seen a close association between exocytosis and conductance, related to 'fusion pore' opening (Spruce et al., 1990). As Figure 1.2 shows, in the final stage of membrane fusion a pathway opens between the vesicular lumen and the extracellular space termed the 'fusion pore'. This produces a small conductance which is detectable during exocytosis in some experimental setups. In our experiments, conductance is defined as the membrane current occurring at the end of a square wave voltage pulse; therefore fusion pore conductances should not contribute to our measurements. By setting the membrane potential to +20mV we were able to induce an inward current, demonstrating that the conductance corresponds to the flow of ions between the extracellular space and the cytoplasm and therefore the opening and closing of a Ca^{2+} activated ion channel. The

conductance profile is typical of a Ca^{2+} activated channel, with Ca^{2+} both activating and inactivating the channel.

Due to close phenotypic similarities between the Ca^{2+} activated channel we were observing and those of TMEM16F described previously (Picollo et al., 2015), we next deleted TMEM16F in Jurkat T cells using the CRISPR-Cas9 method. In response to Ca^{2+} influx TMEM16F-null cells display no Ca^{2+} activated conductance, exocytosis is blocked and instead MEND occurs (Figure 3.6). TMEM16F-null HEK293 cells respond in the same way, with MEND replacing exocytosis (Figure 3.9C). This finding reveals that the Ca^{2+} sensor for large Ca^{2+} activated exocytosis is TMEM16F and uncovers an entirely novel mechanism of membrane fusion.

Following our initial observation that exocytosis is accompanied by a flux of ions through the channel, we next asked whether this flux was necessary for exocytosis. Indeed, replacing all ions with sucrose completely blocks exocytosis while partial inhibition can be achieved by replacing only intracellular ions with sucrose, or by replacing all ions with NMDG and aspartate (Figure 3.3). Under conditions of partial inhibition by ion replacement, the amount of membrane exocytosed is significantly reduced while the kinetics of exocytosis remain the same. This suggests that ion conduction through TMEM16F is directly linked to the mechanism of exocytosis. TMEM16F shares no features with any of the SNARE/Synaptotagmin proteins known to be the machinery of exocytosis in many cell types. Neither intracellular tetanus toxin light chain, which cleaves synaptobrevin-2, nor the absence of ATP and GTP, inhibited fusion. It is likely therefore that this mechanism of exocytosis fits in a new, distinct paradigm.

The close association between channel opening and exocytosis (Figure 3.2) and the apparent resemblance to a ‘fusion pore’ may be informative in conceiving possible models for the mechanism of TMEM16F-induced exocytosis. The SNARE complex has a three-step process for fusion (Figure 1.2). Vesicle membranes are firstly docked in close proximity to the plasma membrane; with an increase in intracellular Ca^{2+} the SNARE complex zippers, bending the membranes and bringing them together to form a stalk. This stalk separates, leading to a hemifusion intermediary. Then finally the fusion pore opens, completing fusion. In this way the SNARE machinery

operates much like a channel, introducing a conduit between the lumen of the vesicle and the extracellular space.

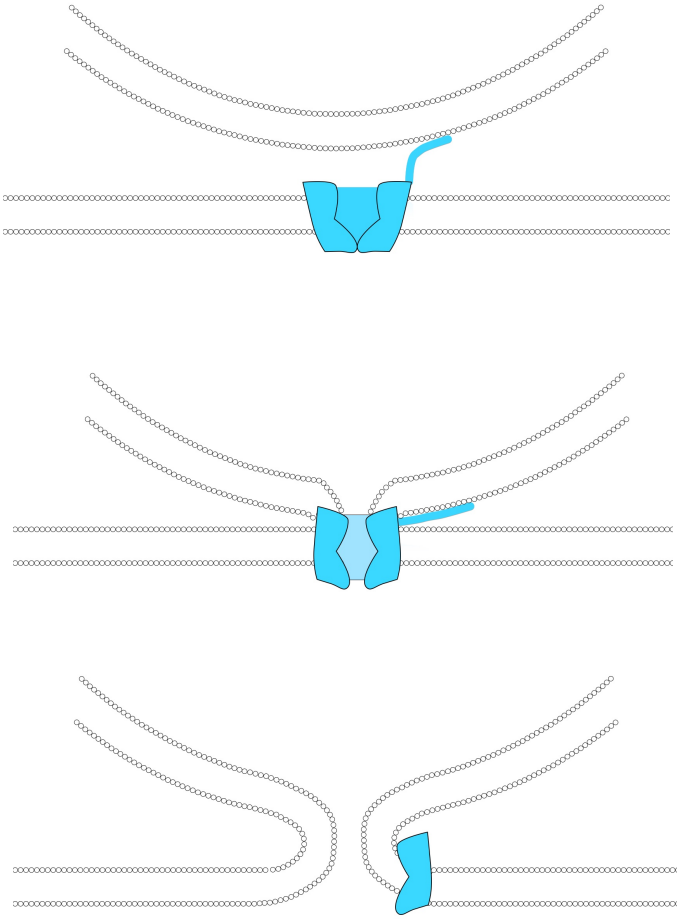

Figure 3.13 **A model of TMEM16F-induced exocytosis**

An equivalent hypothetical mechanism for membrane fusion involving TMEM16F is presented in Figure 3.13. This is of course speculative and will need much further work to verify and refine. TMEM16F alone may carry out some of the functions of SNARE proteins. Firstly for membrane docking, it may be relevant that the yeast homologue of the TMEM16 family, Ist2, functions as a tethering protein between the ER and the PM. It is structurally similar to TMEM proteins with eight transmembrane domains. Ist2 is present in the ER and has a C-terminal domain that

binds to anionic phospholipids on the inner leaflet of the PM. Whether TMEM16F is able to tether membranes close to the PM docked for exocytosis in a similar way to Ist2 will be important to establish. Secondly, Ca^{2+} channel opening could be equivalent to fusion pore opening in breaking PM continuity and allowing vesicular membranes to move into the channel space. TMEM16F channel has a large lumen, described previously as a '6Å pore' (Yang et al., 2012). Ion movement through the channel may be necessary to bring the membranes together and into the channel space. Like all ion channels, TMEM16F is a linear protein that curves around to form a circular channel structure. The linearization of TMEM16F, linking the internal membrane with the PM, may be the final step of fusion in the same way as SNARE complex separation.

3.3.2 Consequences of TMEM16F-induced exocytosis

As discussed earlier, large Ca^{2+} influx leads to microvesicle shedding and phospholipid scrambling for which the mechanisms remain unclear. We sought to better understand whether these are linked to TMEM16F-induced exocytosis.

3.3.2.1 Microvesicle shedding

We were interested in the fate of the plasma membrane following TMEM16F-induced exocytosis. Extended capacitance recording and microscopy of ionomycin-treated WT Jurkat T cells demonstrated a loss of plasma membrane area following large exocytosis that is a consequence of microvesicle shedding, not endocytosis (Figures 3.4 & 3.10). Microvesicle shedding immediately follows TMEM16F-induced exocytosis ,and furthermore in TMEM16F-null cells microvesicle shedding did not occur (Figure 3.12). This strongly implicates TMEM16F as essential for large Ca^{2+} activated microvesicle shedding. This serves to explain the findings from studies on Scott syndrome patients that demonstrate defective release of microvesicles from platelets as well as defective membrane scrambling (Sims et al., 1989; Toti et al., 1996).

A delay has consistently been observed between Ca^{2+} influx and microvesicle release (Cocucci et al., 2007; Lee et al., 1993; MacKenzie et al., 2001; Moskovich and Fishelson, 2007; Stein and Luzio, 1991). It has been hypothesised that this is due to a need for preceding exocytosis (Cocucci et al., 2007). Our data supports this hypothesis and furthermore TMEM16F is also a delayed activation channel with channel opening delayed by minutes at lower intracellular Ca^{2+} concentrations (Grubb et al., 2013; Kim et al., 2015). Both these factors could contribute to a delay between Ca^{2+} influx and microvesicle release.

Though we have established that TMEM16F is necessary for microvesicle shedding in this context of large Ca^{2+} influx, this explanation may not necessarily apply to other contexts where plasma membrane derived microvesicles are released. Microvesicle release in the immune synapse and following membrane injury rely on protein components of the ESCRT complex that is normally associated with endosomal membranes (Choudhuri et al., 2014; Jimenez et al., 2014). It is unclear how these endosomal proteins come to be associated with the plasma membrane. The finding in this case that exocytosis precedes microvesicle shedding could suggest that factors that promote budding and fission of microvesicles are recruited to the membrane by fusion of endosomal membrane carrying ESCRT proteins whether by a SNARE or TMEM16F mediated mechanism.

3.3.2.2 Phospholipid scrambling

A long standing question in physiology has been how phospholipids can be rapidly scrambled following specific stimuli such as Ca^{2+} influx and apoptosis. Analogous to membrane ‘scrambling’ experimentally is the appearance of PS on the outer leaflet of the plasma membrane. It has been supposed that a protein ‘scramblase’ is capable of translocating the hydrophilic heads of phospholipids through a protein domain, allowing their bidirectional movement down a concentration gradient and thus disrupting the normal phospholipid asymmetry. This model existed long before the discovery that TMEM16F is the Ca^{2+} activated phospholipid scramblase. Recently the crystal structure for a fungal TMEM protein was solved and the authors hypothesised that a hydrophilic cleft found in the structure of the protein was the ‘scrambling

domain' (Brunner et al., 2014). Others have recently confirmed that this sequence in mammalian TMEM16F is indeed responsible for phospholipid scrambling (Yu et al., 2015). This 'scrambling domain' would fit perfectly with the long held model.

Here we confirm previous reports that TMEM16F is necessary for Ca^{2+} activated phospholipid scrambling and that this is not due to an inhibition of Ca^{2+} influx (Figure 3.10A). Employing real-time capacitance recording and confocal microscopy using the K7-Rho probe, we show that the kinetics of exocytosis and anionic lipid exposure are identical i.e. the rate of membrane insertion exactly matches that of anionic lipid appearance (K7-Rho binding) on the outer leaflet of the plasma membrane. This close association strongly suggests that scrambling and exocytosis are linked. The first possibility is that TMEM16F is indeed able to translocate phospholipids and that this collapse in phospholipid asymmetry may be the trigger for membrane fusion. The second is that TMEM16F is facilitating exocytosis by another mechanism and that it is the fused membrane that is not asymmetric i.e. has PS on its outer leaflet.

The second possibility has been suggested previously, as described in Chapter 1. Mast cell degranulation leads to membrane scrambling with patches of PS emerging on the membrane at sites of granule exocytosis (Demo et al., 1999). Other groups have provided evidence that Ca^{2+} activated exocytosis of lysosomes may be the cause of membrane scrambling. Here we show that TMEM16F triggers large membrane exocytosis and that it may be unlikely that in doubling the quantity of plasma membrane, all that membrane would be perfectly asymmetric. We found no way of inhibiting TMEM16F induced exocytosis without blocking the function of the channel, so were unable to definitively establish causality between fusion and scrambling. The evidence however points strongly towards the model that membrane exocytosis is the cause of PS emergence on the outer leaflet.

But what of the evidence implicating a "scrambling domain" in TMEM16F as necessary for phospholipid scrambling? Though the authors of recent papers have demonstrated that a domain is necessary for phospholipid scrambling, there is no direct evidence that phospholipids do scramble through that domain i.e. no crystal structure of phospholipids in complex with the domain. This domain could equally

be necessary for TMEM16F induced exocytosis. This alternative hypothesis could explain some of the more puzzling findings made by others. Yang et al found that heterologous overexpression of TMEM16F was not sufficient to enhance membrane scrambling (Yang et al., 2012). With our hypothesis, it would be the available pool of internal, fusible membrane that would limit scrambling, not TMEM16F expression.

Key in definitively uncovering the mechanisms behind microvesicle shedding and phospholipid scrambling will be to identify the membrane that is exocytosed. It is remarkable that a pool equivalent to the whole plasma membrane is in readiness to exocytose within 30 seconds of large Ca^{2+} influx. Characterisation of both the properties of that membrane and the proteins that are associated with it may provide important answers. As detailed in Chapter 1 lysosomes and 'enlargesomes' are shown to fuse with the PM following large Ca^{2+} influx, but work is necessary to clarify this in the context of TMEM16F-induced exocytosis.

For many years it was supposed that the scrambling machinery for Ca^{2+} induced and apoptosis-induced scrambling was shared (Bevers and Williamson, 2010). Ca^{2+} influx occurs during apoptosis following the loss of plasma membrane integrity and dysfunction of Ca^{2+} ATPase pumps. This Ca^{2+} influx may therefore lead to scrambling by TMEM16F and provide the mechanism for apoptotic scrambling. Figure 3.11 demonstrates that TMEM16F is not necessary for apoptotic scrambling. This agrees with recent discoveries of two mechanisms for apoptotic scrambling. Firstly Segawa et al. found that the phospholipid flippase ATP11C is degraded by caspases during apoptosis via a caspase recognition site, mutation of which inhibits apoptotic scrambling (Segawa et al., 2014). So loss of phospholipid asymmetry follows deficient flippase activity rather than a lipid 'scramblase' in apoptosis. Secondly the same group (Suzuki et al., 2013) found that Xk-related protein 8 (Xkr8) also mediates apoptotic scrambling, activated by a caspase-3 cleavage site. The mechanism for phospholipid scrambling by Xkr8 is however unknown.

3.3.3 Ca^{2+} activated MEND in the absence of TMEM16F activity

This work presents two opposing responses to large Ca^{2+} influx that are regulated by TMEM16F activity. In WT cells the plasma membrane area rapidly doubles while in

TMEM16F-null cells, large Ca^{2+} influx triggers the endocytosis of ~50% membrane area in ~ 20 seconds (Figure 3.1 & 3.6). We were interested in the mechanism underlying this significant endocytic event, and how these two opposing phenomena may be physiologically regulated.

Due to the scale and speed of this endocytosis we hypothesised that it was the same seen in BHK, HEK293 and cardiomyocytes coined as MEND (Lariccia et al., 2011). This endocytosis is characterised by its independence from classical endocytic and protein machinery. Our next experiments therefore focussed on establishing whether the endocytosis we saw in Jurkat T cells relied on any of these proteins (Figure 3.7).

First we targeted the clathrin endocytic pathway that relies on intracellular K^+ as well as the protein dynamin. Neither removal of K^+ nor an inhibitory peptide, which blocks dynamin associating to CCPs, had any effect on endocytosis. Next we targeted the cytoskeleton, important for pathways of endocytosis including macropinocytosis and dorsal ruffle endocytosis. Endocytosis was not inhibited by either preventing actin polymerisation with Latrunculin or crosslinking actin with Phalloidin. Lastly, removal of ATP had no effect on endocytosis. This phenotype matches that seen in Lariccia et al. 2010 and strongly suggests this endocytosis is that described as MEND.

The Ca^{2+} sensor and mechanism for MEND are unclear despite much investigation. Most mechanisms of endocytosis involve the assembly of a protein scaffold that bends the plasma membrane, bringing the curved edges together and then pinching off the endocytic vesicle. Previous experiments investigating the mechanism of MEND have ruled out many Ca^{2+} activated proteins including proteases in the mechanism of MEND. Focus has therefore turned from a protein-based mechanism to one where the membrane itself is compositionally changed leading to inward curvature. Following the observation in WT BHK and HEK293 cells that exocytosis always precedes MEND, Tam et al. presented evidence that the exocytosis of acid sphingomyelinases was the mechanism of MEND (Tam et al., 2010). ASM metabolises sphingomyelin to phosphatidylcholine and ceramide; ceramide domains on the outer leaflet of the plasma membrane curve the membrane inwards. This data

however has not been reproducible by others and subsequent findings put the model into question (Hilgemann et al., 2013; Lariccia et al., 2011). One of the main findings incompatible with the idea that ASM secretion is the mechanism for MEND is that exocytosis can be uncoupled from endocytosis by the addition of physiological concentrations of polyamines to the cytoplasmic solution. Polyamines, spermadine, spermine and putrescine are metabolites of the amino acid L-Orthinine and are ubiquitous in eukaryotic cells. They are cationic compounds present at several hundred micromolar concentrations in cells (Igarashi and Kashiwagi, 2000). They have many roles in cell function from gene expression (Gerner and Meyskens, 2004) to enzyme regulation (Coburn et al., 2002). Importantly they also regulate ion channels including NMDA receptors and the inward rectifying K^+ channel (Kir) (Pearson and Nichols, 1998; Williams et al., 1991).

The mechanism of exocytosis inhibition by polyamines was previously unclear and due to their diverse effects on cell function the answer was not obvious (Lariccia et al., 2011). Following our finding that TMEM16F is the Ca^{2+} sensor for this large exocytosis, coupled with the fact that polyamines modulate the activity of the ion channels, we hypothesised that polyamines were blocking TMEM16F and therefore exocytosis. Indeed with increasing concentrations of spermine, TMEM16F peak conductance is significantly reduced and accompanies a switch of phenotypes from exocytosis to endocytosis (Figure 3.8). At 500μM intracellular spermine conductance is completely blocked and endocytosis occurs. With the Kir channel, cationic spermine inhibits by binding to anionic pockets in the channel (Guo and Lu, 2003; Stanfield and Sutcliffe, 2003). Further work will be needed to establish how intracellular polyamines are able to block TMEM16F. Application of extracellular spermine did not block the channel (data not shown) though treatment with cell-permeable EDA had the same effect as spermine in Larricia et al.

These data present a possible mechanism by which cells can physiologically regulate TMEM16F activity, and therefore the plasma membrane response to large Ca^{2+} influx i.e. exocytosis, endocytosis, phospholipid scrambling and microvesicle shedding. Indeed a study carried out on RBC ghosts demonstrated that resealing ghosts in the

presence of spermine recapitulates the phenotype of Scott Syndrome cells (Bucki et al., 1998).

Our data could guide the design of therapeutics that block TMEM16F. PS exposure on platelets is an important step in normal clotting where it provides a surface for activation of the coagulation cascade, lack of which lead to the bleeding disorder Scott Syndrome. Importantly this syndrome has no other reported major systemic symptoms (Sims et al., 1989; Toti et al., 1996). TMEM16F has therefore been suggested as a target for anticoagulation therapy (Morel et al., 2011). Compounds that share the characteristics of polyamines and are cell permeable would be a good starting point for drug screening.

CHAPTER 4

Ca^{2+} ACTIVATED PLASMA MEMBRANE PROTEIN SORTING IN T LYMPHOCYTES

4.1 Introduction

The regulation of protein expression on the surface of cells is vital for effective intercellular communication, allowing multicellular organisms to coordinate the actions of billions of specialised cells. T lymphocytes, which possess the dangerous ability to kill other cells, must be tightly controlled. Having received signals through a variety of receptors, they must integrate these messages through a network of finely balanced stimulatory and inhibitory signalling cascades, and respond appropriately. The consequences of either over-zealous or inadequate T lymphocyte immunity can be devastating to the organism. The kinetics of receptor expression is therefore important in regulating lymphocyte function, for example the T cell receptor is rapidly downregulated following antigen presentation, while the co-receptor PD-1 is upregulated following TCR signalling. In this way, regulating expression in turn regulates signalling.

With a growing understanding of the functional roles of T lymphocyte receptors, the possibility of manipulating their effects for therapeutic purposes has also arisen. The main approach for inhibiting signalling by specific receptors is the use of blocking antibodies that prevent receptor-ligand binding. This approach can either work to enhance or suppress immune responses depending on which receptors are targeted. In the context of cancer, where inappropriate tolerance of tumour cells permits their uncontrolled proliferation, targeting of the inhibitory co-receptors PD-1 and CTLA-4 have proved to be effective anti-cancer agents (Pardoll, 2012).

The inhibitory influence of the PD-L1:PD-1 pathway is clear, but the details of the underlying mechanisms by which this is achieved are still emerging. A better understanding of the pathway could help in three major ways. Firstly, despite good therapeutic outcomes with PD-1:PD-L1 blocking antibodies, the significant incidence of high-grade adverse drug-related events restricts treatment to those with late stage disease. Insights into the factors that mediate these toxicities could open up treatment to a larger cohort (Sharma and Allison, 2015). Secondly, nothing is currently known about the mechanisms by which PD-1 is regulated at the cell surface. There are no endocytosis motifs on the intracellular domain and research so far has only served to demonstrate that the mechanism of PD-1 regulation is

'atypical' (Pentcheva-Hoang et al., 2007). High PD-1 expression on the cell surface is characteristic of 'exhausted' T lymphocytes in the context of chronic viral infection and cancer. Importantly, blocking PD-1 signalling can 'rescue' these cells, returning them to an effector phenotype (Barber et al., 2006; Wherry et al., 2007). An understanding of PD-1 regulation at the cell surface may therefore suggest new therapeutic approaches aimed at downregulating PD-1 expression. Thirdly, it is possible that PD-1 may have yet undefined mechanisms of inhibition that could be targeted. Research has demonstrated that PD-1 activates inhibitory phosphatases (Chemnitz et al., 2004) and leads to the upregulation of inhibitory Cbl-b (Karwacz et al., 2011) and BATF (Quigley et al., 2010), as well as causing cell motility paralysis (Zinselmeyer et al., 2013). Gaining a better understanding of these mechanisms as well as uncovering others that may occur downstream of PD-1 signalling could provide further targets for reversing the inhibitory effects of PD-1.

The starting point for the work outlined in Chapters 3 to 5 was the surprising finding that under certain conditions, including following large Ca^{2+} influx, PD-1 is dramatically downregulated from the surface of cells. This chapter documents how T lymphocyte surface proteins are sorted following Ca^{2+} influx into cells and our investigation into what mediates the specificity of protein sorting.

4.1.1 Research questions:

- Are proteins sorted following large Ca^{2+} influx in Jurkat cells?

- How does TMEM16F activity influence protein sorting?

- What dictates the specificity of protein sorting?

4.2 Results

4.2.1 Ca^{2+} activated downregulation of PD-1 in WT Jurkat T cells by microvesicle shedding

In Chapter 3 we demonstrated that Ca^{2+} influx leads to rapid changes in plasma membrane area regulated by TMEM16F. We next wanted to know whether transmembrane proteins were sorted with this membrane on Jurkat T cells. We monitored a panel of transmembrane proteins that have a variety of roles in T lymphocyte function: the co-stimulatory receptors PD-1 and CD28, the adhesion molecules ICAM-1 and LFA-1, the transferrin receptor which is classically recycled by clathrin-medicated endocytosis, components of antigen recognition machinery CD3ε and CD4, and MHC Class I (HLA ABC). Protein expression was measured in Jurkat T cells using flow cytometry before and after ionomycin treatment.

Figure 1 presents the percentage of protein remaining on the surface of WT Jurkat T cells following Ca^{2+} influx facilitated by ionomycin treatment. Proteins are differentially affected. TfR and HLA ABC are down regulated to ~75% of initial expression whilst PD-1 is reduced to ~10%. Clearly proteins are lost from the surface of cells, but these data give us no information about the destination of this protein - has it been shed or internalised? Our findings in Chapter 3 demonstrated that in WT cells, Ca^{2+} induces a large exocytosis followed by microvesicle shedding. We therefore hypothesised that the loss of proteins from the cell seen in Figure 1 was due to protein shedding in microvesicles.

PD-1 is the receptor most downregulated following Ca^{2+} influx (Figure 1A). To track the destination of PD-1, we conjugated GFP to the C-terminus of PD-1 by overlap extension PCR and expressed this protein in Jurkat T cells with a single promoter lentiviral vector (pSIN-PD1GFP). Flow cytometry of PD1GFP-expressing cells allows us to track total PD-1 (with GFP) and surface PD-1 (using antibody-staining of intact live cells at 4°C).

Figures 2A and 2B show changes in total and surface PD-1 on WT PD1GFP-expressing Jurkat T cells after 15 minutes of ionomycin treatment. There is a ~90%

reduction in surface PD-1 expression, accompanied by a ~40% reduction in total PD-1. As shown in Chapter 3, under these conditions there is a large increase in subcellular-sized events seen by flow cytometry corresponding to shed microvesicles. These microvesicles were gated by flow cytometry, as detailed for Figure 3.12, and surface PD-1 and total GFP was quantified for both WT control and WT PD1GFP expressing cells. Figure 2C demonstrates the presence of surface PD-1 and total GFP in microvesicles shed from PD1GFP expressing cells.

We next wanted to visualise the inclusion of PD-1 in shed microvesicles. Conventional confocal microscopy lacks the resolution necessary for this. We therefore employed super-resolution structured illumination microscopy (SR-SIM) and imaged Jurkat T cells expressing a PD1-mCherry fusion protein (which does not bleach as readily as PD1GFP). Figure 2D and Video 4.1 shows microvesicle shedding of PD-1 following ionomycin treatment in WT Jurkat T cells.

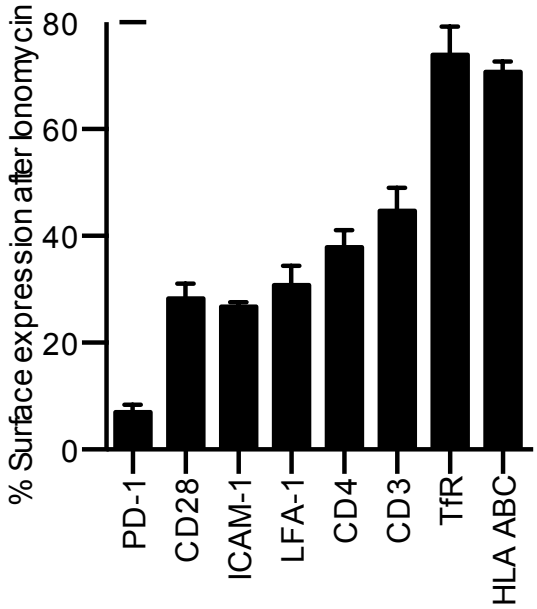

Figure 4.1 **WT Jurkat T cell plasma membrane proteins are down regulated following Ca^{2+} influx.** WT Jurkat T cells expressing PD-1 were treated with 5μM ionomycin for 15 mins in Ringer solution and stained for expression of surface molecules. Data are percentage of initial surface expression following ionomycin treatment.

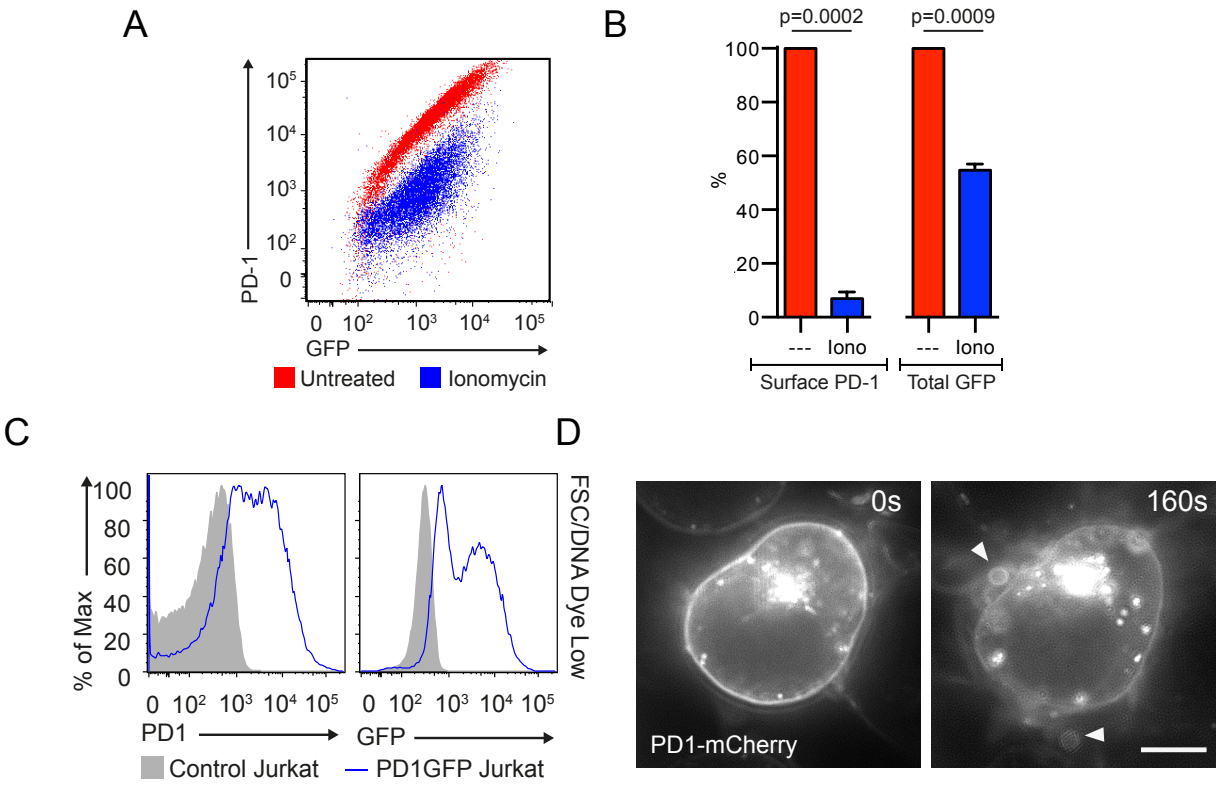

Figure 4.2 **PD-1 is shed from Jurkat T cells in microvesicles following Ca^{2+} influx. A, B** PD1GFP chimera was expressed on WT Jurkat T cells. Surface PD-1 and total GFP with and without ionomycin treatment are shown. **C** WT control and WT PD1GFP chimera expressing Jurkat T cells were stimulated with ionomycin. Microvesicles were gated for as subcellular sized events with low DNA dye uptake. PD-1 and GFP expression on microvesicles from WT control and WT PD1GFP expressing Jurkat T cells is compared. **D** PD1-mCherry chimera was expressed in WT Jurkat T cells and imaged by SR-SIM microscopy before and after ionomycin treatment. Arrows indicate PD1-bearing microvesicles.

4.2.2 Ca^{2+} activated downregulation of PD-1 in TMEM16F-null Jurkat T cells by endocytosis

In the absence of TMEM16F, Ca^{2+} influx activates MEND (Chapter 6, Figure 6). This form of endocytosis is rapid and takes in ~50% of the plasma membrane. We wanted to establish which proteins were sorted by MEND in T lymphocytes. In Figure 3 TMEM16F-null Jurkat T cells were treated with ionomycin for 15 minutes and plasma membrane expression of proteins measured by flow cytometry. PD-1 was selectively down regulated with levels dropping to ~5% of untreated cell levels. Other proteins including CD28, ICAM-1, LFA-1 CD4, CD3 and HLA were maintained at ~60-80% of initial values apart from TfR which fell to ~25%.

Our previous data from Chapter 3 would predict that this downregulation of PD-1 was due to massive endocytosis. To confirm this, we expressed PD1GFP fusion protein used for Figure 2 in TMEM16F-null Jurkat T cells to track both surface and total PD-1. Figures 4A and 4B show that despite a ~95% reduction in surface PD-1, total cell PD-1 (GFP fluorescence) remains constant after Ca^{2+} influx. This confirms that PD-1 protein is internalised from the cell surface and retained in the cell.

Again we employed SR-SIM to visualise the endocytosis of PD-1 in TMEM16F-null cells PD1-mCherry expressing Jurkat T cells. Figure 4C and Video 4.2 show large PD-1 containing vesicles in cells following Ca^{2+} influx.

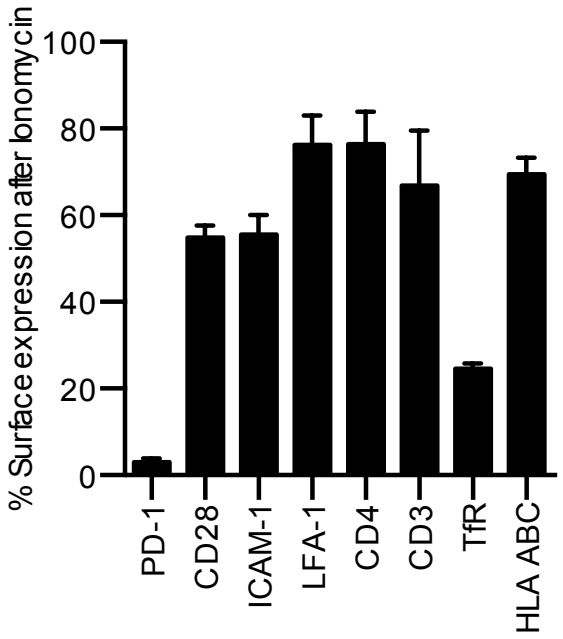

Figure 4.3 **TMEM16F-null Jurkat T cell plasma membrane proteins are downregulated following Ca^{2+} influx.** TMEM16F-null Jurkat T cells expressing PD-1 were treated with ionomycin for 15 mins in Ringer solution and stained for expression of surface molecules. Data are percentage of initial surface expression following ionomycin treatment.

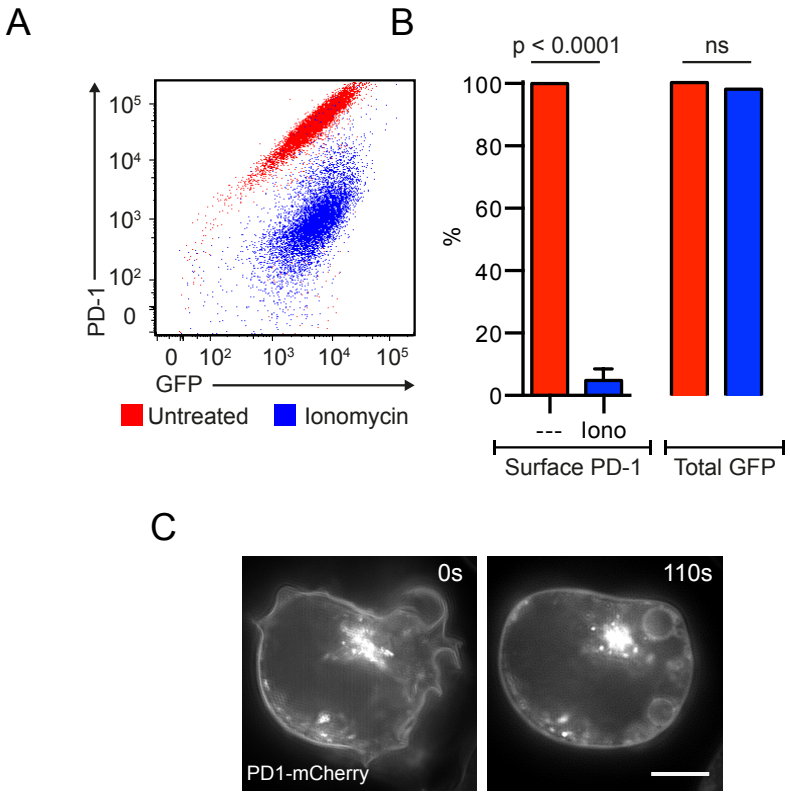

Figure 4.4 **In the absence of TMEM16F PD-1 is endocytosed. A,B** PD1GFP chimera was expressed on TMEM16F-null Jurkat T cells. Surface PD-1 and total GFP with and without ionomycin treatment are shown. **C** PD1-mCherry chimera was expressed in TMEM16F Jurkat T cells and imaged by SR-SIM microscopy before and after ionomycin treatment.

4.2.3 PD-1 sorting is mediated via the transmembrane domain of the receptor

We next wanted to understand what dictates the specificity of PD-1 sorting into both shed and endocytosed vesicles. We hypothesised that PD-1 receptors were situated in specific lipid domains that are susceptible to vesiculation outwards or inwards and that the protein transmembrane domain regulated the inclusion/exclusion of proteins. In all cases PD-1 was the protein most affected, with expression reduced to ~5-10% of baseline following Ca^{2+} influx. HLA ABC however was maintained at the surface with levels dropping to ~70-80%. In order to test whether the transmembrane domain (TM) guides protein sorting, we constructed PD1-HLA chimeras where only the TM was changed.

Figures 5A and 5B show the hydrophobicity profile of both PD-1 and HLA-A2 and the predicted TM domain amino acids using an algorithm designed by ExPASy (http://www.ch.embnet.org/software/TMPRED_form.html). Using overlap-extension PCR we produced two chimeras depicted in Figure 5C. Both chimeras have the extracellular domain of PD-1 and the intracellular domain of HLA-A2. PD1Tm has the PD-1 transmembrane domain and HLATm has the HLA-A2 transmembrane domain. These were cloned into a lentiviral vector and expressed on both WT and TMEM16F-null Jurkat T cells.

Figure 5D shows the expression level of PD1Tm and HLATm chimeric proteins following treatment with 5μM ionomycin. In both cases there is a significant difference between downregulation of the two constructs. The chimera with the PD1Tm was downregulated significantly more (~30% vs ~60%), supporting the hypothesis that intramembrane interactions sort proteins into membrane domains that are preferentially shed and endocytosed.

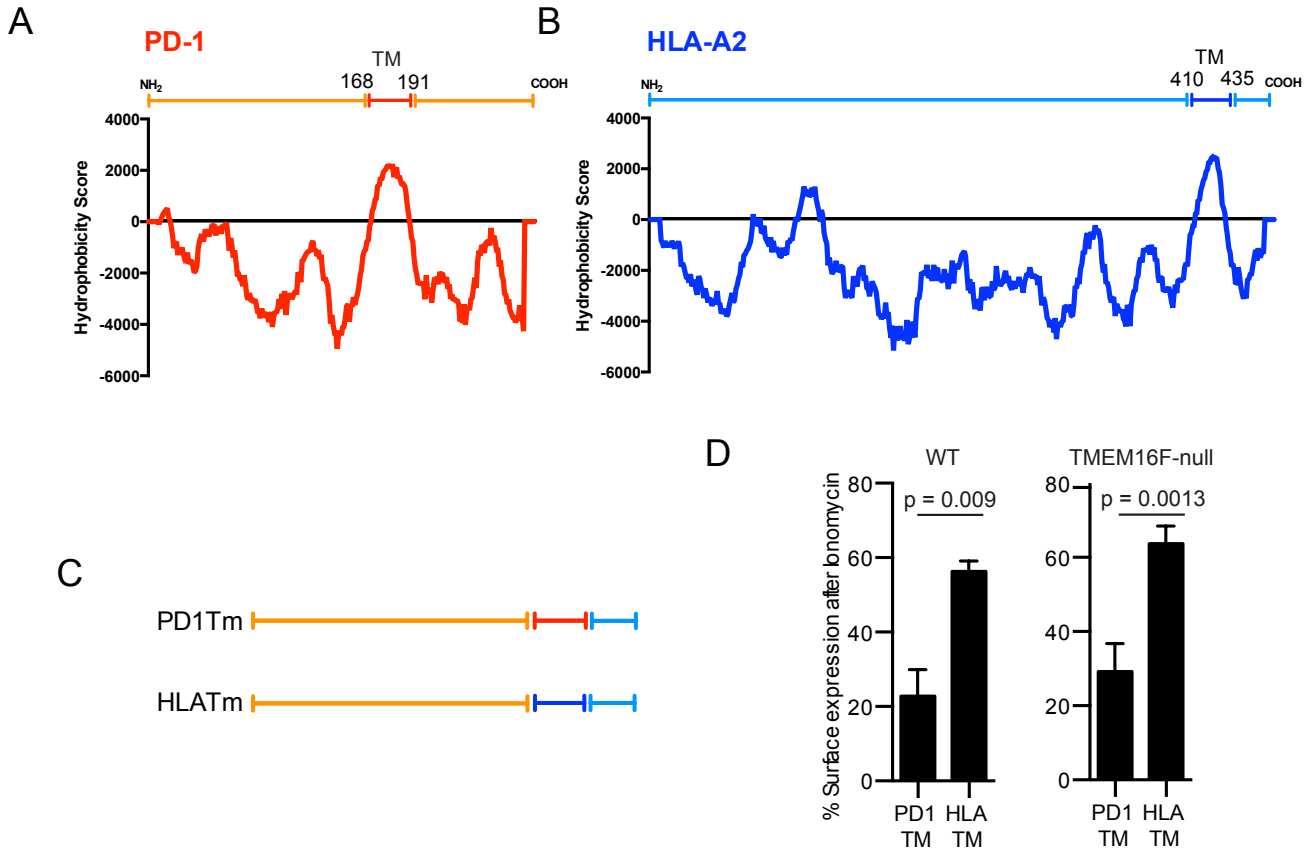

Figure 4.5 **Receptors are sorted via transmembrane domain protein-lipid interactions. A** PD-1 and **B** HLA-A2 hydrophobicity score plotted with predicted transmembrane domain. Data sourced from ExPASy TM prediction algorithm. **C** Illustration of PD1Tm and HLATm constructs. **D** PD1HLA-A2 chimeras were produced and expressed in WT and TMEM16F-null Jurkat T cells. Percentage surface expression remaining after treatment with ionomycin is shown.

4.2.4 Ca^{2+} activated endocytosis of PD-1 in WT Jurkat T cells following excessive Ca^{2+} influx

The Ca^{2+} threshold for microvesicle shedding in WT Jurkat T cells is high, requiring between 2.5 - 5μM ionomycin in physiological Ca^{2+} solution (2mM). By titrating up the amount of ionomycin, we found that when we treated WT Jurkat T cells with 20μM ionomycin, endocytosis occurred.

Using whole-cell patch clamp capacitance recording to monitor membrane area, treatment of cells with 20μM ionomycin led to a rapid exocytosis of ~30% followed by a loss of membrane area to ~70% of baseline expression. This was associated with a downregulation in T lymphocyte protein expression (Figure 6B). Again PD-1 was specifically downregulated. Interestingly the profile of receptors downregulated is not significantly different to those downregulated when WT cells are treated with 5μM ionomycin. As before, it was unclear whether this reduction in membrane area is due to shedding or endocytosis of membrane. In Chapter 3 we used FM4-64 dye as a tracer of membrane movement directionality. The data presented in this chapter so far has demonstrated that we can also use PD1GFP as a tracer of shedding and endocytosis. When WT PD1GFP expressing Jurkat T cells are treated with 20μM ionomycin, PD-1 is endocytosed (Figures 6C and 6D) established by ~95% loss of surface PD-1, accompanied by no significant loss in total PD-1 (GFP).

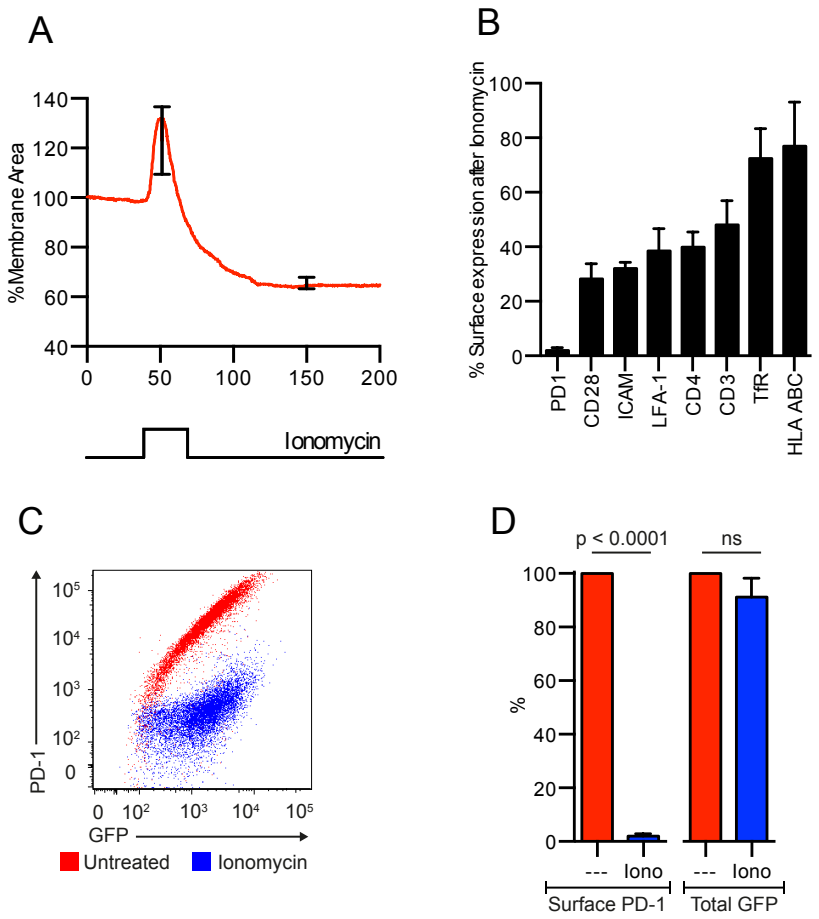

Figure 4.6 **Large Ca^{2+} influx triggers endocytosis without shedding in WT Jurkat T cells. A** Real-time membrane area (capacitance) of WT Jurkat T cells measured by whole-cell patch-clamp treated with 20μM ionomycin. **B** WT Jurkat T cells expressing PD-1 were treated with 20μM ionomycin for 15 mins in Ringer solution and stained for expression of surface molecules. Data are percentage of initial surface expression following ionomycin treatment. **C**, **D** PD1GFP chimera was expressed on WT Jurkat T cells. Surface PD-1 and total GFP with and without 20μM ionomycin treatment are shown.

4.3 Discussion

4.3.1 PD-1 is specifically sorted into microvesicles

The study of plasma membrane derived microvesicles is an emerging field in biology. The known functions of microvesicles are hugely varied with roles demonstrated in coagulation, inflammation, the tumour microenvironment, cell membrane repair and at antigen presentation (Distler et al., 2005; Köppler et al., 2006; Sims et al., 1988); (Choudhuri et al., 2014; Mochizuki and Okada, 2007; Shedden et al., 2003). Release of microvesicles is a secretory pathway employed by macrophages for secreting proteins that lack a leader sequence such as IL-1β (MacKenzie et al., 2001).

The expression of proteins on the membranes of microvesicles is a major regulator of their function. Tumour derived microvesicles for example express high levels of Fas-L that trigger apoptosis in TILs (Albanese et al., 1998; Kim et al., 2005), whilst microvesicles found in the immune synapse are enriched in TCRs that can reverse-signal through pMHC in B cells (Choudhuri et al., 2014). Microvesicle release as a mechanism of protein downregulation may also be important, as is suggested in the case of TCR release in microvesicles at the immune synapse (Choudhuri et al., 2014). The mechanisms that mediate protein inclusion in microvesicles are unclear. In lymphocytes the ESCRT protein TSG101 plays a role in TCR inclusion in microvesicles. Other studies have implicated membrane intrinsic factors such as membrane cholesterol content (Del Conde et al., 2005; Stein and Luzio, 1991).

In Chapter 3 we demonstrated that microvesicle shedding follows Ca^{2+} influx in WT Jurkat T cells. We next wanted to know whether plasma membrane proteins were included in these microvesicles and thereby shed from the cell surface. In Figure 1 we show that surface expression of a panel of T lymphocyte proteins is altered under the same conditions (following 5μM ionomycin treatment). Interestingly proteins are downregulated to a highly variable extent; TfR and HLA ABC are least affected whilst PD-1 expression drops to ~10% of baseline. We confirmed the downregulation of PD-1 was due to loss of protein in microvesicles by using a PD1GFP chimeric protein which allowed us to track surface and total PD-1 (Figures 2A and 2B). Both PD-1 and GFP levels are significantly reduced, indicating that protein has been lost

from the cell. The downregulation of surface PD-1 (~90%) is however greater than that of total PD-1 (~50%). This could suggest that either some PD-1 is endocytosed as well as shed, or that not all the cellular PD-1 was initially on the cell plasma membrane. SR-SIM microscopy reveals that significant amounts of fluorescent PD-1 are indeed held within the cell, presumably in the Golgi and ER, which is likely to account for the ~50% of total PD-1 that is not lost (Figure 2D). Microscopy also allows us to see PD-1 inclusion in shed microvesicles, while no endocytosis is visible. This is in agreement with Chapter 3 Figures 4 and 10 that showed that only microvesicle shedding and no endocytosis follows TMEM16F-induced exocytosis in WT Jurkat T cells. As well as demonstrating the downregulation of PD-1 from the cell plasma membrane following Ca^{2+} influx, we confirmed the presence of PD-1 on the surface of shed microvesicles (defined as DNA dye-negative, subcellular sized events) by FACS (Figure 2C).

These data strongly suggest that there is a mechanism for targeting proteins for inclusion in microvesicles. The simplest model would involve certain membrane regions or 'domains' preferentially vesiculating and the protein cargo located within those domains accompaning. The site of protein:membrane interaction is the transmembrane domain, so we hypothesised that it was this region that guides specificity. The protein consistently most downregulated is PD-1, and the one least downregulated is HLA. We therefore constructed PD-1:HLA chimeric proteins with only the transmembrane domain varied between the two constructs (PD1Tm and HLATm) (Figure 5). The construct containing the PD-1 transmembrane domain was downregulated to a significantly greater extent (~80%) than the one containing the HLA transmembrane domain (~40%). This indicates that the protein transmembrane domain is involved in the sorting of proteins into microvesicles.

4.3.2 PD-1 is specifically sorted into MEND endosomes

We have so far demonstrated that cells can respond in two ways to large Ca^{2+} influx, either by dramatically increasing or decreasing their surface membrane area. TMEM16F activity regulates these phenotypes and can be modulated by intracellular polyamine concentration. So far we have investigated the downregulation of plasma membrane proteins when TMEM16F is active i.e. via protein inclusion in shed microvesicles. We next wanted to know how protein surface expression was altered following Ca^{2+} influx in TMEM16F-null cells i.e. under conditions known to cause MEND.

First we tracked expression of a panel of proteins before and after ionomycin treatment in TMEM16F-null cells (Figure 4). Strikingly, PD-1 is again the receptor most downregulated, this time to ~5% of baseline expression, and again HLA ABC is least affected along with LFA-1, CD3 and CD4 with expression levels reduced to ~80% of baseline. This again suggests a specificity of protein sorting, with PD-1 preferentially affected. To confirm this downregulation was due to endocytosis, we expressed the PD1GFP fusion protein on TMEM16F-null cells and treated them with ionomycin. The 95% decrease in surface PD-1 expression was accompanied by a complete maintenance in total PD-1 (GFP) indicating that PD-1 was downregulated by endocytosis. We visualised PD-1 endocytosis with TMEM16F-null expressing PD1-mCherry chimera with SR-SIM microscopy (Figure 4C, Video 4.2). Large PD-1 containing MEND endosomes are seen to form following Ca^{2+} influx. It is remarkable to compare the phenotypes of WT (Figure 2D) and TMEM16F-null Jurkat T cells (Figure 4C), to recognise that one protein can regulate such different responses and to find that the specificity of protein inclusion in microvesicles and MEND endosomes is conserved.

Experiments focussed towards establishing the Ca^{2+} threshold for microvesicle shedding in WT Jurkat T cells revealed the surprise finding that at high ionomycin concentrations (i.e. very high intracellular Ca^{2+}), MEND occurs in WT cells (Figure 6). When cells are treated with 20μM ionomycin, capacitance recording reveals a rapid exocytosis of membrane over ~5 seconds followed by a loss in membrane area over 100 seconds to ~70% of baseline (Figure 6A). This is accompanied by a

downregulation of surface proteins, specifically PD-1 (Figure 6B). PD1GFP fusion protein was used to track the directionality of membrane movement, and Figures 6C and 6D demonstrate the loss of membrane area and surface PD-1 is due to endocytosis (i.e. total PD1GFP not affected). Initially we hypothesised that very high Ca^{2+} was inhibiting TMEM16F function or leading to rapid channel inactivation, however no significant differences were seen in TMEM16F conductance (data not shown). Our model detailed in Figure 7.1 is that MEND is the default pathway and that either TMEM16F or TMEM16F-induced exocytosis inhibits MEND, hence why MEND only occurs in their absence. At this high Ca^{2+} concentration presumably MEND is able to overcome this inhibition so MEND occurs. If this is a membrane repair pathway, large membrane defects, which lead to a larger Ca^{2+} influx, may be better repaired by endocytosis, not by exocytosis and shedding. However the explanation of this switch is not clear – a full understanding of how the balance of endocytosis and exocytosis is regulated could help in deciphering the mechanisms that underlie these phenomena.

These data indicate that PD-1 is specifically included in both MEND endosomes and shed microvesicles. Specificity of protein sorting into microvesicles is mediated via the protein transmembrane domain. We therefore next wanted to know where this was the mechanism of specificity in MEND protein sorting. Indeed, as Figure 5 shows, the PD-1Tm construct was downregulated significantly more than the HLATm construct in TMEM16F-null cells. This again implicated the transmembrane domain as responsible for the specificity seen and suggests a role of membrane domains.

CHAPTER 5

APOPTOSIS-INDUCED PROTEIN SORTING IN T LYMPHOCYTES

5.1 Introduction

Two hundred billion cells are turned over in the human body each day (Nagata et al., 2010). Apoptosis is essential for normal homeostasis and development in all multicellular organisms. The plasma membrane of an apoptotic cell is very important in safeguarding the control of demolition. Firstly, it maintains a barrier to contain the cellular contents, whose leakage can damage neighbouring cells and lead to inflammation and autoimmunity (Taylor et al., 2008a). Secondly, the plasma membrane undergoes changes that aid the clearance of cell 'corpses' by phagocytes (Poon et al., 2014b).

One of the hallmarks of cells undergoing apoptosis is the loss of plasma membrane phospholipid asymmetry. This has recently been shown to follow Caspase-3 activation of Xkr8 (Suzuki et al., 2013) and inactivation of ATP11C (Segawa et al., 2014). Surface PS constitutes an 'eat-me' signal to phagocyte receptors BAI1 (Park et al., 2007), Stablin 2 (Park et al., 2008) and TIM proteins (Miyanishi et al., 2007) that facilitate engulfment.

Certain cell types including T lymphocytes are broken down into smaller 'apoptotic bodies' that are more readily engulfed by phagocytes. These apoptotic bodies can have functional roles in immune modulation (Berda-Haddad et al., 2011; Xie et al., 2009) and tissue repair (Zernecke et al., 2009). The mechanism by which this occurs is still being characterised. Caspase-3 cleavage of ROCK1 leads to the phosphorylation of myosin light chain, and cell contraction. This results in a period of dynamic membrane blebbing in early apoptosis that is involved in the eventual formation of apoptotic bodies (Sebbagh et al., 2001). This contraction also leads to the fragmentation of the cell nucleus; a characteristic hallmark of apoptotic cells (Croft et al., 2005). Recent work by Poon et al. has discovered a new form of plasma membrane structure termed 'apoptopodia' that forms during apoptosis in T lymphocytes and monocytes (Poon et al., 2014a). These structures are string-like membrane protrusions with apoptotic bodies placed along them resembling 'beads on a sting' (Atkin-Smith et al., 2015). This dramatic membrane remodelling is enhanced by inhibition of the Pannexin 1 small molecule channel.

As well as plasma membrane vesiculation outwards to form apoptotic bodies and apoptopodia, there is also evidence of endocytic events occurring during apoptosis. Lee et al. describe the appearance of large internal vesicles in a variety of cell types during apoptosis initiated in a number of different ways (Lee et al., 2013). These vesicles were seen to originate from the plasma membrane, with a surface biotinylation assay confirming the presence of plasma membrane derived proteins on the membrane of these vesicles.

In Chapters 3 and 4 we have investigated large Ca^{2+} activated plasma membrane vesiculation outwards, producing microvesicles, and inwards, during MEND. We have found that proteins, specifically PD-1, are sorted with these large membrane movements. During apoptosis of lymphocytes, significant membrane remodelling occurs. We therefore next investigated whether expression of surface receptors was altered during apoptosis, and sought to understand the mechanisms underlying this trafficking.

5.1.1 Research questions

- Are proteins sorted from the plasma membrane during apoptosis?

- Is sorting due to membrane shedding or endocytosis?

- Is sorting Ca^{2+} dependent?

- What dictates the specificity of protein sorting?

5.2 Results

5.2.1 Massive PD-1 endocytosis during apoptosis in Jurkat T cells

PD-1 is preferentially sorted with large membrane movements triggered by large Ca^{2+} influx. Apoptosis, the orderly death and breakdown of cells, leads to a number of plasma membrane changes with large intracellular vacuoles, reminiscent of MEND endosomes, seen to appear inside cells (Lee et al., 2013).

We first examined how plasma membrane protein expression, of a panel of proteins detailed in Chapter 4, was altered during apoptosis in Jurkat T cells. We used Etoposide, a topoisomerase inhibitor, to initiate apoptosis. Lack of topoisomerase activity leads to a DNA damage response, phosphorylation of p53, the upregulation of Bax and the subsequent release of cytochrome c from mitochondria (Karpinich et al., 2002). Cells were treated overnight with 2μM Etoposide and protein expression was analysed by FACS. Events with the FSC-SSC profiles of live Jurkat T cells, were analysed.

Figure 5.1 shows the protein surface expression profiles of Jurkat T cells treated with Etoposide. Proteins were differentially affected. CD3 and HLA ABC were less downregulated with levels maintained at ~80%, while ICAM, LFA-1 and CD4 levels were reduced further to ~60%. PD-1 was most affected with expression levels dropping by ~99%. The other receptors most downregulated were TfR (~15%) and CD28 (~10%).

PD-1 was dramatically downregulated during apoptosis, with cells losing ~99% of their surface expression. This is reminiscent of the massive Ca^{2+} activated downregulation of PD-1 described in Chapter 4, where PD-1 is either lost in microvesicles or endocytosed via MEND. We therefore next investigated whether this downregulation was dependent on Ca^{2+}. Under conditions of total Ca^{2+} chelation (4mM EGTA), downregulation occurred normally (Figure 5.2). Interestingly, Figure 5.2A suggests that this large-scale endocytosis of PD-1 is a rapid event affecting the whole cell, as no cells are seen to lie between the two binary states of $PD\text{-}1_{high}$ and $PD\text{-}1_{low}$.

To understand whether PD-1 had been lost from the surface by either endocytosis or microvesicle shedding, we employed the assay described in Chapter 4, using the PD1GFP fusion protein, to track surface and total PD-1. Following Etoposide treatment, a ~99% reduction in surface PD-1 was accompanied by no significant change in total PD-1 (GFP) (Figure 5.2B). This confirms that this downregulation is due to endocytosis of PD-1. Imagestream X images confirmed loss of anti-PD-1 surface staining and maintenance of total PD1GFP. In untreated cells, PD1GFP was distributed on the plasma membrane, whilst in etoposide treated cells there is a diffuse distribution of PD1GFP in the cytosol. Hoechst staining confirms that Etoposide treated cells are undergoing apoptosis, with high Hoescht uptake, and enlarged, fragmented nuclei.

These data demonstrated that apoptosis leads to the remodelling of surface molecules on Jurkat T cells, with PD-1 dramatically downregulated by a massive Ca^{2+}-independent endocytosis.

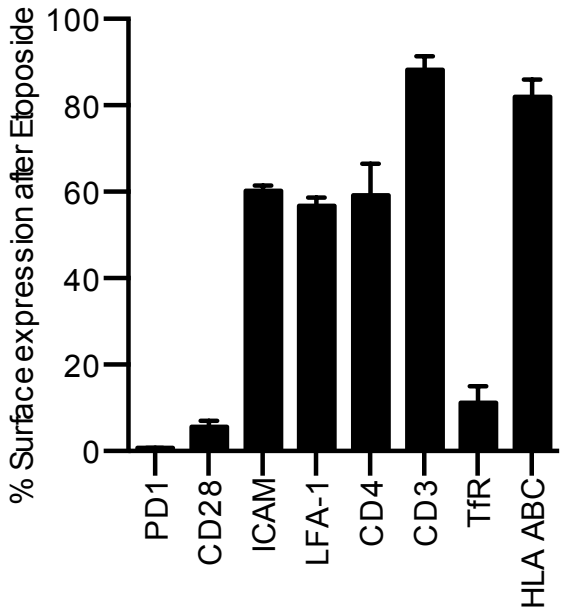

Figure 5.1 **WT Jurkat T cell plasma membrane proteins are downregulated during apoptosis.** WT Jurkat T cells expressing PD-1 were treated with 2μM Etoposide overnight and stained for expression of surface molecules and analysed by FACS. Cells were gated by FSC/SSC to exclude cellular debris. Data are percentage of untreated cell surface expression.

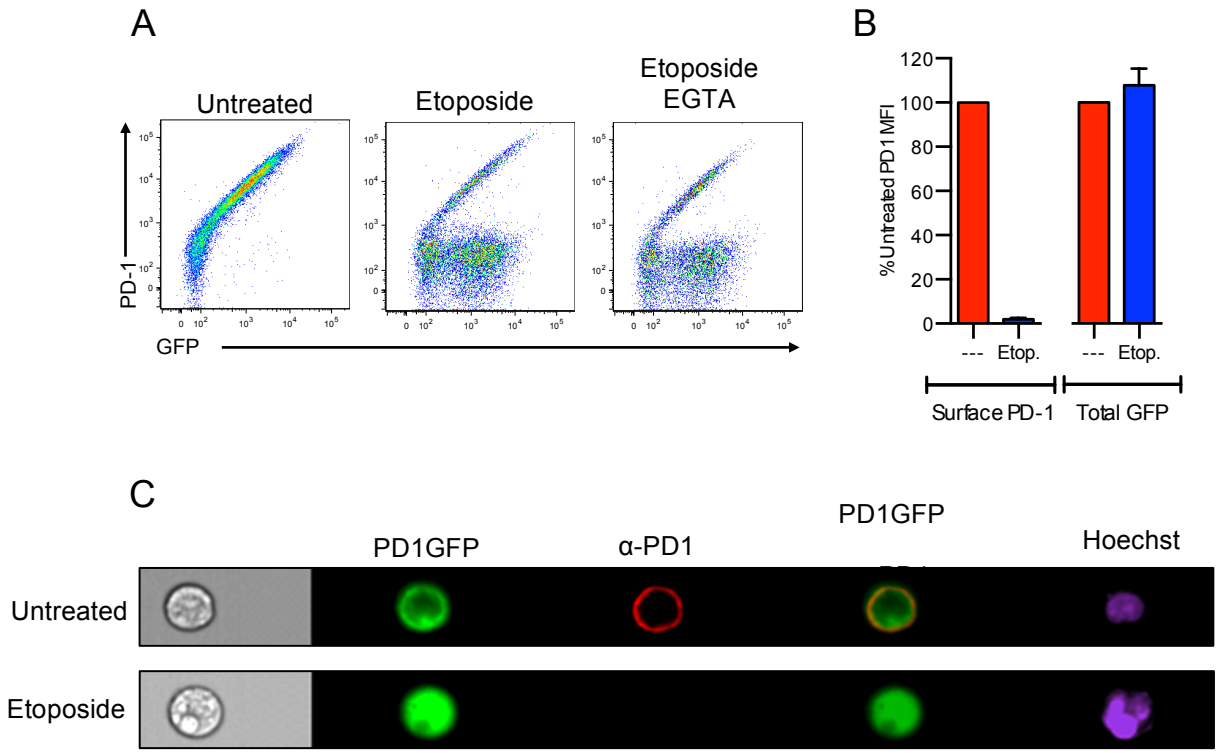

Figure 5.2 **Apoptosis leads to a Ca^{2+} independent massive endocytosis of PD-1.** **A** PD1GFP-expressing Jurkat T cells were treated with 2µM Etoposide overnight and stained for PD-1 in Ringer solution with or without 4mM EGTA. **B** Surface PD-1 and total GFP with and without Etoposide treatment. **C** ImagestreamX micrographs of PD1GFP cells stained with anti-PD-1 antibodies and Hoechst untreated or treated with 2µM Etoposide overnight.

5.2.2 Sorting of PD-1 via the transmembrane domain

Nothing is known about the regulation of PD-1 at the cell surface. Here we present another physiological context, apoptosis, in which PD-1 is dramatically downregulated. We next wanted to gain insights into the mechanism of apoptosis-induced downregulation of PD-1.

Endocytic processes, such as clathrin-mediated endocytosis, often involve the binding of protein adaptors to specific motifs on the intracellular domain of receptors. We therefore wanted to establish whether portions of the PD-1 intracellular domain are important for apoptosis-induced PD-1 endocytosis. We constructed a series of PD-1 receptor truncations with the intracellular domain progressively shortened. These constructs were expressed in Jurkat T cells using dual-promoter lentiviral vectors. Figures 5.3A and 5.3B show the affect of 2μM Etoposide on PD-1 expression. Apoptosis-induced endocytosis of PD-1 is blocked when the receptor is truncated to the 187th amino acid. Downregulation is inhibited to a small but significant extent in the PD1Δ193 truncation with levels dropping to ~3% rather than ~1% in PD1WT. Figure 5.3C shows the hydrophobicity plot of PD-1, with the predicted transmembrane domain lying between the 168th and 191st amino acid. PD-1Δ187 therefore truncates into the transmembrane domain by 4 amino acids. This suggests the transmembrane domain is involved in the sorting of surface proteins during apoptosis.

In the data presented in Chapter 4 we discovered that the transmembrane domain dictates whether proteins are sorted into microvesicles or MEND endosomes following large Ca^{2+} influx. HLA was downregulated to a significantly smaller extent than PD-1, and substitution of the PD-1 and HLA transmembrane domains was able to regulate downregulation (Figure 4.5). Similarly, here we have found that PD-1 is more downregulated than HLA ABC during apoptosis (downregulated by ~99% vs. ~20%). We next triggered apoptosis in cells expressing the PD1Tm and HLATm constructs, described in Figure 4.5. PD-1Tm but not HLATm underwent massive endocytosis during apoptosis (Figure 5.4). This again suggests the role of membrane domains that are preferentially endocytosed along with their protein cargo.

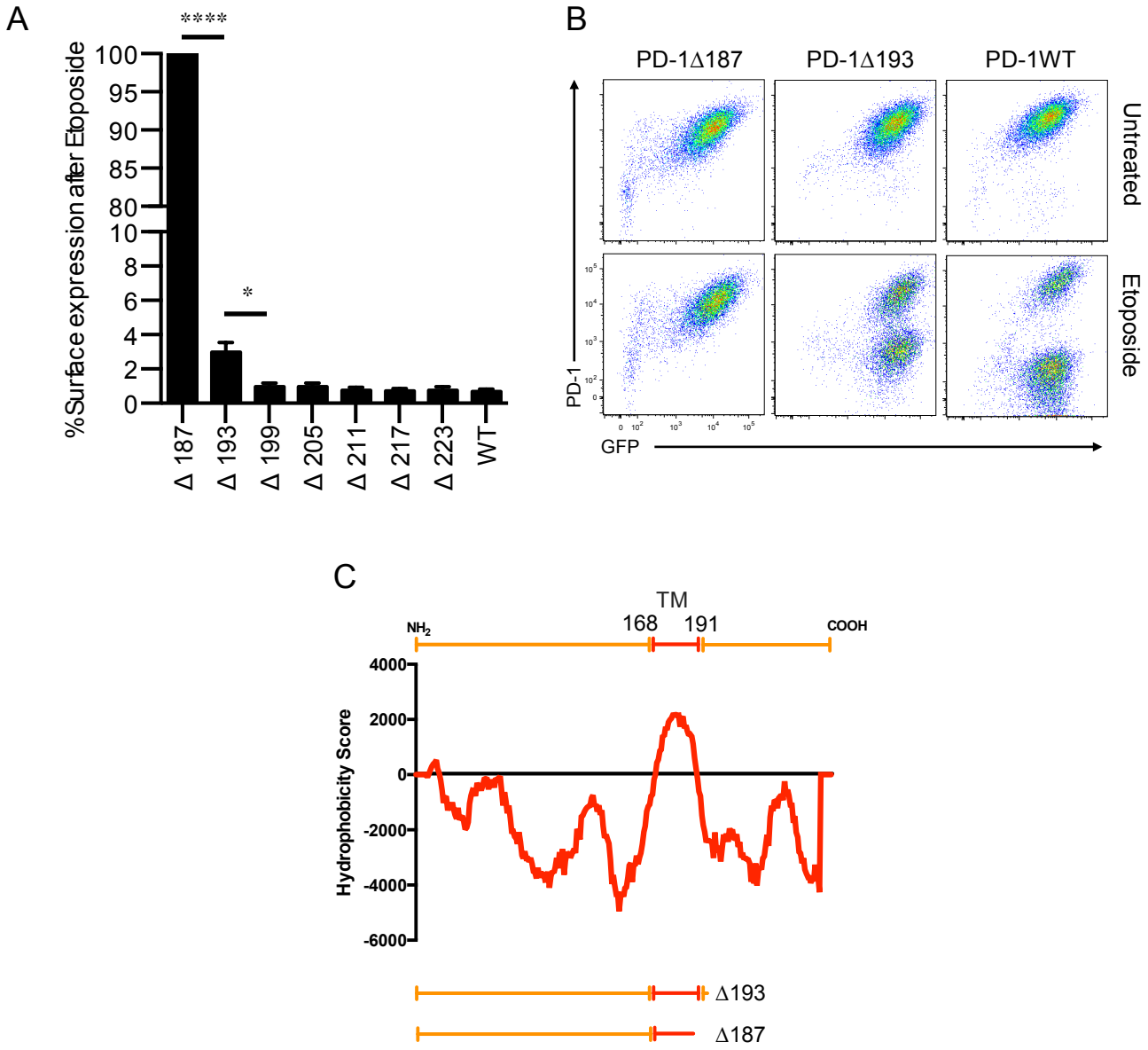

Figure 5.3 **Truncation into the transmembrane domain of PD-1 prevents apoptosis-induced downregulation of PD-1. A** and **B** PD-1 receptors, truncated at different points along the intracellular domain were expressed in Jurkat T cells using a dual promoter lentiviral vector. Cells were treated with 2μM Etoposide overnight and stained for expression of PD1. Data are percentage of untreated cell surface PD-1 expression. P values correspond to * = 0.03 and **** = <0.0001. **C** PD-1 amino acid hydrophobicity plot with predicted transmembrane domain, showing the site of the PD-1Δ193 and PD-1Δ187 truncation. Data sourced from ExPASy TM prediction algorithm.

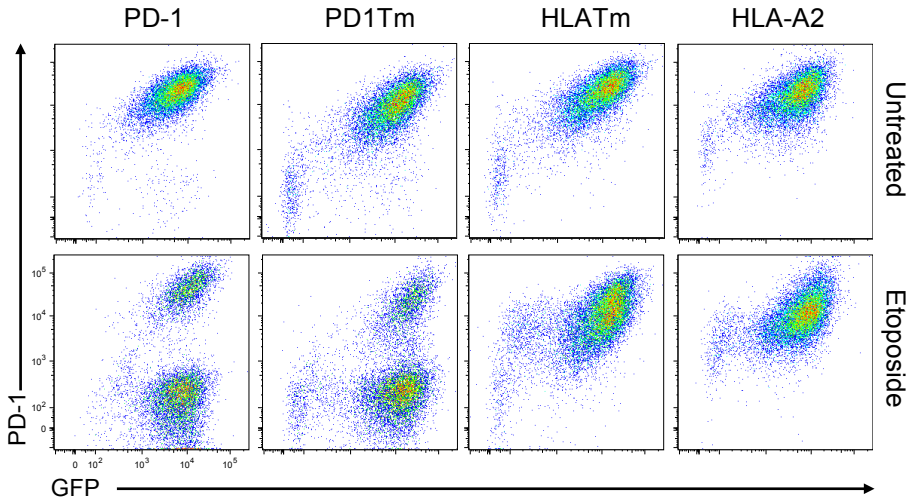

Figure 5.4 **Receptors are sorted for apoptosis-induced endocytosis via their transmembrane domains.** PD-1, PD1Tm, HLATm and HLA-A2 were expressed on Jurkat T cells using a dual promoter lentiviral vector. Cells were treated with 2μM Etoposide overnight and analysed by FACS.

5.3 Discussion

The work presented so far in this thesis has focussed on the effects of Ca^{2+} influx on the plasma membrane of Jurkat T cells, uncovering mechanisms that regulate microvesicle shedding and MEND, as well as investigating how proteins are sorted with these membrane movements. We next chose to explore another physiological context in which significant plasma membrane changes occur - apoptosis.

The plasma membrane plays an essential role in the controlled death, breakdown and clearance of cells. T lymphocytes can undergo large membrane vesiculation outwards and inwards during apoptosis (Lee et al., 2013). The mechanisms of apoptotic body formation are beginning to emerge, whilst very little is known about large endocytic events during apoptosis.

Apoptotic Jurkat T cells did indeed dramatically remodel their plasma membrane protein expression during apoptosis (Figure 5.1). PD-1, CD28 and TfR were most affected with PD-1 surface expression dropping to ~1% of baseline. This downregulation was due to endocytosis, as total PD-1 levels remain constant (Figure 5.2B). We hypothesised that this was Ca^{2+} activated MEND, described in Chapters 3 and 4, which might follow Ca^{2+} influx caused by the loss of plasma membrane integrity during apoptosis. However, endocytosis proceeds normally in the absence of extracellular Ca^{2+} (Figure 5.2B). Endocytosis occurs quickly and is a whole cell effect, with few cells seen to be transitioning between the PD-1_{high} and PD-1_{low} state (Figure 5.2A). We interrogated the intracellular domain of the receptor to establish whether any motifs, necessary for endocytosis, were present. Endocytosis of PD-1 still occurred when the entire PD-1 intracellular domain was truncated, but was completely blocked by removal of ~4 amino acids from the C-terminal end of the transmembrane domain. Substitution of the PD-1 TM for HLA-A1 TM (in chimeras described in Figure 4.5) blocked massive endocytosis of PD-1.

Although this endocytosis is Ca^{2+} independent, it resembles Ca^{2+} activated MEND in the dramatic extent to which PD-1 is specifically downregulated. Like with Ca^{2+} activated MEND, the transmembrane domain is involved in PD-1 targeting for endocytosis, implying the presence of lipid domains susceptible to vesiculation

inwards in which PD-1 is located. Substitution of the transmembrane domain and even removal of ~4 amino acids from the c-terminal end of the TM must exclude PD-1 from these domains and therefore prevent PD-1 internalisation.

As with Ca^{2+} activated MEND, the mechanism for this new form of endocytosis is unclear. This may be the same process observed in Lee et al. where large plasma membrane derived vesicles appear in apoptotic cells. This process was found to be independent of actin and dynamin in the same way as MEND (Lee et al., 2013). This endocytosis may also be the 'delayed' (occurring over minutes rather than seconds) MEND recently described in work by Hilgemann et al. in BHK cells (Hilgemann et al., 2013). In this form of massive endocytosis palmitoylation of surface proteins is the trigger. Mitochondrial PTP opening leads to the release of Coenzyme A (CoA); this is then synthesised into palmitoyl-CoA, which acts as the substrate for DHHC5, an enzyme that then palmitoylates surface proteins. PTP opening is an important step in apoptosis leading to the release of cytochrome c (Ichas and Mazat, 1998). PTP opening does however require elevated intracellular Ca^{2+}, though factors such as ROS and mitochondrial membrane potential can influence the amount of Ca^{2+} required (Brustovetsky et al., 2003).

The physiological role of this apoptosis-induced endocytosis is not clear. Work by Xie et al has demonstrated that IL-1β bound to apoptotic bodies derived from tumour cells is able to induce CTL anergy and inhibit anti-tumour immunity (Xie et al., 2009). The removal of PD-1 and CD28 by endocytosis apoptotic cells and apoptotic bodes may suggest that these immune regulatory molecules are intentionally removed to prevent their competition with receptors bound to live cells.

Further work is needed to uncover both the mechanism of Ca^{2+} independent MEND and its physiological role in T lymphocytes and other cell types. Manipulation of MEND pathway to downregulate surface PD-1 expression may provide a novel therapeutic approach for immunomodulation.

CHAPTER 6

TRANSFER OF PD-L1 FROM TUMOUR CELLS ONTO PD-1 EXPRESSING EFFECTOR T CELLS *IN VITRO* AND *IN VIVO*

6.1 Introduction

Receptors transmit signals across cell membranes following ligand binding. Ligands can be soluble, plasma membrane-bound or associated with other membranous structures such as exosomes and microvesicles. This thesis is focussed on the PD-1:PD-L1 pathway in lymphocytes, with the aim of investigating novel ways by which plasma membrane dynamics may regulate the pathway. Little is know about how PD-1 or PD-L1 is regulated at the plasma membrane and insights in this area may reveal novel inhibitory mechanisms as well as providing potential therapeutic targets for regulating the pathway.

Recently it was discovered that the inhibitory receptor, also in the CD28 family or co-receptors, CTLA-4 is able to transendocytose its ligands CD80 and CD86 from the surface of APCs. This involves the removal and endocytosis of these ligands, eventually leading to their degradation. This constitutes a mechanism of cell-extrinsic inhibition of T lymphocytes, as these ligands are shared with the stimulatory receptor CD28. Depleting the pool of available ligands inhibits lymphocytes by preventing stimulation through CD28. This inhibition may therefore not only effect the CTLA-4-expressing cell that carries out transendocytosis, but also any T lymphocyte that subsequently comes in contact with that APC. This fascinating mechanism of inhibition is thought to be possible owing to the high affinity interaction between CTLA-4 and its ligands (Cheng et al., 2013; Collins et al., 2002). Affinity studies have been carried out on the CD28 family, which confirm this high affinity interaction. These studies also reveal that the PD-1:PD-L1 interaction is much weaker (~5000 times weaker), and is entropy-driven i.e. displacing water molecules. The authors of Cheng et al. conclude that PD-1 would not be capable of a process like transendocytosis due to the transient, weak nature of the PD-1:PD-L1 interaction. Also as PD-1 does not share ligands in the same way as CTLA-4, the function of transendocytosis by PD-1 would not be clear.

Recently it was found that PD-L1 can be detached by a PD-1 expressing cell, in a process similar to transendocytosis, termed trogocytosis (Gary et al., 2012). With trogocytosis, membrane-bound ligands with associated membrane is removed from the ligand expressing cell and rather than being sorted for degradation, the protein

is incorporated onto the receptor-expressing cell's plasma membrane. This occurs between lymphocytes and APCs where pMHC and co-receptors can be exchanged (Busch et al., 2008; Game et al., 2005).

There is, therefore, an apparent contradiction in the literature concerning the PD-1:PD-L1 interaction. Cell-free affinity studies using techniques such as surface plasmon resonance have suggested that the interaction is very weak and transient, while other *in vivo* studies have suggested that PD-L1 can he transferred and expressed on PD-1 expressing cells *in vivo*. No cell-based binding assays have been carried out to measure the stability of PD-1:PD-L1 interactions.

6.1.1 Research question

- Can PD-1 form stable interactions with PD-L1?

- Can PD-1:PD-L1 interactions extend beyond cell-cell contact?

- Does PD-1 undergo ligand-induced downregulation?

- What is the nature of the PD-1:PD-L1 interaction in the tumour microenvironment?

6.2 Results

6.2.1 PD-L1 forms stable complexes with PD-1 which are maintained at the cell surface

To establish whether PD-L1 was able to stably bind PD-1 on T lymphocytes, we conducted an *in vitro* FACS assay using a soluble PD-L1Fc chimeric protein and PD-1 expressing Jurkat T cells. Cells were incubated with soluble PD-L1Fc chimera at 37°C for 1 hour in normal media, then the cells were washed twice in PBS, surface stained for 30 mins at 4°C with both anti-PD-1 and anti-PD-L1 fluorescent antibodies and washed again twice. As Figure 6.1A shows, PD-1 expressing cells incubated with PD-L1Fc become PD-L1 positive i.e.PD-L1 is bound in complex with PD-1 at the cell surface. PD-1 levels remain unchanged suggesting no ligand-induced downregulation.

Next we wanted to understand whether preservation of PD-1:PD-L1 complexes at the cell surface was mediated by any portion of the intracellular domain of PD-1. We performed the PD-L1Fc binding assay on cells expressing PD-1 receptors that had increasing portions of their intracellular domains truncated (Figure 6.1B). PD-L1 bound to these cells was increased by ~3 fold between PD-1Δ217 and Δ211 (Figure 6.1C).

This data suggests that PD-L1 can bind stably to PD-1 and be maintained at the cell surface in complex with PD-1. Data with PD-1 truncations also suggests that factors on the intracellular domain or transmembrane domain of PD-1 regulate the longevity of PD-1:PD-L1 complexes remaining on the cell surface.

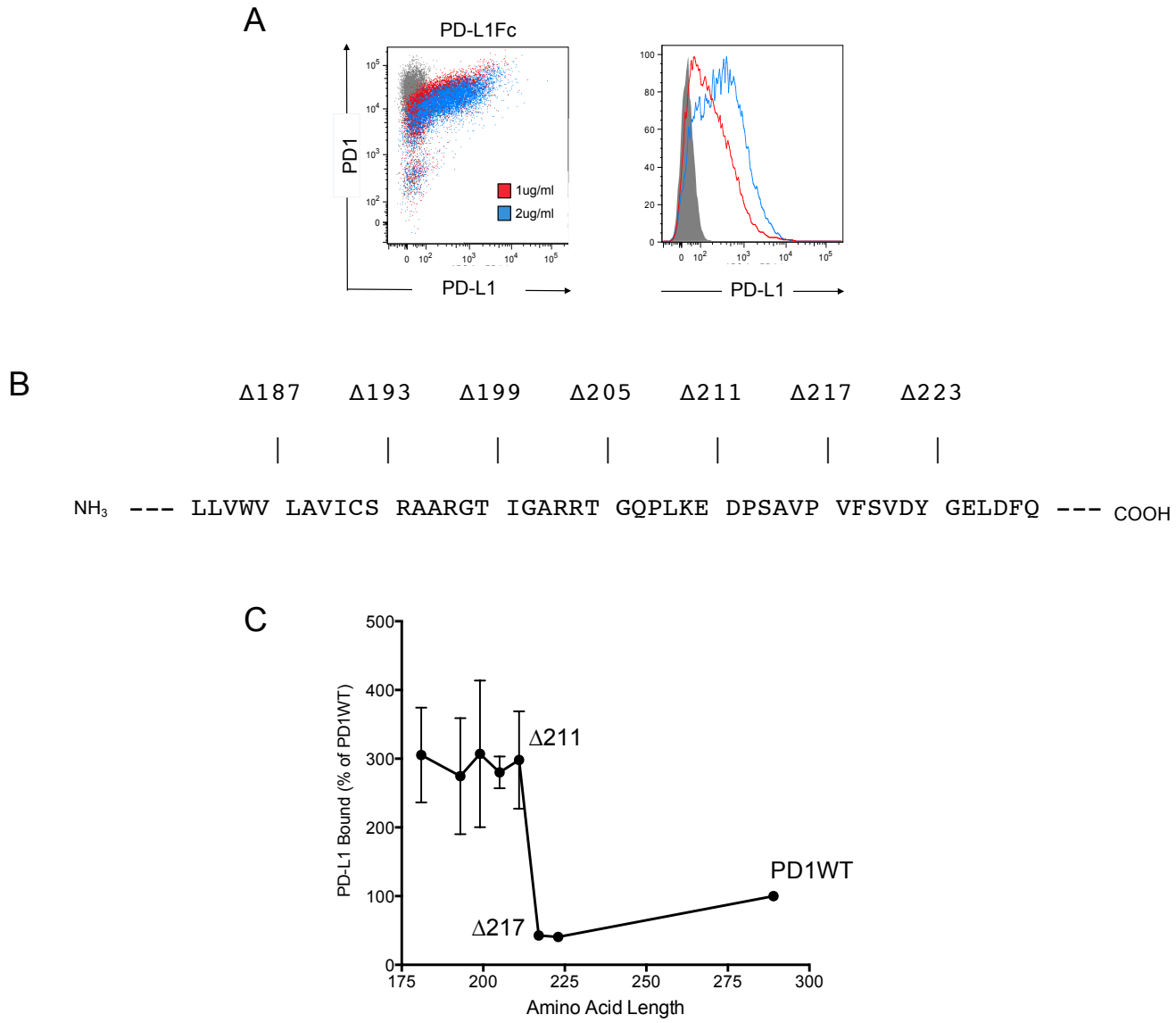

Figure 6.1 **Soluble PD-L1Fc binds stably to PD-1 expressing Jurkat T cells and is maintained at the cell surface. A** PD1WT expressing Jurkat T cells were incubated with 0ug/ml (Grey), 1ug/ml (Red) or 2ug/ml (Blue) PD-L1Fc for 1 hour at 37°C and then stained with anti-PD-1 and anti-PD-L1 antibodies. **B** Amino acid sequence showing the location of each truncation point. **C** PD-1 truncations were incubated in 1ug/ml PD-L1Fc for 1 hour at 37°C. Cells were then stained with anti-PD-L1 antibodies. Results show PD-L1 mean fluorescence intensity as a percentage of PD1WT, plotted against the total amino acid length of the protein.

6.2.2 PD-L1 is transferred onto PD-1 expressing cells by a cell-cell or cell-debris dependent mechanism *in vitro*

Data from Figure 6.1 suggests that PD-L1 can remain in stable complex with PD-1 at the cell surface. Next we wanted to know whether transfer of ligands could occur when PD-L1 bearing cells were co-cultured with PD-1 expressing cells. These proteins were stably expressed on Jurkat T cells using lentiviral vectors as shown in Figure 6.2A.

PD-1 cells were co-cultured with either WT or PD-L1-expressing cells as shown in Figure 6.2B. Cells were then stained for both PD-L1 and PD-1 and single cells gated by SSC-W. Two striking results came from this experiment. Firstly, PD-1 Jurkat T cells cultured with PD-L1 cells downregulate PD-1 and secondly, PD-L1 is transferred onto the PD-1 expressing cells.

To address the mechanism of ligand–induced downregulation of PD-1, we were interested in whether there was a motif on the intracellular domain of the receptor that mediated this downregulation as, for example, in the cases of IL-2R (Takeshita et al., 1992) and the TCR (Dietrich et al., 2002). Downregulation and PD-L1 transfer were however independent of the intracellular domain as they occurred in both PD1WT and PD-1Δ181 expressing cells. There was no change in PD-1 expression in PD1WT cells cultured with WT cells confirming that downregulation was PD-L1 dependent

We were next interested in how PD-L1 is transferred onto PD-1 expressing cells. Several groups have found that PD-L1 can be secreted (Chen et al., 2011; Rossille et al., 2014) and in Figure 6.1 we demonstrate that soluble PD-L1 can form stable complexes with PD-1 at the cell surface. If PD-L1 is being secreted, it would be present in the supernatant of PD-L1 expressing cells. The supernatant was separated by pelleting cells at 2000 rpm for 5 mins. PD1WT cells were cultured with supernatant from WT cells or PD-L1 cells for 2 hours. The complete removal of PD-L1 cells from the supernatant was confirmed by the absence of events in the $PDL1^{high}$ $PD1^{low}$ quadrant. Figure 6.3A shows that there was bound PD-L1 on the surface of PD1WT cells when cultured in crude PD-L1 supernatant. Importantly this did not

lead to a downregulation in PD-1. This PD-L1 binding was, however, abolished when the supernatant was filtered through a 0.45μM filter. This filter allows soluble protein to pass through it, but not cellular debris. We therefore asked whether PD-L1 positive events were present in the subcellular-sized event gate. Indeed they were present in the culture where crude PD-L1 supernatant was used and they were not present in the filtered supernatant. Figure 6.3 shows the back-gating of the PD-L1^{high} sub-cellular events in a FSC and Log SSC plot.

These data so far demonstrates that PD-L1 can be transferred onto PD-1 cells expressing T lymphocytes. This occurs via a cell-cell or cell-debris based dependent way, and not by secretion of PD-L1. PD-1 is downregulated in a ligand dependent manner but only following cell-cell contact, not treatment with soluble PD-L1 or PD-L1 on cell debris.

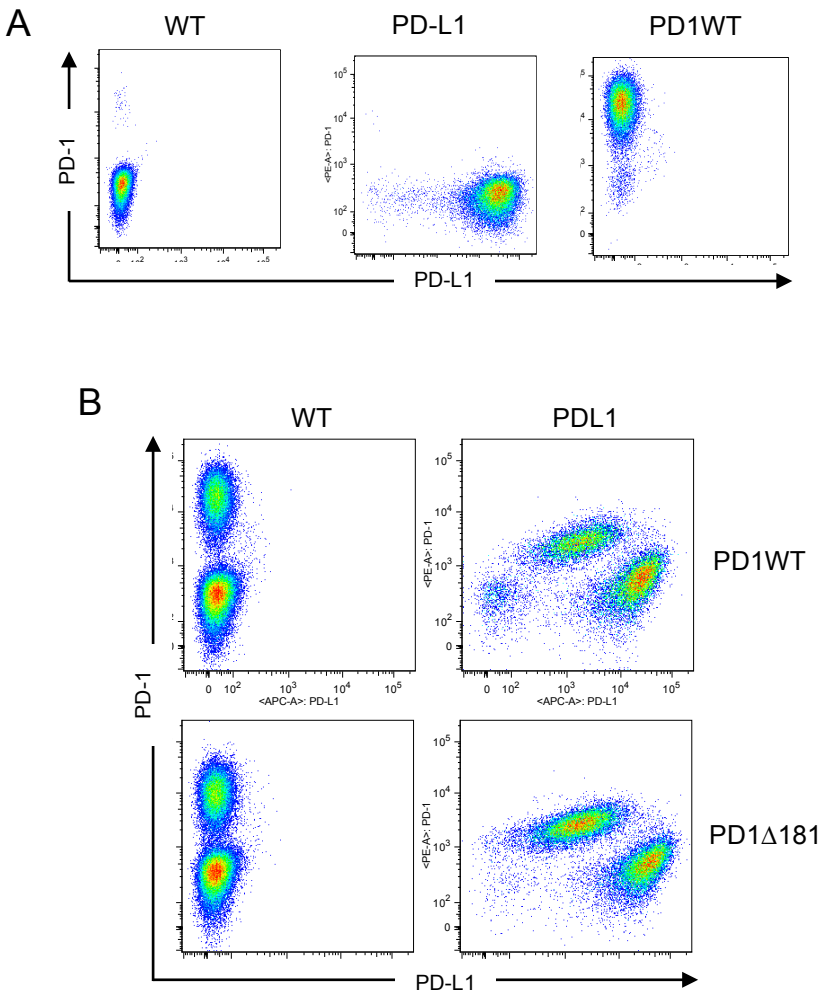

Figure 6.2 **Transfer of PD-L1 onto PD-1 expressing cells during co-culture *in vitro*. A** WT, PD-L1 and PD1WT expressing Jurkat T cells stained anti- PD-1 and PD-L1 antibodies. **B** PD1WT and PD-1Δ181 Jurkat T cells were co-cultured with either WT or PD-L1 expressing Jurkat T cells for 2 hours. Cells were then stained with anti-PD-1 and PD-L1 antibodies.

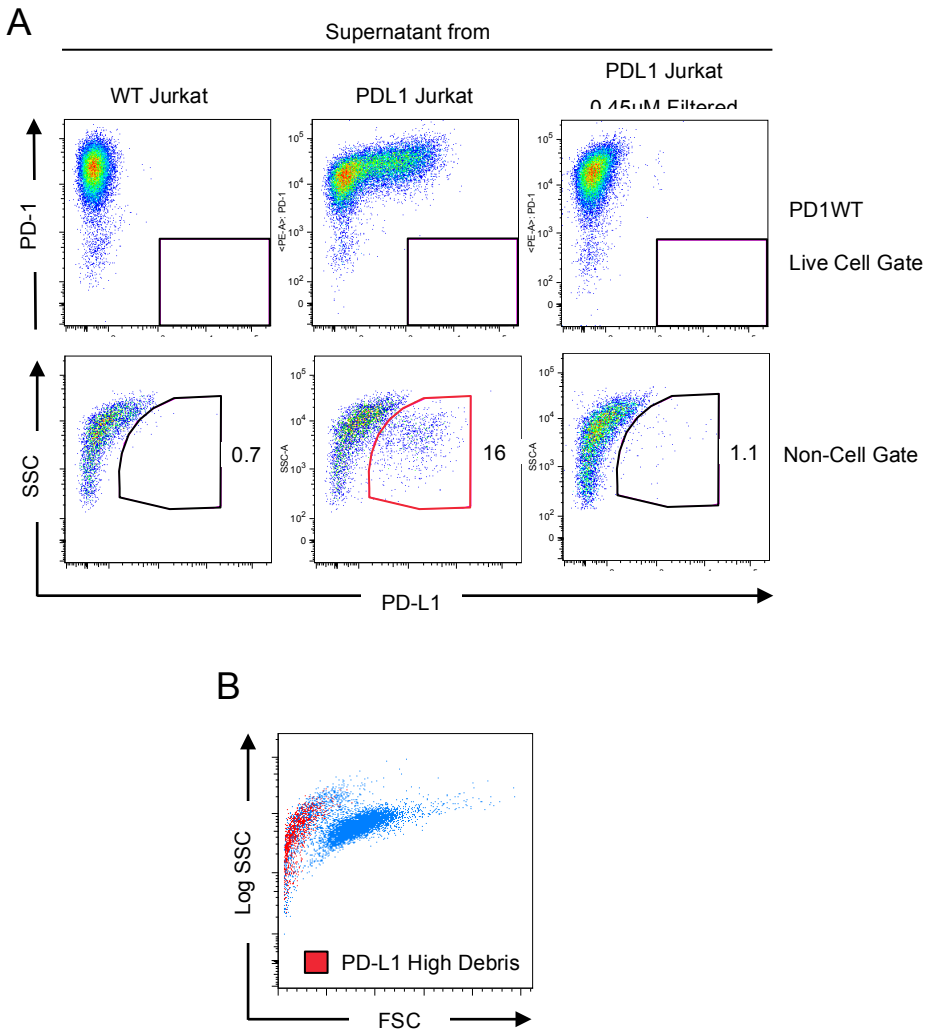

Figure 6.3 **Transfer of PD-L1 is not due to secretion of PD-L1 but is cell-cell or cell-debris dependent. A** PD1WT Jurkat T cells were cultured in crude supernatant from WT and PD-L1 expressing cells and 0.45μM filtered supernatant from PDL1 Jurkat T cells. Data shows events from both the live Cell gate and the non-cell gate. **B** Back-gating of PD-L1 positive non-cell events (red) and all events (blue) on FSC Log SSC plot.

6.2.3 PD-L1 is transferred onto tumour infiltrating lymphocytes *in vivo*

Our *in vitro* data clearly show a transfer of PD-L1 onto PD-1-expressing cells. This experimental system using Jurkat T cells may, however, not accurately represent a process that occurs *in vivo*. We therefore next established an *in vivo* tumour experiment that tested whether PD-L1 from a tumour could transfer onto $CD4^+$ and $CD8^+$ tumour infiltrating lymphocytes. In this case, as we needed to specifically track PD-L1 from the tumour, we therefore produced a PDL1-mCherry fusion protein and expressed it on a B16 melanoma cell line. Figure 4A shows the direct proportionality between PD-L1 and Cherry expression in these B16.PDL1-mCherry cells.

C57BL/6 mice were injected with 2 x 10^6 tumour cells on Day 0. At day 6 and Day 8 they were injected with 1 x 10^6 irradiated GM-CSF-expressing B16 cells (GVAX). This protocol, described in Figure 4B, was performed in collaboration with the Quezada lab and has been optimised for the recruitment of T cells to the tumour (Quezada et al., 2008; van Elsas et al., 1999). At Day 13 mice were sacrificed. Tumour infiltrating lymphocytes were separated by centrifugation with Ficoll. Cells were also isolated from the lymph nodes and spleen of the mice. Figure 4C shows the gating strategy for selectively assaying live $CD4^+$ and $CD8^+$ TILs and Figure 4 show the PD-1 and PD-L1mCherry expression on those cells.

In mice bearing B16.WT tumours, $CD4^+$ and $CD8^+$ TILs express PD-1 but do not fluoresce in the mCherry channel. By contrast, both CD8+ and CD4+ TILs from the B16.PDL1mCherry tumours are positive for PD-L1 mCherry. PD-1 expression on the TILs from the PD-L1mCherry expressing tumour is ~10% of that on TILs from WT.B16 tumours suggesting downregulation of PD-1 by PD-L1 *in vivo*.

This data confirms that PD-L1 is transferred onto both $CD4^+$ and $CD8^+$ TILs and that ligand-induced downregulation of PD-1 also occurs *in vivo*.

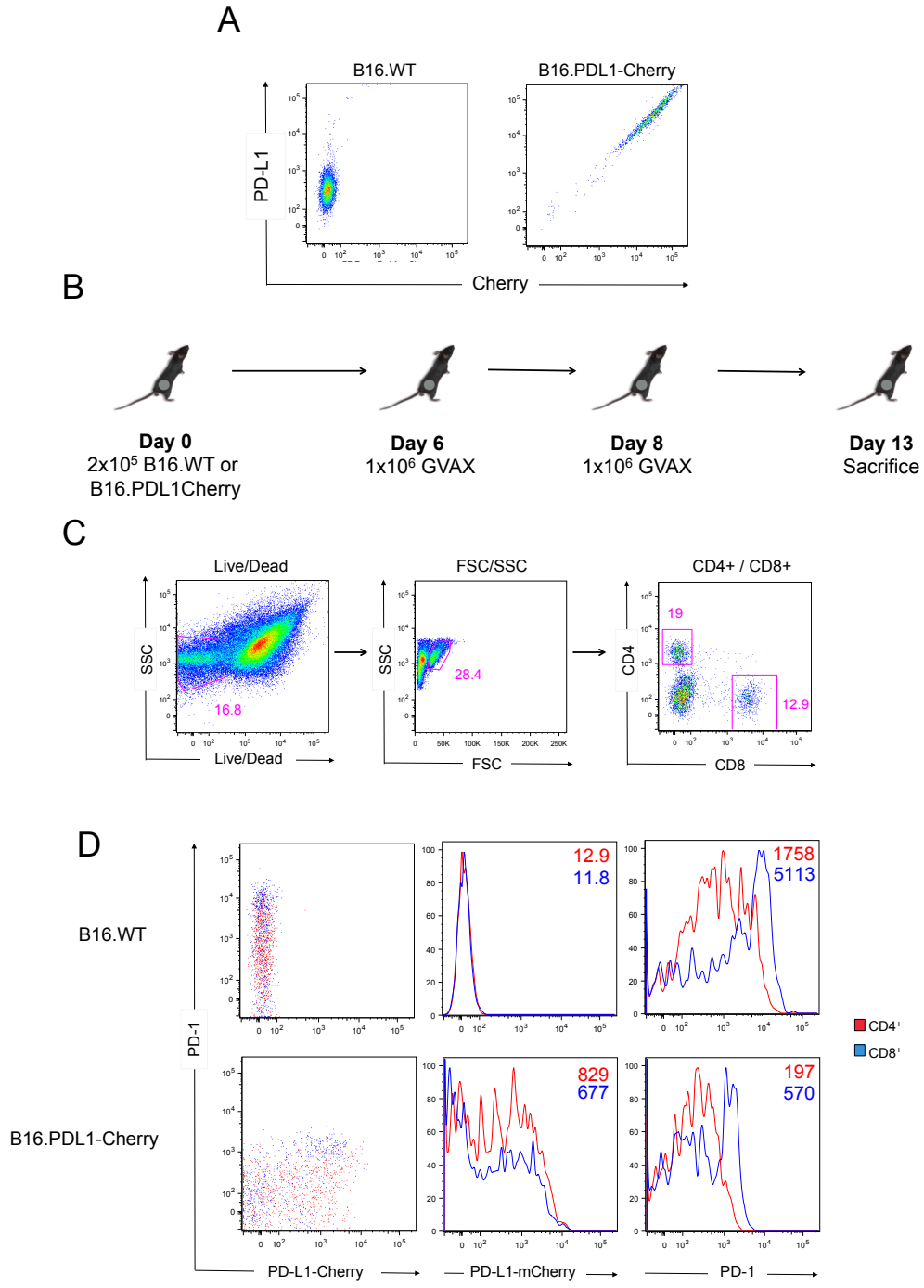

Figure 6.4 **Transfer of PD-L1 onto CD4⁺ and CD8⁺ T cells *in vivo* with B16 Melanoma model. A** B16.WT and B16.PDL1-mCherry cells stained with anti- mouse PD-L1 antibodies. **B** Experimental protocol carried out on C57BL/6 mice. Mice were either injected with 2x10⁶ B16.WT or B16.PDL1-mCherry at Day 0 and then 1x106 GVAX on Days 6 and 8. Mice were sacrificed on Day 13. **C** Gating strategy employed for selectively reviewing live, single, TILs. **D** CD4⁺ and CD8⁺ TILs isolated from either B16.WT or B16.PDL1-Cherry tumours stained with anti-mouse PD-1 antibodies.

6.3 Discussion

6.3.1 PD-L1 transfer onto PD-1 expressing T lymphocytes

We set out to investigate the stability of PD-1:PD-L1 interactions in a cell-based system. Our first step was to incubate PD-1 expressing Jurkat T cells with a soluble PD-L1Fc chimera to see whether the interaction was long-lived enough to detect by FACS. PD-L1 was found to still be in complex with PD-1 on the surface of cells following 5 separate washes and 30 minutes of staining at 4°C (Figure 6.1A). These data strongly suggest that the PD-1:PD-L1 interaction is both stable and long-lived.

The complex of PD-1 and PD-L1 is able to remain in complex at the cell surface. To our surprise, when the same assay was performed on PD-1 receptors that had sections of the intracellular domain truncated (detailed in Chapter 5) we found that with some truncations there is more PD-L1 found in complex with PD-1. As the extracellular domains are kept constant between the truncations, these differences are not due to differences in PD-1:PD-L1 affinity. The level of PD-1 expression was made constant between truncations, with expression titrated by varying concentrations of lentiviral vectors used to transduce cells. What these results may represent is differences in rates of PD-1 recycling. If it takes time for PD-1:PD-L1 complexes to form and the rate of recycling is high, then few complexes will be present at the surface at any point in time; if PD-1 recycling rates are low then more PD-1:PD-L1 complexes would be found at the cell surface. The sharp difference between the Δ217 and Δ211 truncations suggests that the 6 amino acids DPSAVP may form part of a motif involved in receptor turnover. Further investigation is needed to verify this and establish what factors might act on this motif.

Following reports that PD-L1 could be transferred and then expressed on the surface of PD-1 expressing cells via trogocytosis (Gary et al., 2012), we next tested whether we could replicate this finding with co-cultures of Jurkat T cells expressing PD-1 and PD-L1. Indeed a significant amount of PD-L1 was found on the surface of PD-1 expressing cells following co-culture (Figure 6.2). This PD-L1 was present after the multiple washing, re-suspension and staining steps involved in FACS. Interestingly the transfer is entirely one-directional, with PD-L1 transferred only onto PD-1

expressing cells and not visa versa. As both the ligand and receptor bearing cells were kept constant, this is likely to be a consequence PD-L1 or PD-1 properties. Daubeuf et al. made steps to address the issue of what protein properties favoured or facilitated trogocytosis (Daubeuf et al., 2010). They analysed a panel of proteins, comparing for their readiness to be trogocytosed and their plasma membrane anchoring. Further work is needed in this direction to understand what features of PD-L1 allow it to be transferred.

So are we observing trogocytosis of PD-L1, i.e. is PD-L1 now residing in the membrane of the PD-1 expressing cell? This may be the case, as indeed PD-L1 is stainable at the cell surface. There are several factors, however, that suggest this may not be the case. Firstly, the intracellular domain of PD-1 is not necessary for this PD-L1 transfer. In trogocytosis, the ligand must be internalised and incorporated into a host membrane that is then fused with the plasma membrane. In TCR trogocytosis, endocytosis is driven by actin via the Rho GTPase TC21, and NK2D trogocytosis is dependent on clathrin-mediated endocytosis (Martínez-Martín et al., 2011; Nakamura et al., 2013). In both cases, the intracellular domain is necessary for trogocytosis. Secondly, as demonstrated in Figure 6.1, PD-L1 can be held in complex with PD-1 at the cell surface. In those experiments using PD-L1Fc, there is no potential for PD-L1Fc to be expressed on the plasma membrane as it lacks a hydrophobic transmembrane region.

Next we were interested in the mechanism of PD-L1 transfer. A mechanism that would explain the unidirectional nature would be that PD-L1 is secreted (Chen et al., 2011; Rossille et al., 2014). However, when PD-1 expressing cells were incubated in the filtered supernatant from PD-L1 expressing cells, no PD-L1 was transferred. The role of exosomes and small microvesicles can also be ruled out as they would pass through the 0.45μm filter. Surprisingly, if the supernatant was only separated by centrifugation and not filtered, PD-L1 was found bound to the PD-1 expressing cells. This led us to find that PD-L1 is expressed on the surface of subcellular-sized cell debris present in the PD-L1 cell supernatant. This cell debris is likely to be mostly composed of apoptotic bodies and is presumably what is transferred. These data

indicate that the transfer of PD-L1 is not due to PD-L1 secretion, but instead is dependent on either cell-cell or cell-debris contact.

We were then interested in whether these findings *in vitro* were also applicable *in vivo* in a physiologically relevant setting. PD-L1: PD-1 is a crucial pathway in the immune tolerance of cancer cells, especially in immunogenic tumours such as melanoma where PD-1 and PD-L1 blockade has dramatic therapeutic effects. As this was not a closed *in vitro* system we constructed a mouse PDL1-mcherry fusion protein, in order to track tumour-derived PD-L1, and expressed it on B16 mouse melanoma cells (Figure 6.4A) using a lentiviral vector (pSIN-mPDL1-mCherry). In collaboration with Sergio Quezada's lab, an experimental protocol was employed that involved the use of GVAX to recruit tumour reactive lymphocytes to the tumour (Figure 6.4B). At Day 13 $CD4^+$ and $CD8^+$ lymphocytes were isolated from both WT and PDL1-mCherry expressing B16 tumours as well as from the lymph nodes and spleens of mice. The gating strategy ensured only single lymphocytes were analysed (Figure 6.4C). Both $CD4^+$ and $CD8^+$ TILs from both WT and PD-L1 tumours were found to express PD-1. Crucially, those TILs from the PDL1-mCherry tumour were strongly positive for mCherry, indicating that tumour derived PD-L1 had transferred onto the T lymphocytes *in vivo*. PDL1-mCherry was not present on lymphocytes in either the lymph nodes or spleen (data not shown).

Taken together these data demonstrate that PD-L1 is transferred onto PD-1 expressing T lymphocytes in the physiological setting of a melanoma tumour in mice. The physiological significance of this transfer is unclear. If this is indeed trogocytosis, as suggested by Gary et al., then the PD-L1, now expressed on the surface of lymphocytes, may serve to spread the inhibitory microenvironment to T lymphocytes themselves. These may then commit 'fratricide' by inhibiting fellow TILs (Gary et al., 2012). Cheng et al. however, never actually demonstrated that PD-L1 was expressed on the membrane i.e. that trogocytosis had actually occurred. Our data, with PD-L1Fc, demonstrates that stable PD-1:PD-L1 complexes can form at the cell surface. We also show that transfer of ligand is not dependent on the intracellular domain of the receptor, again suggesting that we are seeing surface complexes, not PD-L1 trogocytosis.

If these are indeed surface complexes, then this may suggest other functional roles:

Firstly, in the same way as transendocytosis, by removing the ligand from the APC/target cell, the pool of available PD-L1 able to inhibit subsequent cells is reduced. This may constitute a form of lymphocyte-number specific regulation i.e. a set pool of PD-L1 would be sufficient to inhibit a certain number of lymphocytes, but if numbers reached a critical threshold, the pool could be sufficiently diluted so as to release the PD-L1:PD-1 brake on T lymphocyte function.

Secondly, the transferred PD-L1 may continue to signal through the PD-1 are transferred so inhibition would be sustained beyond cell:cell contact. In the context of a tumour or organ with heterogeneous PD-L1 expression, cells with high PD-L1 expression could thereby protect those with low PD-L1 expression.

Thirdly, the transferred PD-L1 may instead block subsequent signalling through PD-1, preventing serial triggering and eventually depleted functional PD-1. This would therefore have to be offset with compensatory expression of new PD-1 for inhibition to continue.

Further investigation is needed to establish the function of this transferred PD-L1. The matter of receptor:ligand affinity also remains unresolved. SPR-based assays show complete wash off of PD-L1 in 5 - 15 seconds and here we demonstrate stable receptor:ligand complexes that have remained despite repeated washing and resuspension steps over a period of an hour. Presumably for transfer to occur from one cell to the other a high affinity (as in the case of CTLA-4) is necessary. It may be the case that during transfer following cell-cell contact, clusters of PD-1 remove clusters of PD-L1 and associated membrane, so the cumulative affinity is high enough to perform this function. Data with the PD-L1Fc chimera however demonstrates that even the monovalent interaction is relatively stable.

If the interaction of PD-L1:PD-1 is indeed higher than that demonstrated in cell-free assays, this may suggest a mechanism for the motility paralysis seen with by Zinselmeyer et al. Here cells were seen to form very stable immune synapses with clusters of PD-L1 found in the cSMAC (Zinselmeyer et al., 2013). This may have a biophysical explanation, where highly stable PD-L1:PD-1 interactions lead to cells adhering to each other, and thereby inhibiting motility.

6.3.2 Ligand-induced downregulation of PD-1

Many receptors undergo ligand-induced downregulation. In many cases this is a mechanism of negative regulation, terminating signalling and reducing the number of receptors on the surface accessible to more ligand. Other receptors, such as RTKs and EGFR, are endocytosed in order to sustain signalling, remaining active in endosomes (Sorkina et al., 2002).

Here we present data that PD-1 is downregulated following ligand binding. This downregulation has several salient features. It occurs both *in vitro* with human (Figure 6.2) and *in vivo* with mouse PD-L1 and PD-1 (Figure 6.4), it occurs only when the ligand PD-L1 is bound to an opposing cell membrane (Figure 6.2B), and not with soluble PD-L1Fc (Figure 6.1) or PD-L1 bound to cell debris (Figure 6.3A) and it is independent of the intracellular domain of the receptor, occurring both with PD1WT and PD1Δ181 (Figure 6.2).

As PD-L1 has been transferred and is in complex with PD-1, ligand-receptor interactions may be blocking the epitope of the staining antibody, and this could lead to a decrease in PD-1 staining shown in Figure 6.2. However, soluble PD-L1Fc also forms stable complexes at the surface (Figure 6.1) and under these conditions no PD-1 decrease is seen, therefore we can be sure that the reduction in PD-1 is not due to epitope blocking.

The features listed above make this downregulation unlike other forms of ligand-induced downregulation that rely on signalling through the receptor (Sorkin and von Zastrow, 2009). In our experiments however, PD-1 downregulation occurs without the intracellular domain. This suggests that neither internalisation motifs nor PD-1 signalling are necessary for this downregulation. Extracellular or transmembrane interactions may therefore mediate internalisation. The reliance on PD-L1 associated to an opposing cell membrane for downregulation may suggest a role for receptor clustering as the mechanism for downregulation. Clustering of adhesion molecules is sufficient to trigger a clathrin and caveolin independent downregulation (Muro et al., 2003). Indeed PD-1 is known to form microclusters with TCRs when ligated by PD-L1 which are required for inhibition. Lengthening of

the PD-1 extracellular domain with Ig-domain spacers in those experiments inhibited cluster formation (Yokosuka et al., 2012). Undertaking similar experiments will be necessary to clarify the potential roles of the PD-1 extracellular domain and receptor clustering in ligand induced downregulation of PD-1.

CHAPTER 7

CONCLUSIONS AND FUTURE PERSPECTIVES

7.1 Ca^{2+} influx and the plasma membrane

This work aimed to clarify uncertainties surrounding the sequence of events that follow large Ca^{2+} influx in Jurkat T cells. Figure 7.1 presents our model for the membrane movements that follow Ca^{2+} influx. With active TMEM16F, Ca^{2+} causes a rapid exocytosis of internal membranes that leads to plasma membrane scrambling and microvesicle shedding (Figure 1.10 and 1.12). Endocytosis does not occur in the presence of active TMEM16F (Figure 3.1), which implies that either TMEM16F or exocytosis inhibits the MEND pathway. MEND occurs in the absence of TMEM16F activity, perhaps following regulation by intracellular polyamines (Figure 3.8) or low channel expression. Endocytosis is therefore the 'default' or 'backup' pathway. It may be preferable for some cells (of the hematopoietic lineage for example) to scramble their membranes (Elliott et al., 2005; Toti et al., 1996) and shed vesicles as signalling modules (MacKenzie et al., 2001), whereas it may be appropriate for other cell types to take in membrane in response to large Ca^{2+} influx (Idone et al., 2008). We found that at excessive Ca^{2+} concentrations (facilitated by 20µM ionomycin in 2mM $CaCl_2$) in WT Jurkat T cells, MEND occurs even in the presence of TMEM16F activity (Figure 4.6). In this case the MEND pathway may overcome the inhibition exerted by the TMEM16F/exocytosis pathway.

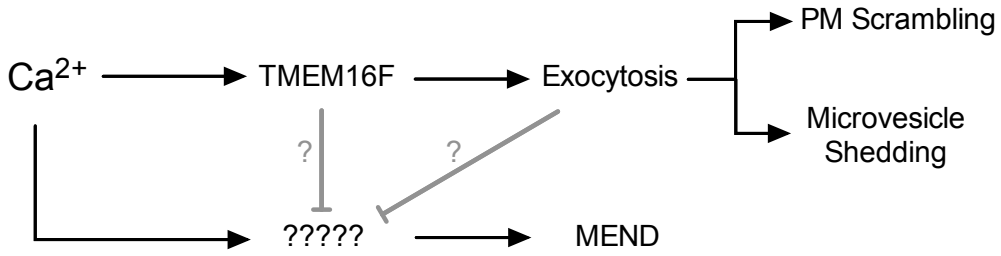

Figure 7.1 **Model of response pathways to large Ca^{2+} influx**

One of the functional roles of these two TMEM16F-regulated phenotypes is likely to be plasma membrane repair. Rapid Ca^{2+} activated exocytosis, endocytosis and microvesicle shedding are necessary for effective repair of membranes in different

cell types (Idone et al., 2008; Jimenez et al., 2014; McNeil and Kirchhausen, 2005). A rapid response to membrane wounding is necessary to ensure cell survival, with patching or removal of damaged membrane having to occur within seconds (McNeil and Kirchhausen, 2005). The speed of both the exo- and endocytic responses is a striking feature of the effects we observed (Figure 3.1 and 1.6). For membrane repair, a primitive mechanism, independent of a large protein complex, with simple regulatory mechanisms is likely to be preferable. For exocytic responses it may therefore not be surprising that the SNARE/Syn machinery, which delivers operative cargos in a highly regulated manner in the neuronal and immunological synapse, is not the same as that needed for membrane repair. MEND also seems to have a primitive mechanism without any reliance on classical endocytic proteins or cytoskeletal scaffolds (Figure 3.7)(Lariccia et al., 2011). Following membrane damage, two possible lines of defence may be necessary: membrane patching then shedding with TMEM16F active, and MEND as a backup pathway in the absence of TMEM16F activity or following large membrane wounds (higher Ca^{2+}) where endocytosis may be a more effective repair pathway.

Further work should be aimed at discovering which other proteins are necessary for TMEM16F-induced exocytosis, and whether our simple mechanistic model described in Figure 3.13 is valid. The close link between exocytosis and channel opening suggests the channel behaves like a fusion pore. It may be informative to establish why ion flux through the channel is required for exocytosis, as well as to ascertain the role of the recently described TMEM16F 'scrambling domain' (Brunner et al., 2014; Yu et al., 2015) and the constitutively active mutants (Suzuki et al., 2010) in the mechanism of membrane fusion. It will also be important to establish the origin of the membrane pool that is fused to the plasma membrane by TMEM16F.

The mechanism for Ca^{2+} dependent (Chapter 3) and independent (Chapter 5) MEND remains unknown. There is cause to believe they may share a mechanism as both specifically sort PD-1 in a manner dependent on the transmembrane domain of the receptor, suggesting the involvement of specific lipid domains in the mechanism. The sensing machinery must either be different in the two cases, or be activated by both Ca^{2+} and factors involved in apoptosis. The uncoupling of exocytosis and

endocytosis in TMEM16F-null cells makes the role of SMase secretion (Tam et al., 2010) unrealistic as previously demonstrated (Lariccia et al., 2011). Following some encouraging results with a small molecule inhibitor of PLA_2 (Lariccia et al., 2011) the role of phospholipases in MEND should be investigated with gene knockout studies.

This work also uncovered some unexpected links between other Ca^{2+} activated plasma membrane responses including microvesicle shedding and phospholipid scrambling. TMEM16F-induced exocytosis was found to precede and be necessary for Ca^{2+} activated microvesicle shedding in Jurkat T cells (Figure 1.12). Both the known delay in channel activation (Grubb et al., 2013) and time taken for exocytosis to occur may explain the consistent observation of a delay between Ca^{2+} influx and microvesicle release (Cocucci et al., 2007; Lee et al., 1993; MacKenzie et al., 2001; Moskovich and Fishelson, 2007; Stein and Luzio, 1991). It will be necessary to establish whether this microvesicle shedding is the same as that seen during membrane repair (Jimenez et al., 2014). TMEM16F has a high Ca^{2+} threshold for activation so it is unlikely that microvesicle release is linked to TMEM16F-induced exocytosis in all physiological contexts of microvesicle release. However, exocytosis itself may be necessary for the biogenesis of microvesicles, either by changing the plasma membrane lipid composition or by trafficking specific protein machinery to the membrane (e.g. ESCRT proteins)(Choudhuri et al., 2014). The machinery for this preceding exocytosis may differ depending on the context i.e. TMEM16F with high Ca^{2+} exocytosis and SNARE/Syn in more regulated settings. Indeed both focussed fusion events, dependent on Syn VII (Soares et al., 2013), and microvesicle release (Choudhuri et al., 2014) take place in the immune synapse during antigen presentation. This would be compatible with the involvement of ESCRT complex proteins and may provide a Ca^{2+} dependent mechanism for their translocation to the plasma membrane.

TMEM16F is the Ca^{2+} activated phospholipid scramblase (Suzuki et al., 2010) but the mechanism for this function has yet to be definitively demonstrated. The long-held model of the scramblase as an ATP-independent phospholipid translocator has endured and been given fresh support following the recent discovery of a hydrophilic cleft in the structure of an ancestral TMEM homologue necessary for membrane

scrambling (Brunner et al., 2014; Yu et al., 2015). Controversy and uncertainty still surround this field as some reports suggest that TMEM16F is not sufficient for plasma membrane scrambling (Yang et al., 2012). Here we show a new function for TMEM16F as a Ca^{2+} sensor for exocytosis, facilitating the rapid doubling of plasma membrane area (Figure 3.1), and furthermore show the kinetic of exocytosis and phospholipid scrambling are identical (Figure 3.10). This strongly suggests that the exocytosis of phospholipid-bearing internal membranes is the cause of TMEM16F-induced phospholipid scrambling. Indeed PS is enriched in certain internal membranes and phospholipid asymmetry is not maintained to the same extent in these as on the plasma membrane (Leventis and Grinstein, 2010; Yeung et al., 2008).

We found no way of selectively blocking exocytosis without also blocking TMEM16F channel activity so were unable to establish whether exocytosis is the cause of membrane scrambling. Our new model is therefore likely to be controversial. It goes against work carried out in artificial membranes that suggests ancestral TMEM homologues are sufficient for scrambling (Brunner et al., 2014; Malvezzi et al., 2013). However, these assays have incorrectly implicated other proteins as the scramblase in the past (Bevers and Williamson, 2010). A point in opposition to our model is the fact that RBCs from Scott syndrome patients, who lack TMEM16F, do not scramble their plasma membrane in response to Ca^{2+} (Bucki et al., 1998; Toti et al., 1996). It is a long established fact that RBCs lack internal membranes. During reticulocyte maturation, the ER, Golgi and other membranes are removed (Griffiths et al., 2012). Therefore in the case of RBCs, TMEM16F-induced plasma membrane scrambling would imply that that the protein has intrinsic scrambling capacity. The alternative is that RBCs do contain a yet undiscovered pool of internal membrane (however small) that participates in exocytosis. These issues will need to be addressing in light of this new function of TMEM16F.

7.2 PD-1 regulation on the plasma membrane

The starting point for this study was a search for mechanisms that regulate PD-1 expression on the cell surface of T lymphocytes. There have been no published mechanisms by which PD-1 is trafficked to and from the plasma membrane. One confocal study found PD-1 to be absent from classical endocytic compartments (Pentcheva-Hoang et al., 2007). Here we report five potential mechanisms of PD-1 regulation on the plasma membrane of Jurkat T cells (Figure 7.2).

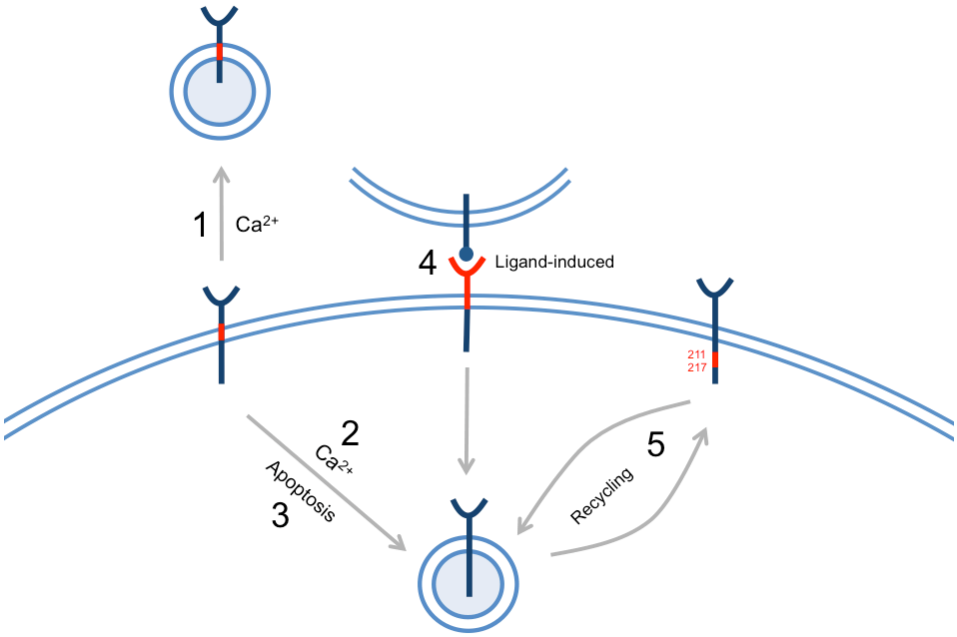

Figure 7.2 **Pathways of PD-1 downregulation**

Pathways 1 and 2 relate to the TMEM16F-regulated plasma membrane responses to Ca^{2+} influx - microvesicle shedding and MEND (Chapter 4 Figures and Videos 4.1 and 4.2). PD-1 is downregulated via either mechanism by 90-95%. Other receptors, including HLA, are only downregulated by 15-25% under the same conditions (Figures 4.1, 4.3, 4.6). This specificity for PD-1 was regulated via the transmembrane domain of the receptor (Figure 4.5). Surprisingly a massive endocytosis of PD-1 also occurs during apoptosis (Figure 7.2 Pathway 3, Figure 5.1 and 5.2) and this is also regulated via the transmembrane domain of the receptor (Figure 5.3 and 5.4). Apoptotic MEND shares similarities with Ca^{2+} activated MEND in protein specificity,

but importantly is Ca^{2+} independent. This suggests that the mechanism for MEND can be triggered by a variety of stimuli. The involvement of the transmembrane domain suggests a role for protein lipid interactions in dictating specificity. The fact that PD-1 is sorted both into microvesicles and MEND endosomes suggests these domains may be susceptible to vesiculation in either direction. The factors in the PD-1 transmembrane domain that dictate this specificity will need to be established. In the original paper that first described Ca^{2+} activated MEND, the authors proposed the model that MEND results from a coalescence of highly ordered membrane domains, rich in cholesterol and sphingolipids, that are then able to spontaneously vesiculate inwards. There is evidence that cholesterol can facilitate both coalescence and membrane bending (Groves, 2007; Sarasij et al., 2007). Indeed Ca^{2+} activated MEND could be blocked when membrane cholesterol was depleted with cyclodextrins. This hypothesis was also reinforced by the work presented in Fine et al 2011 that showed the ability of amphipathic agents to trigger MEND in cells. These may promote domain reorganisation and coalescence. It is as yet unclear how increases in intracellular Ca^{2+} could promote domain coalescence.

The difficulty in verifying a membrane-intrinsic mechanism for MEND or microvesicle shedding, such as domain coalescence leading to vesiculation, is the limited selection of suitable tools available for experimentally altering the membrane. Interventions such as cholesterol stripping using cyclodextrins, or the addition of amphipaths to the membrane, may not be informative as they can have profound effects on the biophysical properties of the membrane and thus not permitting specific conclusions to be drawn.

The functional basis for this protein regulation in T lymphocytes is unclear. There is a growing literature revealing the many roles of shed plasma membrane microvesicles in health and disease (Cocucci et al., 2009). The expression of proteins on these vesicles is closely related to their function (Al-Nedawi et al., 2008; Albanese et al., 1998; Choudhuri et al., 2014; Kim et al., 2005; MacKenzie et al., 2001; Skog et al., 2008). Our findings that demonstrate the specific inclusion and exclusion of proteins on the basis of their transmembrane domains may therefore be of interest in a broad range of contexts from immunity to cancer. It will be important

to next determine whether this mechanism holds true in other cell types as well as in primary human T cells.

We show for the first time that a large endocytic event occurs during apoptosis, which remodels the expression of surface proteins (Pathway 3). Whether this downregulation is physiologically important, in removing functional receptors from the surface of apoptotic cells and bodies, or is incidental to a yet uncharacterised internalisation of the plasma membrane during apoptosis, should be investigated.

As a result of our work investigating the transfer of PD-L1 from tumour cells onto PD-1 expressing lymphocytes, we uncovered two other mechanisms for PD-1 regulation (Chapter 6). Pathway 4 (Figure 7.2) describes ligand-induced downregulation of PD-1 (Figure 6.2, 6.3, 6.4). Crucially this only occurred when ligand was bound to an opposing cell membrane and not when PD-1 expressing cells were incubated with soluble PD-L1Fc or PD-L1 bound to cellular debris. Interestingly the intracellular domain of the receptor was not required for ligand-induced downregulation (Figure 6.2). The necessity for an opposing cell membrane may suggest a role for receptor clustering for internalisation (Muro et al., 2003). The mechanism for this ligand-induced downregulation will need further investigation.

A surprising finding was that the number of PD-1:PD-L1Fc complexes maintained at the cell surface is regulated by a motif between the 211th and 217th amino acid (-DPSAVP-) of the PD-1 intracellular domain (Figure 6.1)(Pathway 5). This truncation cannot have an effect on ligand-receptor affinity, as it affects only intracellular amino acids. A higher number of receptor/ligand complexes could also not be explained by higher expression as this was kept constant between truncations. We therefore hypothesise that this relates to the constitutive receptor-recycling rate, with a longer duration of receptor exposure at the cell surface leading to a higher probability of receptor-ligand complex formation. There are straightforward receptor recycling assays that could be carried out to test this hypothesis as well as further mutagenesis to establish which individual amino acids are responsible for this effect.

7.3 PD-L1 transfer onto T lymphocytes

The PD-1/PD-L1 interaction is a major therapeutic target for the treatment of a broad range of tumour types (Pardoll, 2012). The kinetics of the interaction that leads to the inhibitory influence of this pathway is, however, poorly characterised. Despite very low receptor-ligand affinities being reported in cell-free assays (Cheng et al., 2013), PD-L1 has been found to transfer onto PD-1 expressing T lymphocytes by trogocytosis (Gary et al., 2012). Here we found that PD-L1 and PD-1 can form a stable complex that is maintained at the cell surface (Figure 6.1). This occurs when either soluble PD-L1Fc, PD-L1 bearing cells or debris are incubated with PD-1 expressing cells (Figure 6.1, 6.2). Transfer happened both *in vitro* with Jurkat T cells and *in vivo* in a mouse melanoma model on both $CD4^+$ and $CD8^+$ TILs (Figure 6.4). The strength of the interaction was not quantified but complexes were present after multiple centrifugation, washing and re-suspension steps, suggesting that they may be stable *in vivo*. Interestingly, despite the PD-1:PD-L1 interaction being monovalent, there was no transfer of PD-1 onto PD-L1 expressing cells. This implies a feature of either PD-1, in being securely anchored to the plasma membrane, or PD-L1, in being susceptible to release from the plasma membrane, that allows for this unidirectional transfer. Once the mechanism of transfer is uncovered and can be blocked, it will be important to establish whether this feature of the PD-1:PD-L1 interaction contributes to the inhibitory effects of the pathway. Indeed it is unclear whether this PD-L1:PD-1 complex will continue to signal through PD-1 or block further signalling. In the same way as transendocytosis of ligands carried out by another family member CTLA-4, this transfer of ligands may confer an extrinsic influence on signalling events after the termination of cell-cell contact. It will also be important to establish whether the strength of the interaction is involved in the brake on migration that PD-1:PD-L1 confers. These points should be addressed as they may prove to be an important addition to the understanding of PD-1: PD-L1 biology.

7.4 Possible therapeutic implications

7.4.1 Targeting TMEM16F for anticoagulation

Scott syndrome is a rare inherited bleeding disorder that is caused by the deficient expression of TMEM16F (Suzuki et al., 2010). This symptom is caused by absent PS exposure on the surface of activated platelets, a necessary step in catalysing the clotting cascade (Toti et al., 1996). No other systemic effects have been reported in Scott patients. The Scott syndrome pathway has therefore been suggested as a drug target for anti-coagulation therapy (Morel et al., 2011).

Here we present evidence that intracellular polyamines are able to block TMEM16F activity. This insight could be a good starting point for designing a drug candidate screen. The polyamines we tested were all cell-impermeable so could only be used in whole-cell patch clamp experiments. The candidates should therefore be designed to include cell-permeable polyamine–like compounds. The screening assay would involve a straightforward 96 well FACS-based assay with Jurkat T cells incubated with candidate compounds, triggered with ionomycin in Ringer solution and stained with annexin V. Successful candidates should then proceed to validation *in vivo* with thrombosis assays.

7.4.2 Microvesicle-related therapies

Following the extensive exposition of the physiological roles of microvesicles, their application for therapeutics is now being explored. Microvesicles and exosomes can carry a variety of protein, mRNA and non-coding RNA cargoes (Cocucci et al., 2009). Microvesicles can therefore act as liposomes, transfecting their cargoes into cells of interest. Synthetic RNA delivery approaches such as lipid nanoparticles have met with technical difficulties due to their rapid sequestration by serum proteins (Dobrovolskaia et al., 2008), a problem which microvesicles, as physiological messengers for intercellular communication, do not encounter. One example of such a study was recently carried out by Mizrak et al. and demonstrated the anti-cancer potential of a microvesicle-based therapy (Mizrak et al., 2013). Microvesicles originating from cells that had been genetically engineered to express the enzyme

CD-UTRP, that converts the prodrug 5-fluorocysteine into 5-flurouracil, were injected into schwannoma tumours. This was followed by a significantly improved tumour remission after treatment with the prodrug.

Here we show that the biogenesis of microvesicles following Ca^{2+} influx is linked to the function of TMEM16F. This may inform the design of cell-based protocols for the synthesis of therapeutic microvesicles. Conversely, tumour derived microvesicles are important in regulating the tumour microenvironment (Al-Nedawi et al., 2008; Skog et al., 2008). It will therefore be important to establish whether the biogenesis of tumour-derived microvesicles is linked to TMEM16F and whether interventions that block this pathway could prove therapeutically significant in disrupting this microenvironment.

7.4.3 PD-1 downregulation from the plasma membrane

Regulation of the PD-1 pathway by anti-PD-1 and anti-PD-L1 antibodies has proved a promising therapeutic approach for the treatment of cancer (Pardoll, 2012). Another strategy to modulate the pathway could be to downregulate PD-1 expression at the plasma membrane of lymphocytes. We have uncovered a number of pathways which PD-1 can dramatically downregulate. A better understanding of the mechanism of both MEND and ligand induced PD-1 downregulation may uncover therapeutic targets that can regulate surface expression.

CHAPTER 8

BIBLIOGRAPHY

Abraham, R.T., and Weiss, A. (2004). Jurkat T cells and development of the T-cell receptor signalling paradigm. Nat Rev Immunol *4*, 301-308.

Acharya, U., Edwards, M.B., Jorquera, R.A., Silva, H., Nagashima, K., Labarca, P., and Acharya, J.K. (2006). Drosophila melanogaster Scramblases modulate synaptic transmission. J Cell Biol *173*, 69-82.

Agata, Y., Kawasaki, A., Nishimura, H., Ishida, Y., Tsubata, T., Yagita, H., and Honjo, T. (1996). Expression of the PD-1 antigen on the surface of stimulated mouse T and B lymphocytes. Int Immunol *8*, 765-772.

Ahmadzadeh, M., Johnson, L.A., Heemskerk, B., Wunderlich, J.R., Dudley, M.E., White, D.E., and Rosenberg, S.A. (2009). Tumor antigen-specific CD8 T cells infiltrating the tumor express high levels of PD-1 and are functionally impaired. Blood *114*, 1537-1544.

Al-Nedawi, K., Meehan, B., Micallef, J., Lhotak, V., May, L., Guha, A., and Rak, J. (2008). Intercellular transfer of the oncogenic receptor EGFRvIII by microvesicles derived from tumour cells. Nat Cell Biol *10*, 619-624.

Albanese, J., Meterissian, S., Kontogiannea, M., Dubreuil, C., Hand, A., Sorba, S., and Dainiak, N. (1998). Biologically active Fas antigen and its cognate ligand are expressed on plasma membrane-derived extracellular vesicles. Blood *91*, 3862-3874.

Alegre, ML., Frauwirth, KA., Thompson CB. (2001). T-cell regulation by CD28 and CTLA-4. Nat Rev Immun *1*, 220-228.

Almaça, J., Tian, Y., Aldehni, F., Ousingsawat, J., Kongsuphol, P., Rock, J.R., Harfe, B.D., Schreiber, R., and Kunzelmann, K. (2009). TMEM16 proteins produce volume-regulated chloride currents that are reduced in mice lacking TMEM16A. J Biol Chem *284*, 28571-28578.

Amato, R. (1999). Modest effect of interferon alpha on metastatic renal-cell carcinoma. Lancet *353*, 6-7.

Andrews, N.W. (1995). Lysosome recruitment during host cell invasion by Trypanosoma cruzi. Trends Cell Biol *5*, 133-137.

Andrews, N.W. (2002). Lysosomes and the plasma membrane: trypanosomes reveal a secret relationship. J Cell Biol *158*, 389-394.

Atanassoff, A.P., Wolfmeier, H., Schoenauer, R., Hostettler, A., Ring, A., Draeger, A., and Babiychuk, E.B. (2014). Microvesicle shedding and lysosomal repair fulfill divergent cellular needs during the repair of streptolysin O-induced plasmalemmal damage. PLoS One *9*, e89743.

Atefi, M., Avramis, E., Lassen, A., Wong, D.J., Robert, L., Foulad, D., Cerniglia, M., Titz, B., Chodon, T., Graeber, T.G.*, et al.* (2014). Effects of MAPK and PI3K

pathways on PD-L1 expression in melanoma. Clin Cancer Res *20*, 3446-3457.

Atkin-Smith, G.K., Tixeira, R., Paone, S., Mathivanan, S., Collins, C., Liem, M., Goodall, K.J., Ravichandran, K.S., Hulett, M.D., and Poon, I.K. (2015). A novel mechanism of generating extracellular vesicles during apoptosis via a beads-on-a-string membrane structure. Nat Commun *6*, 7439.

Azuma, K., Ota, K., Kawahara, A., Hattori, S., Iwama, E., Harada, T., Matsumoto, K., Takayama, K., Takamori, S., Kage, M.*, et al.* (2014). Association of PD-L1 overexpression with activating EGFR mutations in surgically resected nonsmall-cell lung cancer. Ann Oncol *25*, 1935-1940.

Babiychuk, E.B., Monastyrskaya, K., Potez, S., and Draeger, A. (2009). Intracellular Ca(2+) operates a switch between repair and lysis of streptolysin O-perforated cells. Cell death and differentiation *16*, 1126-1134.

Badour, K., McGavin, M.K.H., Zhang, J., Freeman, S., Vieira, C., Filipp, D., Julius, M., Mills, G.B., and Siminovitch, K.A. (2007). Interaction of the Wiskott-Aldrich syndrome protein with sorting nexin 9 is required for CD28 endocytosis and cosignaling in T cells. Proceedings of the National Academy of Sciences *104*, 1593-1598.

Bansal, D., Miyake, K., Vogel, S.S., Groh, S., Chen, C.C., Williamson, R., McNeil, P.L., and Campbell, K.P. (2003). Defective membrane repair in dysferlin-deficient muscular dystrophy. Nature *423*, 168-172.

Barber, D.L., Wherry, E.J., Masopust, D., Zhu, B., Allison, J.P., Sharpe, A.H., Freeman, G.J., and Ahmed, R. (2006). Restoring function in exhausted CD8 T cells during chronic viral infection. Nature *439*, 682-687.

Berda-Haddad, Y., Robert, S., Salers, P., Zekraoui, L., Farnarier, C., Dinarello, C.A., Dignat-George, F., and Kaplanski, G. (2011). Sterile inflammation of endothelial cell-derived apoptotic bodies is mediated by interleukin-1α. Proc Natl Acad Sci U S A *108*, 20684-20689.

Betts, M.R., and Koup, R.A. (2004). Detection of T-cell degranulation: CD107a and b. Methods Cell Biol *75*, 497-512.

Bevers, E.M., and Williamson, P.L. (2010). Phospholipid scramblase: an update. FEBS Lett *584*, 2724-2730.

Bi, G.Q., Alderton, J.M., and Steinhardt, R.A. (1995). Calcium-regulated exocytosis is required for cell membrane resealing. J Cell Biol *131*, 1747-1758.

Block, M.R., Glick, B.S., Wilcox, C.A., Wieland, F.T., and Rothman, J.E. (1988). Purification of an N-ethylmaleimide-sensitive protein catalyzing vesicular transport. Proc Natl Acad Sci U S A *85*, 7852-7856.

Bodon, G., Chassefeyre, R., Pernet-Gallay, K., Martinelli, N., Effantin, G., Hulsik, D.L., Belly, A., Goldberg, Y., Chatellard-Causse, C., Blot, B.*, et al.* (2011). Charged multivesicular body protein 2B (CHMP2B) of the endosomal sorting complex required for transport-III (ESCRT-III) polymerizes into helical structures deforming the plasma membrane. J Biol Chem *286*, 40276-40286.

Bollinger, C.R., Teichgräber, V., and Gulbins, E. (2005). Ceramide-enriched membrane domains. Biochim Biophys Acta *1746*, 284-294.

Bradshaw, J.D., Lu, P., Leytze, G., Rodgers, J., Schieven, G.L., Bennett, K.L., Linsley, P.S., and Kurtz, S.E. (1997). Interaction of the cytoplasmic tail of CTLA-4 (CD152) with a clathrin-associated protein is negatively regulated by tyrosine phosphorylation. Biochemistry *36*, 15975-15982.

Brahmer, J.R., Tykodi, S.S., Chow, L.Q.M., Hwu, W.-J., Topalian, S.L., Hwu, P., Drake, C.G., Camacho, L.H., Kauh, J., Odunsi, K.*, et al.* (2012). Safety and Activity of Anti-PD-L1 Antibody in Patients with Advanced Cancer. The New England journal of medicine.

Brezinschek, R.I., Oppenheimer-Marks, N., and Lipsky, P.E. (1999). Activated T cells acquire endothelial cell surface determinants during transendothelial migration. J Immunol *162*, 1677-1684.

Brooks, D.G., Teyton, L., Oldstone, M.B., and McGavern, D.B. (2005). Intrinsic functional dysregulation of CD4 T cells occurs rapidly following persistent viral infection. J Virol *79*, 10514-10527.

Brooks, M., Etter, K., Catalfamo, J., Brisbin, A., Bustamante, C., and Mezey, J. (2010). A genome-wide linkage scan in German shepherd dogs localizes canine platelet procoagulant deficiency (Scott syndrome) to canine chromosome 27. Gene *450*, 70-75.

Brooks, M.B., Catalfamo, J.L., Brown, H.A., Ivanova, P., and Lovaglio, J. (2002). A hereditary bleeding disorder of dogs caused by a lack of platelet procoagulant activity. Blood *99*, 2434-2441.

Brown, D. (2003). The ins and outs of aquaporin-2 trafficking. Am J Physiol Renal Physiol *284*, F893-901.

Brunner, J.D., Lim, N.K., Schenck, S., Duerst, A., and Dutzler, R. (2014). X-ray structure of a calcium-activated TMEM16 lipid scramblase. Nature *516*, 207-212.

Brustovetsky, N., Brustovetsky, T., Purl, K.J., Capano, M., Crompton, M., and Dubinsky, J.M. (2003). Increased susceptibility of striatal mitochondria to calcium-induced permeability transition. J Neurosci *23*, 4858-4867.

Bucki, R., Bachelot-Loza, C., Zachowski, A., Giraud, F., and Sulpice, J.C. (1998). Calcium induces phospholipid redistribution and microvesicle release in human erythrocyte membranes by independent pathways. Biochemistry *37*, 15383-15391.

Burnet, F.M. (1970). The concept of immunological surveillance. Prog Exp Tumor Res *13*, 1-27.

Busch, A., Quast, T., Keller, S., Kolanus, W., Knolle, P., Altevogt, P., and Limmer, A. (2008). Transfer of T cell surface molecules to dendritic cells upon CD4+ T cell priming involves two distinct mechanisms. J Immunol *181*, 3965-3973.

Castoldi, E., Collins, P.W., Williamson, P.L., and Bevers, E.M. (2011). Compound heterozygosity for 2 novel TMEM16F mutations in a patient with Scott syndrome. Blood *117*, 4399-4400.

Cauwenberghs, S., Feijge, M.A., Harper, A.G., Sage, S.O., Curvers, J., and Heemskerk, J.W. (2006). Shedding of procoagulant microparticles from unstimulated platelets by integrin-mediated destabilization of actin cytoskeleton. FEBS Lett *580*, 5313-5320.

Cerny, J., Feng, Y., Yu, A., Miyake, K., Borgonovo, B., Klumperman, J., Meldolesi, J., McNeil, P.L., and Kirchhausen, T. (2004). The small chemical vacuolin-1 inhibits Ca(2+)-dependent lysosomal exocytosis but not cell resealing. EMBO Rep *5*, 883-888.

Chakrabarti, S., Kobayashi, K.S., Flavell, R.A., Marks, C.B., Miyake, K., Liston, D.R., Fowler, K.T., Gorelick, F.S., and Andrews, N.W. (2003). Impaired membrane resealing and autoimmune myositis in synaptotagmin VII-deficient mice. J Cell Biol *162*, 543-549.

Chan, A.C., Iwashima, M., Turck, C.W., and Weiss, A. (1992). ZAP-70: a 70 kd protein-tyrosine kinase that associates with the TCR zeta chain. Cell *71*, 649-662.

Chapon, M., Randriamampita, C., Maubec, E., Badoual, C., Fouquet, S., Wang, S.F., Marinho, E., Farhi, D., Garcette, M., Jacobelli, S.*, et al.* (2011). Progressive upregulation of PD-1 in primary and metastatic melanomas associated with blunted TCR signaling in infiltrating T lymphocytes. J Invest Dermatol *131*, 1300-1307.

Chemnitz, J.M., Parry, R.V., Nichols, K.E., June, C.H., and Riley, J.L. (2004). SHP-1 and SHP-2 associate with immunoreceptor tyrosine-based switch motif of programmed death 1 upon primary human T cell stimulation, but only receptor ligation prevents T cell activation. The Journal of Immunology *173*, 945-954.

Chen, L., and Flies, D.B. (2013). Molecular mechanisms of T cell co-stimulation and co-inhibition. Nat Rev Immunol *13*, 227-242.

Chen, Y., Wang, Q., Shi, B., Xu, P., Hu, Z., Bai, L., and Zhang, X. (2011). Development of a sandwich ELISA for evaluating soluble PD-L1 (CD274) in human sera of different ages as well as supernatants of PD-L1+ cell lines. Cytokine.

Cheng, X., Veverka, V., Radhakrishnan, A., Waters, L.C., Muskett, F.W., Morgan, S.H., Huo, J., Yu, C., Evans, E.J., Leslie, A.J., *et al.* (2013). Structure and interactions of the human programmed cell death 1 receptor. J Biol Chem *288*, 11771-11785.

Chicka, M.C., Hui, E., Liu, H., and Chapman, E.R. (2008). Synaptotagmin arrests the SNARE complex before triggering fast, efficient membrane fusion in response to Ca2+. Nat Struct Mol Biol *15*, 827-835.

Chieregatti, E., and Meldolesi, J. (2005). Regulated exocytosis: new organelles for non-secretory purposes. Nat Rev Mol Cell Biol *6*, 181-187.

Chikuma, S., Imboden, J.B., Bluestone, J.A. (2003). Negative regulation of T cell receptor-lipid raft interaction by cytotoxic T lymphocyte-associated antigen 4. J Exp Med *197*, 129-135.

Chikuma, S., Terawaki, S., Hayashi, T., Nabeshima, R., Yoshida, T., Shibayama, S., Okazaki, T., and Honjo, T. (2009). PD-1-mediated suppression of IL-2 production induces CD8+ T cell anergy in vivo. J Immunol *182*, 6682-6689.

Choudhuri, K., Llodrá, J., Roth, E.W., Tsai, J., Gordo, S., Wucherpfennig, K.W., Kam, L.C., Stokes, D.L., and Dustin, M.L. (2014). Polarized release of T-cell-receptor-enriched microvesicles at the immunological synapse. Nature *507*, 118-123.

Clapham, D.E. (2007). Calcium signaling. Cell *131*, 1047-1058.

Clayton, E.L., and Cousin, M.A. (2009). The molecular physiology of activity-dependent bulk endocytosis of synaptic vesicles. J Neurochem *111*, 901-914.

Coburn, R.F., Jones, D.H., Morgan, C.P., Baron, C.B., and Cockcroft, S. (2002). Spermine increases phosphatidylinositol 4,5-bisphosphate content in permeabilized and nonpermeabilized HL60 cells. Biochim Biophys Acta *1584*, 20-30.

Cocucci, E., Racchetti, G., and Meldolesi, J. (2009). Shedding microvesicles: artefacts no more. Trends Cell Biol *19*, 43-51.

Cocucci, E., Racchetti, G., Podini, P., and Meldolesi, J. (2007). Enlargeosome traffic: exocytosis triggered by various signals is followed by endocytosis, membrane shedding or both. Traffic *8*, 742-757.

Cocucci, E., Racchetti, G., Podini, P., Rupnik, M., and Meldolesi, J. (2004). Enlargeosome, an exocytic vesicle resistant to nonionic detergents, undergoes endocytosis via a nonacidic route. Mol Biol Cell *15*, 5356-5368.

Collins, A.V., Brodie, D.W., Gilbert, R.J., Iaboni, A., Manso-Sancho, R., Walse, B., Stuart, D.I., van der Merwe, P.A., and Davis, S.J. (2002). The interaction properties of costimulatory molecules revisited. Immunity *17*, 201-210.

Coorssen, J.R., Schmitt, H., and Almers, W. (1996). Ca2+ triggers massive exocytosis in Chinese hamster ovary cells. EMBO J *15*, 3787-3791.

Croft, D.R., Coleman, M.L., Li, S., Robertson, D., Sullivan, T., Stewart, C.L., and Olson, M.F. (2005). Actin-myosin-based contraction is responsible for apoptotic nuclear disintegration. J Cell Biol *168*, 245-255.

Danilchik, M.V., Bedrick, S.D., Brown, E.E., and Ray, K. (2003). Furrow microtubules and localized exocytosis in cleaving Xenopus laevis embryos. J Cell Sci *116*, 273-283.

Daubeuf, S., Aucher, A., Bordier, C., Salles, A., Serre, L., Gaibelet, G., Faye, J.C., Favre, G., Joly, E., and Hudrisier, D. (2010). Preferential transfer of certain plasma membrane proteins onto T and B cells by trogocytosis. PLoS One *5*, e8716.

DEL CASTILLO, J., and KATZ, B. (1954). Quantal components of the end-plate potential. J Physiol *124*, 560-573.

Del Conde, I., Shrimpton, C.N., Thiagarajan, P., and López, J.A. (2005). Tissue-factor-bearing microvesicles arise from lipid rafts and fuse with activated platelets to initiate coagulation. Blood *106*, 1604-1611.

Demo, S.D., Masuda, E., Rossi, A.B., Throndset, B.T., Gerard, A.L., Chan, E.H., Armstrong, R.J., Fox, B.P., Lorens, J.B., Payan, D.G., *et al.* (1999). Quantitative measurement of mast cell degranulation using a novel flow cytometric annexin-V binding assay. Cytometry *36*, 340-348.

Detrait, E., Eddleman, C.S., Yoo, S., Fukuda, M., Nguyen, M.P., Bittner, G.D., and Fishman, H.M. (2000). Axolemmal repair requires proteins that mediate synaptic vesicle fusion. J Neurobiol *44*, 382-391.

Di, A., Nelson, D.J., Bindokas, V., Brown, M.E., Libunao, F., and Palfrey, H.C. (2003). Dynamin regulates focal exocytosis in phagocytosing macrophages. Mol Biol Cell *14*, 2016-2028.

Dietrich, J., Menné, C., and Geisler, C. (2002). Ligand-induced TCR down-regulation is not dependent on constitutive TCR cycling. The Journal of Immunology *168*, 5434-5440.

Distler, J.H., Jüngel, A., Huber, L.C., Seemayer, C.A., Reich, C.F., Gay, R.E., Michel, B.A., Fontana, A., Gay, S., Pisetsky, D.S., *et al.* (2005). The induction of matrix metalloproteinase and cytokine expression in synovial fibroblasts stimulated with immune cell microparticles. Proc Natl Acad Sci U S A *102*, 2892-2897.

Dobrovolskaia, M.A., Aggarwal, P., Hall, J.B., and McNeil, S.E. (2008). Preclinical studies to understand nanoparticle interaction with the immune system and its potential effects on nanoparticle biodistribution. Mol Pharm *5*, 487-495.

Dranoff, G. (2004). Cytokines in cancer pathogenesis and cancer therapy. Nat Rev Cancer *4*, 11-22.

Dunn, G.P., Old, L.J., and Schreiber, R.D. (2004). The three Es of cancer immunoediting. Annu Rev Immunol *22*, 329-360.

Elliott, J.I. (2006). Phosphatidylserine exposure in B lymphocytes: a role for lipid packing. Blood *108*, 1611-1617.

Elliott, J.I., Surprenant, A., Marelli-Berg, F.M., Cooper, J.C., Cassady-Cain, R.L., Wooding, C., Linton, K., Alexander, D.R., and Higgins, C.F. (2005). Membrane phosphatidylserine distribution as a non-apoptotic signalling mechanism in lymphocytes. Nat Cell Biol *7*, 808-816.

Fadeel, B., Gleiss, B., Högstrand, K., Chandra, J., Wiedmer, T., Sims, P.J., Henter, J.I., Orrenius, S., and Samali, A. (1999). Phosphatidylserine exposure during apoptosis is a cell-type-specific event and does not correlate with plasma membrane phospholipid scramblase expression. Biochem Biophys Res Commun *266*, 504-511.

Fadeel, B., and Xue, D. (2009). The ins and outs of phospholipid asymmetry in the plasma membrane: roles in health and disease. Crit Rev Biochem Mol Biol *44*, 264-277.

FATT, P., and KATZ, B. (1952). Spontaneous subthreshold activity at motor nerve endings. J Physiol *117*, 109-128.

Fine, M., Llaguno, M.C., Lariccia, V., Lin, M.-J., Yaradanakul, A., and Hilgemann, D.W. (2011). Massive endocytosis driven by lipidic forces originating in the outer plasmalemmal monolayer: a new approach to membrane recycling and lipid domains. The Journal of general physiology *137*, 137-154.

Fischer, K., Voelkl, S., Berger, J., Andreesen, R., Pomorski, T., and Mackensen, A. (2006). Antigen recognition induces phosphatidylserine exposure on the cell surface of human CD8+ T cells. Blood *108*, 4094-4101.

French, J.D., Kotnis, G.R., Said, S., Raeburn, C.D., McIntyre, R.C., Klopper, J.P., and Haugen, B.R. (2012). Programmed death-1+ T cells and regulatory T cells are enriched in tumor-involved lymph nodes and associated with aggressive features in papillary thyroid cancer. J Clin Endocrinol Metab *97*, E934-943.

Frigola, X., Inman, B.A., Lohse, C.M., Krco, C.J., Cheville, J.C., Thompson, R.H., Leibovich, B., Blute, M.L., Dong, H., and Kwon, E.D. (2011). Identification of a soluble form of B7-H1 that retains immunosuppressive activity and is

associated with aggressive renal cell carcinoma. Clin Cancer Res *17*, 1915-1923.

Game, D.S., Rogers, N.J., and Lechler, R.I. (2005). Acquisition of HLA-DR and costimulatory molecules by T cells from allogeneic antigen presenting cells. Am J Transplant *5*, 1614-1625.

Gao, Q., Wang, X.Y., Qiu, S.J., Yamato, I., Sho, M., Nakajima, Y., Zhou, J., Li, B.Z., Shi, Y.H., Xiao, Y.S.*, et al.* (2009). Overexpression of PD-L1 significantly associates with tumor aggressiveness and postoperative recurrence in human hepatocellular carcinoma. Clin Cancer Res *15*, 971-979.

Gary, R., Voelkl, S., Palmisano, R., Ullrich, E., Bosch, J.J., and Mackensen, A. (2012). Antigen-Specific Transfer of Functional Programmed Death Ligand 1 from Human APCs onto CD8+ T Cells via Trogocytosis. The Journal of Immunology *188*, 744-752.

Geppert, M., Goda, Y., Hammer, R.E., Li, C., Rosahl, T.W., Stevens, C.F., and Südhof, T.C. (1994). Synaptotagmin I: a major Ca2+ sensor for transmitter release at a central synapse. Cell *79*, 717-727.

Gerner, E.W., and Meyskens, F.L. (2004). Polyamines and cancer: old molecules, new understanding. Nat Rev Cancer *4*, 781-792.

Ginestra, A., La Placa, M.D., Saladino, F., Cassarà, D., Nagase, H., and Vittorelli, M.L. (1998). The amount and proteolytic content of vesicles shed by human cancer cell lines correlates with their in vitro invasiveness. Anticancer Res *18*, 3433-3437.

Giusti, I., D'Ascenzo, S., Millimaggi, D., Taraboletti, G., Carta, G., Franceschini, N., Pavan, A., and Dolo, V. (2008). Cathepsin B mediates the pH-dependent proinvasive activity of tumor-shed microvesicles. Neoplasia *10*, 481-488.

Goñi, F.M., and Alonso, A. (2009). Effects of ceramide and other simple sphingolipids on membrane lateral structure. Biochim Biophys Acta *1788*, 169-177.

Grabs, D., Slepnev, V.I., Songyang, Z., David, C., Lynch, M., Cantley, L.C., and De Camilli, P. (1997). The SH3 domain of amphiphysin binds the proline-rich domain of dynamin at a single site that defines a new SH3 binding consensus sequence. J Biol Chem *272*, 13419-13425.

Griff, I.C., Schekman, R., Rothman, J.E., and Kaiser, C.A. (1992). The yeast SEC17 gene product is functionally equivalent to mammalian alpha-SNAP protein. J Biol Chem *267*, 12106-12115.

Griffiths, R.E., Kupzig, S., Cogan, N., Mankelow, T.J., Betin, V.M., Trakarnsanga, K., Massey, E.J., Parsons, S.F., Anstee, D.J., and Lane, J.D. (2012). The ins and outs of human reticulocyte maturation: autophagy and the endosome/exosome pathway. Autophagy *8*, 1150-1151.

Groves, J.T. (2007). Bending mechanics and molecular organization in biological membranes. Annu Rev Phys Chem *58*, 697-717.

Grubb, S., Poulsen, K.A., Juul, C.A., Kyed, T., Klausen, T.K., Larsen, E.H., and Hoffmann, E.K. (2013). TMEM16F (Anoctamin 6), an anion channel of delayed Ca(2+) activation. J Gen Physiol *141*, 585-600.

Guo, D., and Lu, Z. (2003). Interaction mechanisms between polyamines and IRK1 inward rectifier K+ channels. J Gen Physiol *122*, 485-500.

Halimani, M., Pattu, V., Marshall, M.R., Chang, H.F., Matti, U., Jung, M., Becherer, U., Krause, E., Hoth, M., Schwarz, E.C.*, et al.* (2014). Syntaxin11 serves as a t-SNARE for the fusion of lytic granules in human cytotoxic T lymphocytes. Eur J Immunol *44*, 573-584.

Hamid, O., Robert, C., Daud, A., Hodi, F.S., Hwu, W.J., Kefford, R., Wolchok, J.D., Hersey, P., Joseph, R.W., Weber, J.S.*, et al.* (2013). Safety and tumor responses with lambrolizumab (anti-PD-1) in melanoma. N Engl J Med *369*, 134-144.

Hamon, Y., Broccardo, C., Chambenoit, O., Luciani, M.F., Toti, F., Chaslin, S., Freyssinet, J.M., Devaux, P.F., McNeish, J., Marguet, D.*, et al.* (2000). ABC1 promotes engulfment of apoptotic cells and transbilayer redistribution of phosphatidylserine. Nat Cell Biol *2*, 399-406.

Hanson, P.I., Roth, R., Lin, Y., and Heuser, J.E. (2008). Plasma membrane deformation by circular arrays of ESCRT-III protein filaments. J Cell Biol *180*, 389-402.

Heckman, K.L., and Pease, L.R. (2007). Gene splicing and mutagenesis by PCR-driven overlap extension. Nat Protoc *2*, 924-932.

Heijnen, H.F., Schiel, A.E., Fijnheer, R., Geuze, H.J., and Sixma, J.J. (1999). Activated platelets release two types of membrane vesicles: microvesicles by surface shedding and exosomes derived from exocytosis of multivesicular bodies and alpha-granules. Blood *94*, 3791-3799.

Heuser, J.E., Reese, T.S., Dennis, M.J., Jan, Y., Jan, L., and Evans, L. (1979). Synaptic vesicle exocytosis captured by quick freezing and correlated with quantal transmitter release. J Cell Biol *81*, 275-300.

Hilgemann, D.W., Fine, M., Linder, M.E., Jennings, B.C., and Lin, M.J. (2013). Massive endocytosis triggered by surface membrane palmitoylation under mitochondrial control in BHK fibroblasts. Elife *2*, e01293.

Hino, R., Kabashima, K., Kato, Y., Yagi, H., Nakamura, M., Honjo, T., Okazaki, T., and Tokura, Y. (2010). Tumor cell expression of programmed cell death-1 ligand 1 is a prognostic factor for malignant melanoma. Cancer *116*, 1757-1766.

Hodi, F.S., Butler, M., Oble, D.A., Seiden, M.V., Haluska, F.G., Kruse, A., Macrae, S., Nelson, M., Canning, C., Lowy, I., *et al.* (2008). Immunologic and clinical effects of antibody blockade of cytotoxic T lymphocyte-associated antigen 4 in previously vaccinated cancer patients. Proc Natl Acad Sci U S A *105*, 3005-3010.

Hodi, F.S., O'Day, S.J., McDermott, D.F., Weber, R.W., Sosman, J.A., Haanen, J.B., Gonzalez, R., Robert, C., Schadendorf, D., Hassel, J.C., *et al.* (2010). Improved survival with ipilimumab in patients with metastatic melanoma. N Engl J Med *363*, 711-723.

Holderfield, M., Deuker, M.M., McCormick, F., and McMahon, M. (2014). Targeting RAF kinases for cancer therapy: BRAF-mutated melanoma and beyond. Nat Rev Cancer *14*, 455-467.

Holevinsky, K.O., and Nelson, D.J. (1998). Membrane capacitance changes associated with particle uptake during phagocytosis in macrophages. Biophys J *75*, 2577-2586.

Holopainen, J.M., Angelova, M.I., and Kinnunen, P.K. (2000). Vectorial budding of vesicles by asymmetrical enzymatic formation of ceramide in giant liposomes. Biophys J *78*, 830-838.

Huang, J.F., Yang, Y., Sepulveda, H., Shi, W., Hwang, I., Peterson, P.A., Jackson, M.R., Sprent, J., and Cai, Z. (1999). TCR-Mediated internalization of peptide-MHC complexes acquired by T cells. Science *286*, 952-954.

Hui, E., Johnson, C.P., Yao, J., Dunning, F.M., and Chapman, E.R. (2009). Synaptotagmin-mediated bending of the target membrane is a critical step in Ca(2+)-regulated fusion. Cell *138*, 709-721.

Ichas, F., and Mazat, J.P. (1998). From calcium signaling to cell death: two conformations for the mitochondrial permeability transition pore. Switching from low- to high-conductance state. Biochim Biophys Acta *1366*, 33-50.

Idone, V., Tam, C., Goss, J.W., Toomre, D., Pypaert, M., and Andrews, N.W. (2008). Repair of injured plasma membrane by rapid Ca2+-dependent endocytosis. J Cell Biol *180*, 905-914.

Igarashi, K., and Kashiwagi, K. (2000). Polyamines: mysterious modulators of cellular functions. Biochem Biophys Res Commun *271*, 559-564.

Imboden, J.B., Weiss, A., and Stobo, J.D. (1985). The antigen receptor on a human T cell line initiates activation by increasing cytoplasmic free calcium. J Immunol *134*, 663-665.

Ito, T., Ueno, T., Clarkson, M.R., Yuan, X., Jurewicz, M.M., Yagita, H., Azuma, M., Sharpe, A.H., Auchincloss, H., Sayegh, M.H., *et al.* (2005). Analysis of the

role of negative T cell costimulatory pathways in CD4 and CD8 T cell-mediated alloimmune responses in vivo. J Immunol *174*, 6648-6656.

Ivanov, A.I. (2008). Pharmacological inhibition of endocytic pathways: is it specific enough to be useful? Methods Mol Biol *440*, 15-33.

Iwai, Y., Ishida, M., Tanaka, Y., Okazaki, T., Honjo, T., and Minato, N. (2002). Involvement of PD-L1 on tumor cells in the escape from host immune system and tumor immunotherapy by PD-L1 blockade. Proc Natl Acad Sci U S A *99*, 12293-12297.

Iwai, Y., Terawaki, S., and Honjo, T. (2005). PD-1 blockade inhibits hematogenous spread of poorly immunogenic tumor cells by enhanced recruitment of effector T cells. Int Immunol *17*, 133-144.

Iwai, Y., Terawaki, S., Ikegawa, M., Okazaki, T., and Honjo, T. (2003). PD-1 inhibits antiviral immunity at the effector phase in the liver. J Exp Med *198*, 39-50.

Jahn, R., and Fasshauer, D. (2012). Molecular machines governing exocytosis of synaptic vesicles. Nature *490*, 201-207.

Jaiswal, J.K., Chakrabarti, S., Andrews, N.W., and Simon, S.M. (2004). Synaptotagmin VII restricts fusion pore expansion during lysosomal exocytosis. PLoS Biol *2*, E233.

Jimenez, A.J., Maiuri, P., Lafaurie-Janvore, J., Divoux, S., Piel, M., and Perez, F. (2014). ESCRT machinery is required for plasma membrane repair. Science *343*, 1247136.

Karim, R., Jordanova, E.S., Piersma, S.J., Kenter, G.G., Chen, L., Boer, J.M., Melief, C.J., and van der Burg, S.H. (2009). Tumor-expressed B7-H1 and B7-DC in relation to PD-1+ T-cell infiltration and survival of patients with cervical carcinoma. Clin Cancer Res *15*, 6341-6347.

Karpinich, N.O., Tafani, M., Rothman, R.J., Russo, M.A., and Farber, J.L. (2002). The course of etoposide-induced apoptosis from damage to DNA and p53 activation to mitochondrial release of cytochrome c. J Biol Chem *277*, 16547-16552.

Karwacz, K., Bricogne, C., Macdonald, D., Arce, F., Bennett, C.L., Collins, M., and Escors, D. (2011). PD-L1 co-stimulation contributes to ligand-induced T cell receptor down-modulation on CD8(+) T cells. EMBO molecular medicine.

Keir, M.E., Butte, M.J., Freeman, G.J., and Sharpe, A.H. (2008). PD-1 and its ligands in tolerance and immunity. Annu Rev Immunol *26*, 677-704.

Keyel, P.A., Loultcheva, L., Roth, R., Salter, R.D., Watkins, S.C., Yokoyama, W.M., and Heuser, J.E. (2011). Streptolysin O clearance through sequestration into blebs that bud passively from the plasma membrane. J Cell Sci *124*, 2414-2423.

Khaled, Y.S., Ammori, B.J., and Elkord, E. (2013). Myeloid-derived suppressor cells in cancer: recent progress and prospects. Immunol Cell Biol *91*, 493-502.

Kim, H.J., Jun, I., Yoon, J.S., Jung, J., Kim, Y.K., Kim, W.K., Kim, B.J., Song, J., Kim, S.J., Nam, J.H.*, et al.* (2015). Selective serotonin reuptake inhibitors facilitate ANO6 (TMEM16F) current activation and phosphatidylserine exposure. Pflugers Arch.

Kim, J.W., Wieckowski, E., Taylor, D.D., Reichert, T.E., Watkins, S., and Whiteside, T.L. (2005). Fas ligand-positive membranous vesicles isolated from sera of patients with oral cancer induce apoptosis of activated T lymphocytes. Clin Cancer Res *11*, 1010-1020.

Klueg, K.M., and Muskavitch, M.A. (1999). Ligand-receptor interactions and trans-endocytosis of Delta, Serrate and Notch: members of the Notch signalling pathway in Drosophila. J Cell Sci *112 (Pt 19)*, 3289-3297.

Kmit, A., van Kruchten, R., Ousingsawat, J., Mattheij, N.J.A., Senden-Gijsbers, B., Heemskerk, J.W.M., Schreiber, R., Bevers, E.M., and Kunzelmann, K. (2013). Calcium-activated and apoptotic phospholipid scrambling induced by Ano6 can occur independently of Ano6 ion currents. Cell Death & Disease *4*, e611.

Kner, P., Chhun, B.B., Griffis, E.R., Winoto, L., and Gustafsson, M.G. (2009). Super-resolution video microscopy of live cells by structured illumination. Nat Methods *6*, 339-342.

Krummel, M.F., and Allison, J.P. (1995). CD28 and CTLA-4 have opposing effects on the response of T cells to stimulation. J Exp Med *182*, 459-465.

Köppler, B., Cohen, C., Schlöndorff, D., and Mack, M. (2006). Differential mechanisms of microparticle transfer toB cells and monocytes: anti-inflammatory propertiesof microparticles. Eur J Immunol *36*, 648-660.

Lariccia, V., Fine, M., Magi, S., Lin, M.-J., Yaradanakul, A., Llaguno, M.C., and Hilgemann, D.W. (2011). Massive calcium-activated endocytosis without involvement of classical endocytic proteins. The Journal of general physiology *137*, 111-132.

Lee, S.H., Meng, X.W., Flatten, K.S., Loegering, D.A., and Kaufmann, S.H. (2013). Phosphatidylserine exposure during apoptosis reflects bidirectional trafficking between plasma membrane and cytoplasm. Cell Death Differ *20*, 64-76.

Lee, T.L., Lin, Y.C., Mochitate, K., and Grinnell, F. (1993). Stress-relaxation of fibroblasts in collagen matrices triggers ectocytosis of plasma membrane vesicles containing actin, annexins II and VI, and beta 1 integrin receptors. J Cell Sci *105 (Pt 1)*, 167-177.

Leventis, P.A., and Grinstein, S. (2010). The distribution and function of phosphatidylserine in cellular membranes. Annu Rev Biophys *39*, 407-427.

Lewis, R.S., and Cahalan, M.D. (1995). Potassium and calcium channels in lymphocytes. Annu Rev Immunol *13*, 623-653.

Lindau, M., and Neher, E. (1988). Patch-clamp techniques for time-resolved capacitance measurements in single cells. Pflugers Arch *411*, 137-146.

Liu, J., Aoki, M., Illa, I., Wu, C., Fardeau, M., Angelini, C., Serrano, C., Urtizberea, J.A., Hentati, F., Hamida, M.B., *et al.* (1998). Dysferlin, a novel skeletal muscle gene, is mutated in Miyoshi myopathy and limb girdle muscular dystrophy. Nat Genet *20*, 31-36.

Loo, L.S., Hwang, L.A., Ong, Y.M., Tay, H.S., Wang, C.C., and Hong, W. (2009). A role for endobrevin/VAMP8 in CTL lytic granule exocytosis. Eur J Immunol *39*, 3520-3528.

Lorenz, D., Krylov, A., Hahm, D., Hagen, V., Rosenthal, W., Pohl, P., and Maric, K. (2003). Cyclic AMP is sufficient for triggering the exocytic recruitment of aquaporin-2 in renal epithelial cells. EMBO Rep *4*, 88-93.

MacKenzie, A., Wilson, H.L., Kiss-Toth, E., Dower, S.K., North, R.A., and Surprenant, A. (2001). Rapid secretion of interleukin-1beta by microvesicle shedding. Immunity *15*, 825-835.

Maine, C.J., Aziz, N.H., Chatterjee, J., Hayford, C., Brewig, N., Whilding, L., George, A.J., and Ghaem-Maghami, S. (2014). Programmed death ligand-1 over-expression correlates with malignancy and contributes to immune regulation in ovarian cancer. Cancer Immunol Immunother *63*, 215-224.

Malhotra, V., Orci, L., Glick, B.S., Block, M.R., and Rothman, J.E. (1988). Role of an N-ethylmaleimide-sensitive transport component in promoting fusion of transport vesicles with cisternae of the Golgi stack. Cell *54*, 221-227.

Malvezzi, M., Chalat, M., Janjusevic, R., Picollo, A., Terashima, H., Menon, A.K., and Accardi, A. (2013). Ca2+-dependent phospholipid scrambling by a reconstituted TMEM16 ion channel. Nat Commun *4*, 2367.

Manodori, A.B., Barabino, G.A., Lubin, B.H., and Kuypers, F.A. (2000). Adherence of phosphatidylserine-exposing erythrocytes to endothelial matrix thrombospondin. Blood *95*, 1293-1300.

Marcet-Palacios, M., Odemuyiwa, S.O., Coughlin, J.J., Garofoli, D., Ewen, C., Davidson, C.E., Ghaffari, M., Kane, K.P., Lacy, P., Logan, M.R., *et al.* (2008). Vesicle-associated membrane protein 7 (VAMP-7) is essential for target cell killing in a natural killer cell line. Biochem Biophys Res Commun *366*, 617-623.

Marraffini, L.A., and Sontheimer, E.J. (2010). CRISPR interference: RNA-directed adaptive immunity in bacteria and archaea. Nat Rev Genet *11*, 181-190.

Marston, D.J., Dickinson, S., and Nobes, C.D. (2003). Rac-dependent trans-endocytosis of ephrinBs regulates Eph-ephrin contact repulsion. Nat Cell Biol *5*, 879-888.

Martens, S., Kozlov, M.M., and McMahon, H.T. (2007). How synaptotagmin promotes membrane fusion. Science *316*, 1205-1208.

Martin, S., Pombo, I., Poncet, P., David, B., Arock, M., and Blank, U. (2000). Immunologic stimulation of mast cells leads to the reversible exposure of phosphatidylserine in the absence of apoptosis. Int Arch Allergy Immunol *123*, 249-258.

Martinez, I., Chakrabarti, S., Hellevik, T., Morehead, J., Fowler, K., and Andrews, N.W. (2000). Synaptotagmin VII regulates Ca(2+)-dependent exocytosis of lysosomes in fibroblasts. J Cell Biol *148*, 1141-1149.

Martins, J.R., Faria, D., Kongsuphol, P., Reisch, B., Schreiber, R., and Kunzelmann, K. (2011). Anoctamin 6 is an essential component of the outwardly rectifying chloride channel. Proc Natl Acad Sci U S A *108*, 18168-18172.

Martínez-Martín, N., Fernández-Arenas, E., Cemerski, S., Delgado, P., Turner, M., Heuser, J., Irvine, D.J., Huang, B., Bustelo, X.R., Shaw, A.*, et al.* (2011). T cell receptor internalization from the immunological synapse is mediated by TC21 and RhoG GTPase-dependent phagocytosis. Immunity *35*, 208-222.

Massi, D., Brusa, D., Merelli, B., Ciano, M., Audrito, V., Serra, S., Buonincontri, R., Baroni, G., Nassini, R., Minocci, D.*, et al.* (2014). PD-L1 marks a subset of melanomas with a shorter overall survival and distinct genetic and morphological characteristics. Ann Oncol *25*, 2433-2442.

Matsuzaki, J., Gnjatic, S., Mhawech-Fauceglia, P., Beck, A., Miller, A., Tsuji, T., Eppolito, C., Qian, F., Lele, S., Shrikant, P.*, et al.* (2010). Tumor-infiltrating NY-ESO-1-specific CD8+ T cells are negatively regulated by LAG-3 and PD-1 in human ovarian cancer. Proc Natl Acad Sci U S A *107*, 7875-7880.

Matti, U., Pattu, V., Halimani, M., Schirra, C., Krause, E., Liu, Y., Weins, L., Chang, H.F., Guzman, R., Olausson, J.*, et al.* (2013). Synaptobrevin2 is the v-SNARE required for cytotoxic T-lymphocyte lytic granule fusion. Nat Commun *4*, 1439.

McNeil, P.L., and Kirchhausen, T. (2005). An emergency response team for membrane repair. Nat Rev Mol Cell Biol *6*, 499-505.

Menke, J., Lucas, J.A., Zeller, G.C., Keir, M.E., Huang, X.R., Tsuboi, N., Mayadas, T.N., Lan, H.Y., Sharpe, A.H., and Kelley, V.R. (2007). Programmed death 1

ligand (PD-L) 1 and PD-L2 limit autoimmune kidney disease: distinct roles. J Immunol *179*, 7466-7477.

Mirnikjoo, B., Balasubramanian, K., and Schroit, A.J. (2009). Suicidal Membrane Repair Regulates Phosphatidylserine Externalization during Apoptosis. The Journal of biological chemistry *284*, 22512-22516.

Miyanishi, M., Tada, K., Koike, M., Uchiyama, Y., Kitamura, T., and Nagata, S. (2007). Identification of Tim4 as a phosphatidylserine receptor. Nature *450*, 435-439.

Mizrak, A., Bolukbasi, M.F., Ozdener, G.B., Brenner, G.J., Madlener, S., Erkan, E.P., Ströbel, T., Breakefield, X.O., and Saydam, O. (2013). Genetically engineered microvesicles carrying suicide mRNA/protein inhibit schwannoma tumor growth. Mol Ther *21*, 101-108.

Mochizuki, S., and Okada, Y. (2007). ADAMs in cancer cell proliferation and progression. Cancer Sci *98*, 621-628.

Morel, O., Jesel, L., Freyssinet, J.M., and Toti, F. (2011). Cellular mechanisms underlying the formation of circulating microparticles. Arterioscler Thromb Vasc Biol *31*, 15-26.

Moskophidis, D., Lechner, F., Pircher, H., and Zinkernagel, R.M. (1993). Virus persistence in acutely infected immunocompetent mice by exhaustion of antiviral cytotoxic effector T cells. Nature *362*, 758-761.

Moskovich, O., and Fishelson, Z. (2007). Live cell imaging of outward and inward vesiculation induced by the complement c5b-9 complex. The Journal of biological chemistry *282*, 29977-29986.

Mougiakakos, D., Choudhury, A., Lladser, A., Kiessling, R., and Johansson, C.C. (2010). Regulatory T cells in cancer. Adv Cancer Res *107*, 57-117.

Muenst, S., Schaerli, A.R., Gao, F., Däster, S., Trella, E., Droeser, R.A., Muraro, M.G., Zajac, P., Zanetti, R., Gillanders, W.E., *et al.* (2014). Expression of programmed death ligand 1 (PD-L1) is associated with poor prognosis in human breast cancer. Breast Cancer Res Treat *146*, 15-24.

Muro, S., Wiewrodt, R., Thomas, A., Koniaris, L., Albelda, S.M., Muzykantov, V.R., and Koval, M. (2003). A novel endocytic pathway induced by clustering endothelial ICAM-1 or PECAM-1. J Cell Sci *116*, 1599-1609.

Nagata, S., Hanayama, R., and Kawane, K. (2010). Autoimmunity and the clearance of dead cells. Cell *140*, 619-630.

Nakamura, K., Nakayama, M., Kawano, M., Amagai, R., Ishii, T., Harigae, H., and Ogasawara, K. (2013). Fratricide of natural killer cells dressed with tumor-derived NKG2D ligand. Proc Natl Acad Sci U S A *110*, 9421-9426.

Naramura, M., Jang, I.-K., Kole, H., Huang, F., Haines, D., and Gu, H. (2002). c-Cbl and Cbl-b regulate T cell responsiveness by promoting ligand-induced TCR down-modulation. Nature Immunology *3*, 1192-1199.

Nishimura, H., Nose, M., Hiai, H., Minato, N., and Honjo, T. (1999). Development of lupus-like autoimmune diseases by disruption of the PD-1 gene encoding an ITIM motif-carrying immunoreceptor. Immunity *11*, 141-151.

Nishimura, H., Okazaki, T., Tanaka, Y., and Nakatani, K. (2001). Autoimmune Dilated Cardiomyopathy in PD-1 Receptor-Deficient Mice. Science.

Novick, P., Field, C., and Schekman, R. (1980). Identification of 23 complementation groups required for post-translational events in the yeast secretory pathway. Cell *21*, 205-215.

Oestreich, K.J., Yoon, H., Ahmed, R., and Boss, J.M. (2008). NFATc1 regulates PD-1 expression upon T cell activation. The Journal of Immunology *181*, 4832-4839.

Ohigashi, Y., Sho, M., Yamada, Y., Tsurui, Y., Hamada, K., Ikeda, N., Mizuno, T., Yoriki, R., Kashizuka, H., Yane, K.*, et al.* (2005). Clinical significance of programmed death-1 ligand-1 and programmed death-1 ligand-2 expression in human esophageal cancer. Clin Cancer Res *11*, 2947-2953.

Okazaki, T., Maeda, A., Nishimura, H., Kurosaki, T., and Honjo, T. (2001). PD-1 immunoreceptor inhibits B cell receptor-mediated signaling by recruiting src homology 2-domain-containing tyrosine phosphatase 2 to phosphotyrosine. Proceedings of the National Academy of Sciences of the United States of America *98*, 13866-13871.

Ory, S., Ceridono, M., Momboisse, F., Houy, S., Chasserot-Golaz, S., Heintz, D., Calco, V., Haeberlé, A.M., Espinoza, F.A., Sims, P.J.*, et al.* (2013). Phospholipid scramblase-1-induced lipid reorganization regulates compensatory endocytosis in neuroendocrine cells. J Neurosci *33*, 3545-3556.

Pardoll, D.M. (2012). The blockade of immune checkpoints in cancer immunotherapy. Nature reviews Cancer *12*, 252-264.

Park, D., Tosello-Trampont, A.C., Elliott, M.R., Lu, M., Haney, L.B., Ma, Z., Klibanov, A.L., Mandell, J.W., and Ravichandran, K.S. (2007). BAI1 is an engulfment receptor for apoptotic cells upstream of the ELMO/Dock180/Rac module. Nature *450*, 430-434.

Park, S.Y., Jung, M.Y., Kim, H.J., Lee, S.J., Kim, S.Y., Lee, B.H., Kwon, T.H., Park, R.W., and Kim, I.S. (2008). Rapid cell corpse clearance by stabilin-2, a membrane phosphatidylserine receptor. Cell Death Differ *15*, 192-201.

Parry, R.V., Chemnitz, J.M., Frauwirth, K.A., Lanfranco, A.R., Braunstein, I., Kobayashi, S.V., Linsley, P.S., Thompson, C.B., and Riley, J.L. (2005). CTLA-4 and PD-1 receptors inhibit T-cell activation by distinct mechanisms. Molecular and Cellular Biology *25*, 9543-9553.

Parsa, A.T., Waldron, J.S., Panner, A., Crane, C.A., Parney, I.F., Barry, J.J., Cachola, K.E., Murray, J.C., Tihan, T., Jensen, M.C., *et al.* (2007). Loss of tumor suppressor PTEN function increases B7-H1 expression and immunoresistance in glioma. Nat Med *13*, 84-88.

Paulusma, C.C., and Elferink, R.P. (2010). P4 ATPases--the physiological relevance of lipid flipping transporters. FEBS Lett *584*, 2708-2716.

Pearson, W.L., and Nichols, C.G. (1998). Block of the Kir2.1 channel pore by alkylamine analogues of endogenous polyamines. J Gen Physiol *112*, 351-363.

Peggs, K.S., Quezada, S.A., Chambers, C.A., Korman, A.J., and Allison, J.P. (2009). Blockade of CTLA-4 on both effector and regulatory T cell compartments contributes to the antitumor activity of anti-CTLA-4 antibodies. J Exp Med *206*, 1717-1725.

Pentcheva-Hoang, T., Chen, L., Pardoll, D.M., and Allison, J.P. (2007). Programmed death-1 concentration at the immunological synapse is determined by ligand affinity and availability. Proc Natl Acad Sci U S A *104*, 17765-17770.

Perin, M.S., Fried, V.A., Mignery, G.A., Jahn, R., and Südhof, T.C. (1990). Phospholipid binding by a synaptic vesicle protein homologous to the regulatory region of protein kinase C. Nature *345*, 260-263.

Picollo, A., Malvezzi, M., and Accardi, A. (2015). TMEM16 proteins: unknown structure and confusing functions. Journal of Molecular Biology *427*, 94-105.

Pilzer, D., Gasser, O., Moskovich, O., Schifferli, J.A., and Fishelson, Z. (2005). Emission of membrane vesicles: roles in complement resistance, immunity and cancer. Springer Semin Immunopathol *27*, 375-387.

Pomorski, T., and Menon, A.K. (2006). Lipid flippases and their biological functions. Cell Mol Life Sci *63*, 2908-2921.

Poon, I.K., Chiu, Y.H., Armstrong, A.J., Kinchen, J.M., Juncadella, I.J., Bayliss, D.A., and Ravichandran, K.S. (2014a). Unexpected link between an antibiotic, pannexin channels and apoptosis. Nature *507*, 329-334.

Poon, I.K., Lucas, C.D., Rossi, A.G., and Ravichandran, K.S. (2014b). Apoptotic cell clearance: basic biology and therapeutic potential. Nat Rev Immunol *14*, 166-180.

Powles, T., Eder, J.P., Fine, G.D., Braiteh, F.S., Loriot, Y., Cruz, C., Bellmunt, J., Burris, H.A., Petrylak, D.P., Teng, S.L.*, et al.* (2014). MPDL3280A (anti-PD-L1) treatment leads to clinical activity in metastatic bladder cancer. Nature *515*, 558-562.

Quezada, S.A., Peggs, K.S., Simpson, T.R., Shen, Y., Littman, D.R., and Allison, J.P. (2008). Limited tumor infiltration by activated T effector cells restricts the therapeutic activity of regulatory T cell depletion against established melanoma. Journal of Experimental Medicine *205*, 2125-2138.

Quigley, M., Pereyra, F., Nilsson, B., and Porichis, F. (2010). Transcriptional analysis of HIV-specific CD8+ T cells shows that PD-1 inhibits T cell function by upregulating BATF. Nature Medicine.

Qureshi, O.S., Kaur, S., Hou, T.Z., Jeffery, L.E., Poulter, N.S., Briggs, Z., Kenefeck, R., Willox, A.K., Royle, S.J., Rappoport, J.Z.*, et al.* (2012). Constitutive clathrin-mediated endocytosis of CTLA-4 persists during T cell activation. J Biol Chem *287*, 9429-9440.

Qureshi, O.S., Zheng, Y., Nakamura, K., Attridge, K., Manzotti, C., Schmidt, E.M., Baker, J., Jeffery, L.E., Kaur, S., Briggs, Z.*, et al.* (2011). Trans-endocytosis of CD80 and CD86: a molecular basis for the cell-extrinsic function of CTLA-4. Science *332*, 600-603.

Reddy, A., Caler, E.V., and Andrews, N.W. (2001). Plasma membrane repair is mediated by Ca(2+)-regulated exocytosis of lysosomes. Cell *106*, 157-169.

Riley, J.L., and June, C.H. (2005). The CD28 family: a T-cell rheostat for therapeutic control of T-cell activation. Blood *105*, 13-21.

Riond, J., Elhmouzi, J., Hudrisier, D., and Gairin, J.E. (2007). Capture of membrane components via trogocytosis occurs in vivo during both dendritic cells and target cells encounter by CD8(+) T cells. Scand J Immunol *66*, 441-450.

Rizo, J., and Südhof, T.C. (2012). The membrane fusion enigma: SNAREs, Sec1/Munc18 proteins, and their accomplices--guilty as charged? Annu Rev Cell Dev Biol *28*, 279-308.

Robert, C., Long, G.V., Brady, B., Dutriaux, C., Maio, M., Mortier, L., Hassel, J.C., Rutkowski, P., McNeil, C., Kalinka-Warzocha, E.*, et al.* (2015). Nivolumab in previously untreated melanoma without BRAF mutation. N Engl J Med *372*, 320-330.

Rosenberg, S.A., Yang, J.C., and Restifo, N.P. (2004). Cancer immunotherapy: moving beyond current vaccines. Nat Med *10*, 909-915.

Rosing, J., van Rijn, J.L., Bevers, E.M., van Dieijen, G., Comfurius, P., and Zwaal, R.F. (1985). The role of activated human platelets in prothrombin and factor X activation. Blood *65*, 319-332.

Rossille, D., Gressier, M., Damotte, D., Maucort-Boulch, D., Pangault, C., Semana, G., Le Gouill, S., Haioun, C., Tarte, K., Lamy, T., *et al.* (2014). High level of soluble programmed cell death ligand 1 in blood impacts overall survival in aggressive diffuse large B-Cell lymphoma: results from a French multicenter clinical trial. Leukemia *28*, 2367-2375.

Rowe, H.M., Lopes, L., Brown, N., Efklidou, S., Smallie, T., Karrar, S., Kaye, P.M., and Collins, M.K. (2009). Expression of vFLIP in a lentiviral vaccine vector activates NF-{kappa}B, matures dendritic cells, and increases CD8+ T-cell responses. J Virol *83*, 1555-1562.

Rudd, C.E. (2008). The reverse stop-signal model for CTLA4 function. Nat Rev Immunol *8*, 153-160.

Sander, J.D., and Joung, J.K. (2014). CRISPR-Cas systems for editing, regulating and targeting genomes. Nat Biotechnol *32*, 347-355.

Sanjana, N.E., Shalem, O., and Zhang, F. (2014). Improved vectors and genome-wide libraries for CRISPR screening. Nat Methods *11*, 783-784.

Sarasij, R.C., Mayor, S., and Rao, M. (2007). Chirality-induced budding: a raft-mediated mechanism for endocytosis and morphology of caveolae? Biophys J *92*, 3140-3158.

Schadendorf, D., Hodi, F.S., Robert, C., Weber, J.S., Margolin, K., Hamid, O., Patt, D., Chen, T.T., Berman, D.M., and Wolchok, J.D. (2015). Pooled Analysis of Long-Term Survival Data From Phase II and Phase III Trials of Ipilimumab in Unresectable or Metastatic Melanoma. J Clin Oncol *33*, 1889-1894.

Scheffer, L.L., Sreetama, S.C., Sharma, N., Medikayala, S., Brown, K.J., Defour, A., and Jaiswal, J.K. (2014). Mechanism of Ca^{2+}-triggered ESCRT assembly and regulation of cell membrane repair. Nat Commun *5*, 5646.

Schonn, J.S., Maximov, A., Lao, Y., Südhof, T.C., and Sørensen, J.B. (2008). Synaptotagmin-1 and -7 are functionally overlapping Ca2+ sensors for exocytosis in adrenal chromaffin cells. Proc Natl Acad Sci U S A *105*, 3998-4003.

Schneider, H., Smith, X., Liu, H., Bismuth, G., Rudd, C.E. (2007) CTLA-4 disrupts ZAP70 microcluster formation with reduced T cell/APC dwell times and calcium mobilization. Euro J Immun *38*, 40-47.

Sebbagh, M., Renvoizé, C., Hamelin, J., Riché, N., Bertoglio, J., and Bréard, J. (2001). Caspase-3-mediated cleavage of ROCK I induces MLC phosphorylation and apoptotic membrane blebbing. Nat Cell Biol *3*, 346-352.

Segawa, K., Kurata, S., Yanagihashi, Y., Brummelkamp, T.R., Matsuda, F., and Nagata, S. (2014). Caspase-mediated cleavage of phospholipid flippase for apoptotic phosphatidylserine exposure. Science *344*, 1164-1168.

Seliger, B., and Massa, C. (2013). The dark side of dendritic cells: development and exploitation of tolerogenic activity that favor tumor outgrowth and immune escape. Front Immunol *4*, 419.

Sfanos, K.S., Bruno, T.C., Meeker, A.K., De Marzo, A.M., Isaacs, W.B., and Drake, C.G. (2009). Human prostate-infiltrating CD8+ T lymphocytes are oligoclonal and PD-1+. Prostate *69*, 1694-1703.

Shamim, M., Nanjappa, S.G., Singh, A., Plisch, E.H., LeBlanc, S.E., Walent, J., Svaren, J., Seroogy, C., and Suresh, M. (2007). Cbl-b regulates antigen-induced TCR down-regulation and IFN-gamma production by effector CD8 T cells without affecting functional avidity. The Journal of Immunology *179*, 7233-7243.

Sharma, P., and Allison, J.P. (2015). The future of immune checkpoint therapy. Science *348*, 56-61.

Shedden, K., Xie, X.T., Chandaroy, P., Chang, Y.T., and Rosania, G.R. (2003). Expulsion of small molecules in vesicles shed by cancer cells: association with gene expression and chemosensitivity profiles. Cancer Res *63*, 4331-4337.

Sheppard, K.-A., Fitz, L.J., Lee, J.M., Benander, C., George, J.A., Wooters, J., Qiu, Y., Jussif, J.M., Carter, L.L., Wood, C.R., *et al.* (2004). PD-1 inhibits T-cell receptor induced phosphorylation of the ZAP70/CD3zeta signalosome and downstream signaling to PKCtheta. FEBS letters *574*, 37-41.

Shi, F., Shi, M., Zeng, Z., Qi, R.Z., Liu, Z.W., Zhang, J.Y., Yang, Y.P., Tien, P., and Wang, F.S. (2011). PD-1 and PD-L1 upregulation promotes CD8(+) T-cell apoptosis and postoperative recurrence in hepatocellular carcinoma patients. Int J Cancer *128*, 887-896.

Shi, S.J., Wang, L.J., Wang, G.D., Guo, Z.Y., Wei, M., Meng, Y.L., Yang, A.G., and Wen, W.H. (2013). B7-H1 expression is associated with poor prognosis in colorectal carcinoma and regulates the proliferation and invasion of HCT116 colorectal cancer cells. PLoS One *8*, e76012.

Sims, P.J., Faioni, E.M., Wiedmer, T., and Shattil, S.J. (1988). Complement proteins C5b-9 cause release of membrane vesicles from the platelet surface that are enriched in the membrane receptor for coagulation factor Va and express prothrombinase activity. J Biol Chem *263*, 18205-18212.

Sims, P.J., Wiedmer, T., Esmon, C.T., Weiss, H.J., and Shattil, S.J. (1989). Assembly of the platelet prothrombinase complex is linked to vesiculation of the platelet plasma membrane. Studies in Scott syndrome: an isolated defect in platelet procoagulant activity. J Biol Chem *264*, 17049-17057.

Skog, J., Würdinger, T., van Rijn, S., Meijer, D.H., Gainche, L., Sena-Esteves, M., Curry, W.T., Carter, B.S., Krichevsky, A.M., and Breakefield, X.O. (2008).

Glioblastoma microvesicles transport RNA and proteins that promote tumour growth and provide diagnostic biomarkers. Nat Cell Biol *10*, 1470-1476.

Soares, H., Henriques, R., Sachse, M., Ventimiglia, L., Alonso, M.A., Zimmer, C., Thoulouze, M.I., and Alcover, A. (2013). Regulated vesicle fusion generates signaling nanoterritories that control T cell activation at the immunological synapse. J Exp Med *210*, 2415-2433.

Sorkin, A., and von Zastrow, M. (2009). Endocytosis and signalling: intertwining molecular networks. Nat Rev Mol Cell Biol *10*, 609-622.

Sorkina, T., Huang, F., Beguinot, L., and Sorkin, A. (2002). Effect of tyrosine kinase inhibitors on clathrin-coated pit recruitment and internalization of epidermal growth factor receptor. J Biol Chem *277*, 27433-27441.

Spruce, A.E., Breckenridge, L.J., Lee, A.K., and Almers, W. (1990). Properties of the fusion pore that forms during exocytosis of a mast cell secretory vesicle. Neuron *4*, 643-654.

Stanfield, P.R., and Sutcliffe, M.J. (2003). Spermine is fit to block inward rectifier (Kir) channels. J Gen Physiol *122*, 481-484.

Stein, A., Radhakrishnan, A., Riedel, D., Fasshauer, D., and Jahn, R. (2007). Synaptotagmin activates membrane fusion through a Ca2+-dependent trans interaction with phospholipids. Nat Struct Mol Biol *14*, 904-911.

Stein, J.M., and Luzio, J.P. (1991). Ectocytosis caused by sublytic autologous complement attack on human neutrophils. The sorting of endogenous plasma-membrane proteins and lipids into shed vesicles. Biochem J *274 (Pt 2)*, 381-386.

Steinhardt, R.A., Bi, G., and Alderton, J.M. (1994). Cell membrane resealing by a vesicular mechanism similar to neurotransmitter release. Science *263*, 390-393.

Stinchcombe, J.C., and Griffiths, G.M. (2007). Secretory mechanisms in cell-mediated cytotoxicity. Annu Rev Cell Dev Biol *23*, 495-517.

Stöckli, J., Fazakerley, D.J., and James, D.E. (2011). GLUT4 exocytosis. J Cell Sci *124*, 4147-4159.

Sun, S., Fei, X., Mao, Y., Wang, X., Garfield, D.H., Huang, O., Wang, J., Yuan, F., Sun, L., Yu, Q.*, et al.* (2014). PD-1(+) immune cell infiltration inversely correlates with survival of operable breast cancer patients. Cancer Immunol Immunother *63*, 395-406.

Suzuki, J., Denning, D.P., Imanishi, E., Horvitz, H.R., and Nagata, S. (2013). Xk-related protein 8 and CED-8 promote phosphatidylserine exposure in apoptotic cells. Science *341*, 403-406.

Suzuki, J., Umeda, M., Sims, P.J., and Nagata, S. (2010). Calcium-dependent phospholipid scrambling by TMEM16F. Nature *468*, 834-838.

Söllner, T., Whiteheart, S.W., Brunner, M., Erdjument-Bromage, H., Geromanos, S., Tempst, P., and Rothman, J.E. (1993). SNAP receptors implicated in vesicle targeting and fusion. Nature *362*, 318-324.

Südhof, T.C. (2013). Neurotransmitter release: the last millisecond in the life of a synaptic vesicle. Neuron *80*, 675-690.

Takeshita, T., Asao, H., Ohtani, K., Ishii, N., Kumaki, S., Tanaka, N., Munakata, H., Nakamura, M., and Sugamura, K. (1992). Cloning of the gamma chain of the human IL-2 receptor. Science *257*, 379-382.

Tam, C., Idone, V., Devlin, C., Fernandes, M.C., Flannery, A., He, X., Schuchman, E., Tabas, I., and Andrews, N.W. (2010). Exocytosis of acid sphingomyelinase by wounded cells promotes endocytosis and plasma membrane repair. J Cell Biol *189*, 1027-1038.

Taylor, R.C., Cullen, S.P., and Martin, S.J. (2008a). Apoptosis: controlled demolition at the cellular level. Nat Rev Mol Cell Biol *9*, 231-241.

Taylor, S.R., Gonzalez-Begne, M., Dewhurst, S., Chimini, G., Higgins, C.F., Melvin, J.E., and Elliott, J.I. (2008b). Sequential shrinkage and swelling underlie P2X7-stimulated lymphocyte phosphatidylserine exposure and death. J Immunol *180*, 300-308.

Terawaki, S., Chikuma, S., Shibayama, S., Hayashi, T., Yoshida, T., Okazaki, T., and Honjo, T. (2011). IFN-gamma Directly Promotes Programmed Cell Death-1 Transcription and Limits the Duration of T Cell-Mediated Immunity. The Journal of Immunology *186*, 2772-2779.

Thomas, P., Lee, A.K., Wong, J.G., and Almers, W. (1994). A triggered mechanism retrieves membrane in seconds after Ca(2+)-stimulated exocytosis in single pituitary cells. J Cell Biol *124*, 667-675.

Thompson, R.H., Dong, H., Lohse, C.M., Leibovich, B.C., Blute, M.L., Cheville, J.C., and Kwon, E.D. (2007). PD-1 is expressed by tumor-infiltrating immune cells and is associated with poor outcome for patients with renal cell carcinoma. Clin Cancer Res *13*, 1757-1761.

Tian, Y., Schreiber, R., and Kunzelmann, K. (2012). Anoctamins are a family of Ca2+-activated Cl- channels. J Cell Sci *125*, 4991-4998.

Tivol, E.A., Borriello, F., Schweitzer, A.N., Lynch, W.P., Bluestone, J.A., and Sharpe, A.H. (1995). Loss of CTLA-4 leads to massive lymphoproliferation and fatal multiorgan tissue destruction, revealing a critical negative regulatory role of CTLA-4. Immunity *3*, 541-547.

Togo, T., Alderton, J.M., Bi, G.Q., and Steinhardt, R.A. (1999). The mechanism of facilitated cell membrane resealing. J Cell Sci *112 (Pt 5)*, 719-731.

Togo, T., Krasieva, T.B., and Steinhardt, R.A. (2000). A decrease in membrane tension precedes successful cell-membrane repair. Molecular Biology of the Cell *11*, 4339-4346.

Topalian, S.L., Hodi, F.S., Brahmer, J.R., Gettinger, S.N., Smith, D.C., McDermott, D.F., Powderly, J.D., Carvajal, R.D., Sosman, J.A., Atkins, M.B.*, et al.* (2012). Safety, Activity, and Immune Correlates of Anti-PD-1 Antibody in Cancer. The New England journal of medicine.

Toti, F., Satta, N., Fressinaud, E., Meyer, D., and Freyssinet, J.M. (1996). Scott syndrome, characterized by impaired transmembrane migration of procoagulant phosphatidylserine and hemorrhagic complications, is an inherited disorder. Blood *87*, 1409-1415.

Valdez, A.C., Cabaniols, J.P., Brown, M.J., and Roche, P.A. (1999). Syntaxin 11 is associated with SNAP-23 on late endosomes and the trans-Golgi network. J Cell Sci *112 (Pt 6)*, 845-854.

van den Eijnde, S.M., van den Hoff, M.J., Reutelingsperger, C.P., van Heerde, W.L., Henfling, M.E., Vermeij-Keers, C., Schutte, B., Borgers, M., and Ramaekers, F.C. (2001). Transient expression of phosphatidylserine at cell-cell contact areas is required for myotube formation. J Cell Sci *114*, 3631-3642.

van der Bruggen, P., Traversari, C., Chomez, P., Lurquin, C., De Plaen, E., Van den Eynde, B., Knuth, A., and Boon, T. (1991). A gene encoding an antigen recognized by cytolytic T lymphocytes on a human melanoma. Science *254*, 1643-1647.

van Elsas, A., Hurwitz, A.A., and Allison, J.P. (1999). Combination immunotherapy of B16 melanoma using anti-cytotoxic T lymphocyte-associated antigen 4 (CTLA-4) and granulocyte/macrophage colony-stimulating factor (GM-CSF)-producing vaccines induces rejection of subcutaneous and metastatic tumors accompanied by autoimmune depigmentation. J Exp Med *190*, 355-366.

van Meer, G., Voelker, D.R., and Feigenson, G.W. (2008). Membrane lipids: where they are and how they behave. Nat Rev Mol Cell Biol *9*, 112-124.

Vanneman, M., and Dranoff, G. (2012). Combining immunotherapy and targeted therapies in cancer treatment. Nat Rev Cancer *12*, 237-251.

Varma, R., Campi, G., Yokosuka, T., Saito, T., and Dustin, M.L. (2006). T cell receptor-proximal signals are sustained in peripheral microclusters and terminated in the central supramolecular activation cluster. Immunity *25*, 117-127.

Veillette, A., Bookman, M.A., Horak, E.M., and Bolen, J.B. (1988). The CD4 and CD8 T cell surface antigens are associated with the internal membrane tyrosine-protein kinase p56lck. Cell *55*, 301-308.

Velu, V., Titanji, K., Zhu, B., Husain, S., Pladevega, A., Lai, L., Vanderford, T.H., Chennareddi, L., Silvestri, G., Freeman, G.J., *et al.* (2009). Enhancing SIV-specific immunity in vivo by PD-1 blockade. Nature *458*, 206-210.

Vogel, S.S., Smith, R.M., Baibakov, B., Ikebuchi, Y., and Lambert, N.A. (1999). Calcium influx is required for endocytotic membrane retrieval. Proc Natl Acad Sci U S A *96*, 5019-5024.

Walunas, T.L., Bakker, C.Y., and Bluestone, J.A. (1996). CTLA-4 ligation blocks CD28-dependent T cell activation. J Exp Med *183*, 2541-2550.

Walunas, T.L., Lenschow, D.J., Bakker, C.Y., Linsley, P.S., Freeman, G.J., Green, J.M., Thompson, C.B., and Bluestone, J.A. (1994). CTLA-4 can function as a negative regulator of T cell activation. Immunity *1*, 405-413.

Wang, J. (2005). Establishment of NOD-Pdcd1-/- mice as an efficient animal model of type I diabetes. Proceedings of the National Academy of Sciences *102*, 11823-11828.

Wang, T., Liu, G., and Wang, R. (2014). The Intercellular Metabolic Interplay between Tumor and Immune Cells. Front Immunol *5*, 358.

Wang, T.M., and Hilgemann, D.W. (2008). Ca-dependent nonsecretory vesicle fusion in a secretory cell. J Gen Physiol *132*, 51-65.

Waterhouse, P., Penninger, J.M., Timms, E., Wakeham, A., Shahinian, A., Lee, K.P., Thompson, C.B., Griesser, H., and Mak, T.W. (1995). Lymphoproliferative disorders with early lethality in mice deficient in Ctla-4. Science *270*, 985-988.

Weber, J.S., O'Day, S., Urba, W., Powderly, J., Nichol, G., Yellin, M., Snively, J., and Hersh, E. (2008). Phase I/II study of ipilimumab for patients with metastatic melanoma. J Clin Oncol *26*, 5950-5956.

Weisberg, E., Manley, P.W., Cowan-Jacob, S.W., Hochhaus, A., and Griffin, J.D. (2007). Second generation inhibitors of BCR-ABL for the treatment of imatinib-resistant chronic myeloid leukaemia. Nat Rev Cancer *7*, 345-356.

Weiss, A., Koretzky, G., Schatzman, R.C., and Kadlecek, T. (1991). Functional activation of the T-cell antigen receptor induces tyrosine phosphorylation of phospholipase C-gamma 1. Proc Natl Acad Sci U S A *88*, 5484-5488.

Weiss, H.J., Vicic, W.J., Lages, B.A., and Rogers, J. (1979). Isolated deficiency of platelet procoagulant activity. Am J Med *67*, 206-213.

Wherry, E.J., Blattman, J.N., and Ahmed, R. (2005). Low CD8 T-cell proliferative potential and high viral load limit the effectiveness of therapeutic vaccination. J Virol *79*, 8960-8968.

Wherry, E.J., Ha, S.J., Kaech, S.M., Haining, W.N., Sarkar, S., Kalia, V., Subramaniam, S., Blattman, J.N., Barber, D.L., and Ahmed, R. (2007). Molecular signature of CD8+ T cell exhaustion during chronic viral infection. Immunity *27*, 670-684.

Williams, K., Romano, C., Dichter, M.A., and Molinoff, P.B. (1991). Modulation of the NMDA receptor by polyamines. Life Sci *48*, 469-498.

Williamson, P., Christie, A., Kohlin, T., Schlegel, R.A., Comfurius, P., Harmsma, M., Zwaal, R.F., and Bevers, E.M. (2001). Phospholipid scramblase activation pathways in lymphocytes. Biochemistry *40*, 8065-8072.

Wilschut, J., Düzgüneş, N., and Papahadjopoulos, D. (1981). Calcium/magnesium specificity in membrane fusion: kinetics of aggregation and fusion of phosphatidylserine vesicles and the role of bilayer curvature. Biochemistry *20*, 3126-3133.

Wilson, D.W., Wilcox, C.A., Flynn, G.C., Chen, E., Kuang, W.J., Henzel, W.J., Block, M.R., Ullrich, A., and Rothman, J.E. (1989). A fusion protein required for vesicle-mediated transport in both mammalian cells and yeast. Nature *339*, 355-359.

Woon, L.A., Holland, J.W., Kable, E.P., and Roufogalis, B.D. (1999). Ca2+ sensitivity of phospholipid scrambling in human red cell ghosts. Cell Calcium *25*, 313-320.

Xie, Y., Bai, O., Yuan, J., Chibbar, R., Slattery, K., Wei, Y., Deng, Y., and Xiang, J. (2009). Tumor apoptotic bodies inhibit CTL responses and antitumor immunity via membrane-bound transforming growth factor-beta1 inducing CD8+ T-cell anergy and CD4+ Tr1 cell responses. Cancer Res *69*, 7756-7766.

Yang, H., Kim, A., David, T., Palmer, D., Jin, T., Tien, J., Huang, F., Cheng, T., Coughlin, S.R., Jan, Y.N.*, et al.* (2012). TMEM16F forms a Ca2+-activated cation channel required for lipid scrambling in platelets during blood coagulation. Cell *151*, 111-122.

Yang, J.C., Hughes, M., Kammula, U., Royal, R., Sherry, R.M., Topalian, S.L., Suri, K.B., Levy, C., Allen, T., Mavroukakis, S.*, et al.* (2007). Ipilimumab (anti-CTLA4 antibody) causes regression of metastatic renal cell cancer associated with enteritis and hypophysitis. J Immunother *30*, 825-830.

Yang, X., Kaeser-Woo, Y.J., Pang, Z.P., Xu, W., and Südhof, T.C. (2010). Complexin clamps asynchronous release by blocking a secondary Ca(2+) sensor via its accessory α helix. Neuron *68*, 907-920.

Yaradanakul, A., Wang, T.-M., Lariccia, V., Lin, M.-J., Shen, C., Liu, X., and Hilgemann, D.W. (2008). Massive Ca-induced membrane fusion and phospholipid changes triggered by reverse Na/Ca exchange in BHK fibroblasts. The Journal of general physiology *132*, 29-50.

Yeung, T., Gilbert, G.E., Shi, J., Silvius, J., Kapus, A., and Grinstein, S. (2008). Membrane Phosphatidylserine Regulates Surface Charge and Protein Localization. Science *319*, 210-213.

Yokosuka, T., Takamatsu, M., Kobayashi-Imanishi, W., Hashimoto-Tane, A., Azuma, M., and Saito, T. (2012). Programmed cell death 1 forms negative costimulatory microclusters that directly inhibit T cell receptor signaling by recruiting phosphatase SHP2. Journal of Experimental Medicine *209*, 1201-1217.

Yu, K., Whitlock, J.M., Lee, K., Ortlund, E.A., Cui, Y.Y., and Hartzell, H.C. (2015). Identification of a lipid scrambling domain in ANO6/TMEM16F. Elife *4*, e06901.

Zajac, A.J., Blattman, J.N., Murali-Krishna, K., Sourdive, D.J., Suresh, M., Altman, J.D., and Ahmed, R. (1998). Viral immune evasion due to persistence of activated T cells without effector function. J Exp Med *188*, 2205-2213.

Zernecke, A., Bidzhekov, K., Noels, H., Shagdarsuren, E., Gan, L., Denecke, B., Hristov, M., Köppel, T., Jahantigh, M.N., Lutgens, E.*, et al.* (2009). Delivery of microRNA-126 by apoptotic bodies induces CXCL12-dependent vascular protection. Sci Signal *2*, ra81.

Zhang, X., Schwartz, J.C., Guo, X., Bhatia, S., Cao, E., Lorenz, M., Cammer, M., Chen, L., Zhang, Z.Y., Edidin, M.A.*, et al.* (2004). Structural and functional analysis of the costimulatory receptor programmed death-1. Immunity *20*, 337-347.

Zhang, Y., Huang, S., Gong, D., Qin, Y., and Shen, Q. (2010). Programmed death-1 upregulation is correlated with dysfunction of tumor-infiltrating CD8+ T lymphocytes in human non-small cell lung cancer. Cell Mol Immunol *7*, 389-395.

Zhao, J., Zhou, Q., Wiedmer, T., and Sims, P.J. (1998). Level of expression of phospholipid scramblase regulates induced movement of phosphatidylserine to the cell surface. J Biol Chem *273*, 6603-6606.

Zhou, Q., Zhao, J., Al-Zoghaibi, F., Zhou, A., Wiedmer, T., Silverman, R.H., and Sims, P.J. (2000). Transcriptional control of the human plasma membrane phospholipid scramblase 1 gene is mediated by interferon-alpha. Blood *95*, 2593-2599.

Zhou, Q., Zhao, J., Stout, J.G., Luhm, R.A., Wiedmer, T., and Sims, P.J. (1997). Molecular cloning of human plasma membrane phospholipid scramblase. A

protein mediating transbilayer movement of plasma membrane phospholipids. J Biol Chem *272*, 18240-18244.

Zinselmeyer, B.H., Heydari, S., Sacristán, C., Nayak, D., Cammer, M., Herz, J., Cheng, X., Davis, S.J., Dustin, M.L., and McGavern, D.B. (2013). PD-1 promotes immune exhaustion by inducing antiviral T cell motility paralysis. Journal of Experimental Medicine *210*, 757-774.

Zufferey, R., Dull, T., Mandel, R.J., Bukovsky, A., Quiroz, D., Naldini, L., and Trono, D. (1998). Self-inactivating lentivirus vector for safe and efficient in vivo gene delivery. J Virol *72*, 9873-9880.

zur Stadt, U., Schmidt, S., Kasper, B., Beutel, K., Diler, A.S., Henter, J.I., Kabisch, H., Schneppenheim, R., Nürnberg, P., Janka, G.*, et al.* (2005). Linkage of familial hemophagocytic lymphohistiocytosis (FHL) type-4 to chromosome 6q24 and identification of mutations in syntaxin 11. Hum Mol Genet *14*, 827-834.

Züllig, S., Neukomm, L.J., Jovanovic, M., Charette, S.J., Lyssenko, N.N., Halleck, M.S., Reutelingsperger, C.P., Schlegel, R.A., and Hengartner, M.O. (2007). Aminophospholipid translocase TAT-1 promotes phosphatidylserine exposure during C. elegans apoptosis. Curr Biol *17*, 994-999.

APPENDIX I – VIDEO LEGENDS

Video 3.1. Ca^{2+} induced exocytosis and shedding probed with FM4-64 in WT Jurkat T cells. WT Jurkat cells were plated in a chambered coverslip in Ringer with 5μM FM 4-64. 5μM ionomycin was added at 30 seconds. The scale bar represents 10μm.

Video 3.2. Ca^{2+} induced PS exposure probed with K7-Rhodamine in WT Jurkat T cells. WT Jurkat cells were plated in a chambered coverslip in Ringer with 3μM K7-Rhodamine. 5μM ionomycin was added at 50 seconds. The scale bar represents 10μm.

Video 4.1. In WT Jurkat T cells PD-1 is shed following ionomycin treatment. PD1-mCherry expressing WT Jurkat T cells were imaged by SR-SIM Microscopy. Ionomycin was added to the opposite side of the chambered cover slip 10 seconds before the video starts. Scale bar represents 10μm.

Video 4.2. In TMEM16F-null Jurkat T cells PD-1 is endocytosed following ionomycin treatment. PD1-mCherry expressing TMEM16F-null Jurkat T cells were imaged by SR-SIM Microscopy. Ionomycin was added to the opposite side of the chambered cover slip 10 seconds before the video starts. Scale bar represents 10μm.